Published in Handbook on the Physics and Chemistry of Rare Earths, Volume 64 (2023) Pages 175-246
https://doi.org/10.1016/bs.hpcre.2023.10.004

Modern rare-earth-containing magnetocaloric materials: standing on the shoulders of *giant* $Gd_5Si_2Ge_2$

JIA YAN LAW* AND VICTORINO FRANCO

DEPARTMENT OF CONDENSED MATTER PHYSICS, ICMS-CSIC, UNIVERSIDAD DE SEVILLA, SEVILLA, SPAIN

* Corresponding author email: jylaw@us.es

Abstract

The magnetocaloric effect (MCE) is a phenomenon where varying magnetic fields cause temperature changes in magnetic materials, primarily near their thermomagnetic phase transitions. Its first observation was the induced temperature change of 0.7 K (for 1.5 T at 630 K) in a nickel sample near its thermomagnetic phase transition, but the heart of modern magnetocaloric materials research was shaped by Vitalij K. Pecharsky's and Karl A. Gschneidner Jr.'s discovery of the giant magnetocaloric effect (GMCE) in the famous $Gd_5Si_2Ge_2$. Significant MCE values are achieved when structural transformations coincide with magnetic transitions. This chapter focuses on rare-earth (RE)-containing magnetocaloric compounds that stand on the shoulders of the "*giant* $Gd_5Si_2Ge_2$", i.e., whose MCE values meet the GMCE threshold and pays attention to their material criticality assessment. It highlights recent breakthroughs related to first-order thermomagnetic phase transitions (FOMT) and magnetocalorics, including the quantitative criteria to identify FOMT and the critical point at which FOMT crossovers to second-order thermomagnetic phase transition (SOMT). The chapter examines the massive magnetocaloric materials library, including lanthanide metals, binary lanthanide-metalloid compounds, binary lanthanides-transition metals, ternary intermetallics, RE oxides, and alloys with multiple principal elements (known as high entropy alloys). The book chapter also discusses a directed search strategy for designing intermetallics with multi-principal elements exhibiting FOMT and GMCE, which can largely balance criticality and enable a combination of properties with mechanical stability if it is properly applied when searching for and developing modern magnetocaloric materials containing highly critical rare-earth elements.

Published in Handbook on the Physics and Chemistry of Rare Earths, Volume 64 (2023) Pages 175-246
https://doi.org/10.1016/bs.hpcre.2023.10.004

Keywords

Giant magnetocaloric effect; First-order thermomagnetic phase transitions; Criticality; Supply risk index; Gas Liquefaction; Multiple principal elements; High entropy alloys

Chapter Outline

List of symbols and acronyms

AFM	antiferromagnetic
FIM	ferrimagnetic
FOMT	first-order thermomagnetic phase transition
FM	ferromagnetic
FSMA	ferromagnetic shape memory alloy
GGG	gallium gadolinium garnet
GMCE	giant magnetocaloric effect
H	magnetic field
HAFM	helicoidal antiferromagnetic
HTM	high temperature modification

Published in Handbook on the Physics and Chemistry of Rare Earths, Volume 64 (2023) Pages 175-246
https://doi.org/10.1016/bs.hpcre.2023.10.004

hcp	hexagonal closed-packed
H_{CR}	critical magnetic field
HEA	high-entropy alloy
H_{mix}	enthalpy of mixing
IEM	itinerant electron metamagnetic
LTM	low temperature modification
M	magnetization
MCE	magnetocaloric effect
ML	machine learning
PM	paramagnetic
RC	refrigeration capacity
RCP	relative cooling power
RE	rare earth
$S_{isothermal}$	isothermal magnetic entropy
S_{mix}	entropy of mixing
S_R	rotational isothermal entropy
SG	space group
SOMT	second-order thermomagnetic phase transition
SR	spin reorientation
SRI	supply risk index
T_{ad}	reversible adiabatic temperature
T_C	Curie transition temperature
T_N	Néel transition temperature
T_{SR}	spin reorientation transition temperature
TM	transition metal

1 Introduction

The magnetocaloric effect (MCE) was first found when the magnetization of a nickel sample near its thermomagnetic phase transition induced a temperature change of 0.7 K (for 1.5 T at 630 K) [1]. This phenomenon made it possible to reach temperatures below 1 K by adiabatically demagnetizing a paramagnetic material [2]. Thus, MCE is commonly referred to as the effect of varying the applied magnetic fields causing reversible temperature changes in materials where the practical useful magnitude is usually found near their thermomagnetic phase transitions. Therefore, the heart of MCE consists of magnetic moments and external magnetic fields coupled together to the lattice degrees of freedom, and significantly large values can be realized in instances where structural transformations concomitate with magnetic transitions, which was first uncovered by Vitalij K. Pecharsky and Karl A. Gschneidner Jr. in $Gd_5Si_2Ge_2$. This material displays the famous giant magnetocaloric effect (GMCE) near room temperature [3]. Such a milestone paved the way for magnetic refrigeration to reach practical applications and initiated the search for new magnetocaloric materials.

Published in Handbook on the Physics and Chemistry of Rare Earths, Volume 64 (2023) Pages 175-246
https://doi.org/10.1016/bs.hpcre.2023.10.004

The "*giant* $Gd_5Si_2Ge_2$" and the impact of its breakthrough in magnetocalorics: What happens then and what is GMCE? How large is then considered a GMCE?

At the heart of the MCE, its isothermal magnetic entropy change ($\Delta S_{\text{isothermal}}$) is associated with magnetic moments coupled together with external magnetic fields, which is why one observes the practical useful MCE is found close to thermomagnetic phase transitions, such as near the Curie transition temperatures (T_C) for ferromagnets. Therefore, using the following equation derived from the Maxwell relation, the MCE can be indirectly calculated from the isothermal entropy change associated with magnetization:

$$\Delta S_{\text{isothermal}} = \mu_0 \int_{H_{\text{initial}}}^{H_{\text{final}}} \left(\partial M / \partial T\right)_H \, dH,$$

where *H* refers to the magnetic field, *M* to magnetization, and *T* represents temperature. The reversible adiabatic temperature change (ΔT_{ad}) of the magnetic material under varying magnetic fields is another characteristic that is used to describe the MCE, though $\Delta S_{\text{isothermal}}$ is more frequently found to characterize the performance of magnetocaloric materials because magnetometer measurements of magnetization are more easily available and accessible.

In instances where structural transformations coincide with magnetic transitions, it is more likely to achieve noticeably higher MCE values, as in the case of GMCE found in $Gd_5Si_2Ge_2$, than when only magnetic phase transitions occur. **Figure 1 (A)** shows a schematic representation of the MCE adopting the Brayton cycle while **Figure 1 (B)** presents the discovery of GMCE in $Gd_5Si_2Ge_2$ in 1997 where it shows MCE maximizes near the thermomagnetic phase transition temperatures. It should be noted that the negative sign of $\Delta S_{\text{isothermal}}$ refers to the conventional MCE, which is found in materials with magnetization that decreases with increasing temperature, i.e., with a $\partial M / \partial T < 0$. As a result, the opposite ($\partial M / \partial T > 0$), which occurs when magnetization increases with rising temperature, results in a positive $\Delta S_{\text{isothermal}}$ sign, also known as the inverse MCE.

Published in Handbook on the Physics and Chemistry of Rare Earths, Volume 64 (2023) Pages 175-246
https://doi.org/10.1016/bs.hpcre.2023.10.004

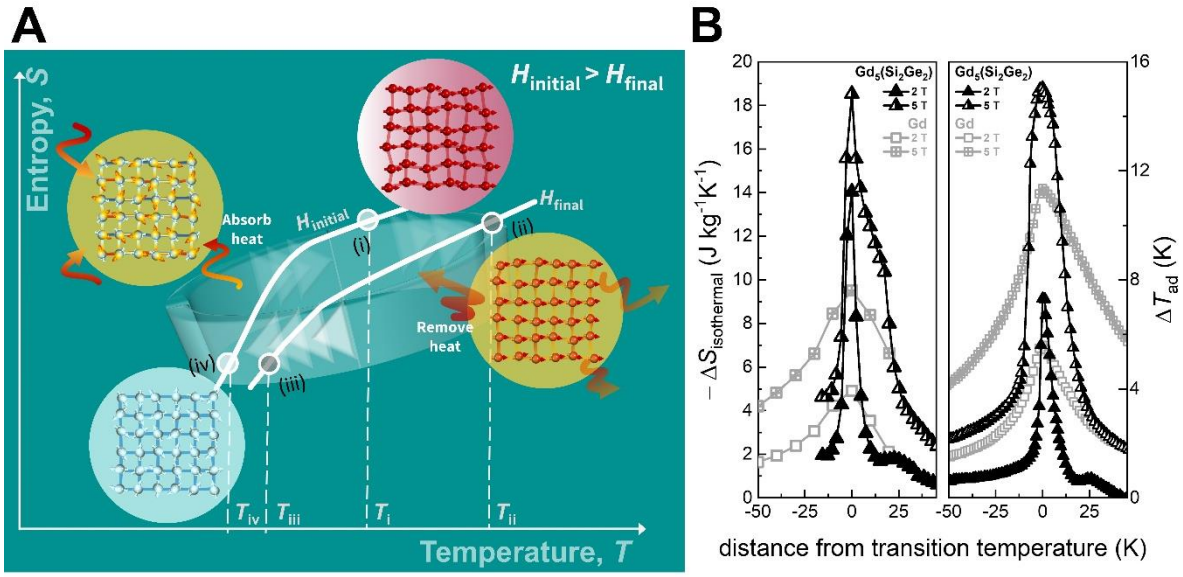

Figure 1. (A) Schematic representation of the magnetocaloric effect following a Brayton cycle: adiabatic magnetization (i)→(ii), isofield temperature change (ii)→(iii), adiabatic demagnetization (iii)→(iv), and isofield temperature change (iv)→(i). When the material is adiabatically magnetized (from magnetic field values $H_{initial}$→H_{final}), its magnetic moments align to the magnetic field, causing the material to heat up. This extra heat can be removed by a fluid through heat transfer while keeping the material magnetized. As it gets demagnetized adiabatically, the magnetic moments randomize, causing an increase in the magnetic entropy and thus a drop in the material temperature (since total entropy is constant). In the last step (iv), the material can be placed in thermal contact with the load for cooling during an isofield process. The demagnetized material heats up and can revert to stage (i) for another magnetic refrigeration cycle. Such systems can establish half of the theoretical Carnot efficiency and much higher than that of conventional compressed gas refrigeration (38% of theoretical Carnot efficiency). **(B)** The discovery of the giant magnetocaloric effect in $Gd_5Si_2Ge_2$ reported by V.K. Pecharsky and K.A. Jr. Gschneidner in 1997 [3]. In this representation, it can be seen that the MCE maximizes near the thermomagnetic transition temperature. *Data in panel **(B)** from V.K. Pecharsky, K.A. Gschneidner, Jr., Giant magnetocaloric effect in $Gd_5(Si_2Ge2)$, Phys. Rev. Lett. 78 (23) (1997) 4494–4497 [3].*

For $Gd_5Si_2Ge_2$, its ferromagnetic ordering is accompanied by a reversible breaking or making of bonds between Si/Ge sites, resulting in a significant entropy change and adiabatic temperature change as shown in **Figure 1 (B)** [3]. Such a transition, which couples structural transformation with magnetic phase transition, is associated with a first-order thermomagnetic phase transition (FOMT) that could result in an abrupt change in magnetization. On the other hand, the magnetic phase transition implying order-disorder in the magnetic sublattice during transition is known as the second-order thermomagnetic phase transition (SOMT), which typically gives smaller MCE than those arising from FOMT. This means that FOMT materials undergo significant transformations that are mediated by the lattice subsystem (i.e., the latent heat), which indicates that FOMT can be classified into two

types: magnetostructural and magnetoelastic. Upon completion of the first-order thermomagnetic phase transition, the magnetocaloric response reaches saturation, while for second-order transitions, a large MCE value is highly dependent on much higher fields. The huge difference of FOMT versus SOMT materials can be interpreted from the comparison of $Gd_5Si_2Ge_2$ (FOMT) versus Gd (SOMT) as shown in **Figure 1 (B)**. For 2 T, the former showed a maximum $\Delta S_{isothermal}$ of -14 J $kg^{-1}K^{-1}$ while the corresponding value for Gd was -5 J $kg^{-1}K^{-1}$, leading to the coining of "GMCE" for $Gd_5Si_2Ge_2$, and a breakthrough in magnetocalorics. Accordingly, GMCE could be considered when the MCE values are double of those of Gd, which has been discussed and suggested in ref.[4]. In addition, it is interesting to note that, prior to $Gd_5(Si,Ge)_4$, FeRh[5, 6] and $La_{0.8}Ca_{0.2}MnO_3$[7] are known examples of magnetocaloric materials with significantly large MCE; however, it is the later references on $Gd_5(Si, Ge)_4$ family that coined the term "GMCE materials". The variation of Si:Ge ratio enabled a wide range of tunable transition temperatures from ~30 to ~276 K, maintaining a reversible GMCE [8]. Despite that a large MCE of -13 K (2 T) was observed from a FOMT around 308 K in FeRh [5, 6], this substantial value is unfortunately irreversible and only observed upon applying the magnetic field to a virgin sample [4]. Meanwhile, $La_{0.8}Ca_{0.2}MnO_3$ showed comparable MCE values to Gd but is not significant enough to justify the claim of GMCE [7].

The 1997 breakthrough of $Gd_5Si_2Ge_2$ nonetheless led to the development of more magnetocaloric materials with exceptional GMCE values within a few years of its discovery, as we present in **Figure 2** where the flourishing rush for designing FOMTs for advanced magnetocaloric materials sits on the "*giant* $Gd_5Si_2Ge_2$". The figure also includes the year of reporting for the compound with GMCE, with the diameter of the sphere corresponding to the GMCE magnitude. Relevant examples of these advanced materials include MnAs, the $NaZn_{13}$-structure $La(Fe,Si)_{13}$ and their hydrides $La(Fe,Si)_{13}H$, the compounds with Fe_2P structure (Mn-Fe-P-Si-Ge-As), as well as off-stoichiometric Ni_2MnY-based (where Y = Ga, In, or Sn) ferromagnetic shape memory alloys (FSMA), the MM'X family (where M and M' are transition metals and X are metalloids), high-entropy alloys (HEA) though at ascent stage, etc. The infographic also includes a timeline for Gd, FeRh, and $HoCo_2$, but they appear outside the flourish as their first reports date from before 1997.

Published in Handbook on the Physics and Chemistry of Rare Earths, Volume 64 (2023) Pages 175-246
https://doi.org/10.1016/bs.hpcre.2023.10.004

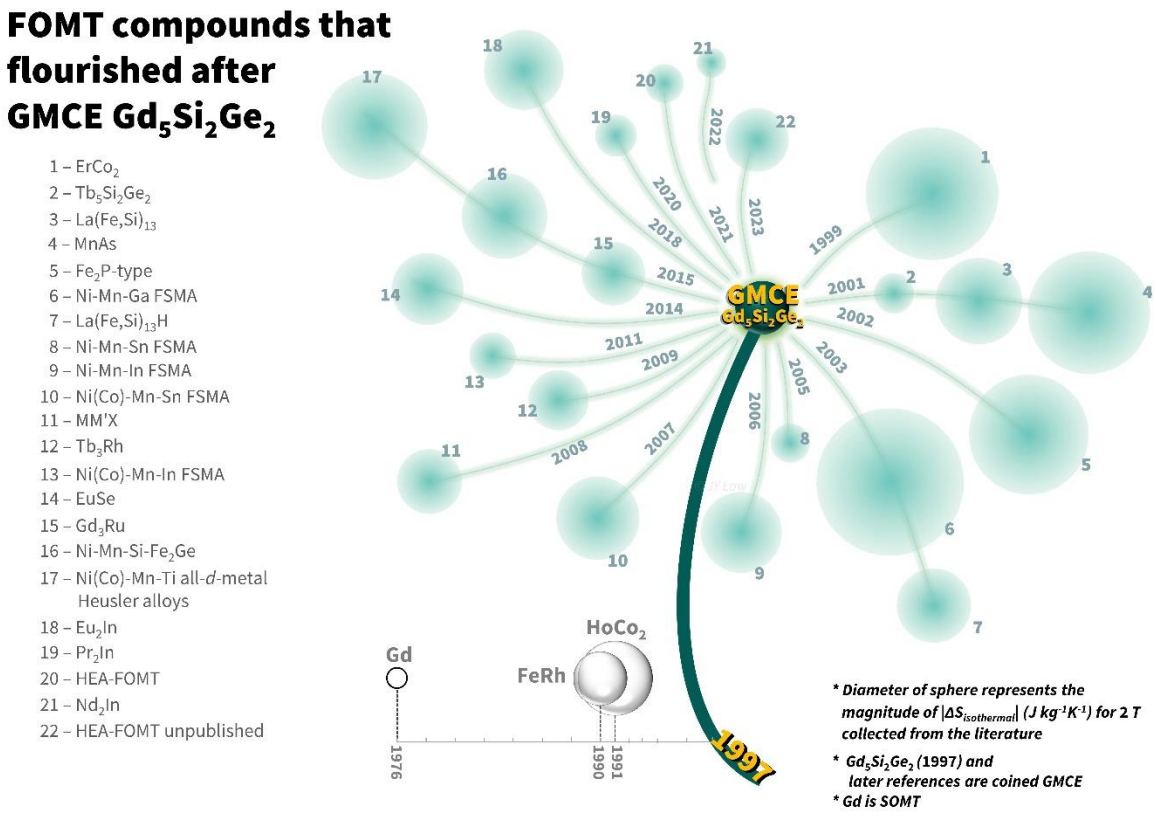

Figure 2. Infographic on the flourish of FOMT compounds from the "giant $Gd_5Si_2Ge_2$" after 1997. Diameter of the sphere represents the magnitude of $|\Delta S_{isothermal}|$ for 2 T collected from references [3, 6, 8-34]. The year that the compounds were first reported for their GMCE is indicated. Note that all the compounds undergo FOMT except Gd with SOMT.

According to **Figure 2**, these advanced FOMT compounds can be divided into two categories: for cryogenic applications, a common choice is lanthanide-based compositions due to their low transition temperatures. On the other hand, the other rare-earth-free (RE-free) or RE-containing ones are the ideal candidates for applications near room temperature or above. Based on the current interests of the community and energy concerns today, we will name the relevant ones below.

The magnetocaloric compounds that are used in prototypes, apart from Gd, include those of the Fe_2P-type and $NaZn_{13}$-type. Their first reports with GMCE are: $MnFeP_{0.45}As_{0.55}$ [33] and related alloys [35], as well as $La(Fe,Si)_{13}$ [34] and their hydrides [32]. Afterward, many chemical substitution efforts were made to optimize MCE, where these two material families became well-established enough to be considered by companies to scale-up for use in prototypes. In Fe_2P family, there are a number of compositions with GMCE values without the presence of arsenic [10, 36]. The GMCE of $La(Fe,Si)_{13}$ is typically below room temperature [34, 37, 38], but

after hydrogenation, they were discovered to have potential near room temperature [32, 39]. Additionally, this family of compounds not only has easily adjustable transition temperatures but also can be tuned from FOMT to SOMT, where the critical point of FOMT crossing over to SOMT exhibits both benefits of these two groups. The current interests of them evolved to additive manufacturing[40], composite development [41] as well as hysteresis management [42, 43].

The next noteworthy compounds shown in **Figure 2** are FSMA, MM'X, Ni(Co)-Mn-Ti all-*d*-metal Heusler alloys, and HEA-FOMT, which are all worthy of further mention. Their GMCE values are attributed to the magnetostructural transformation they undergo, which enable extended potentials to multi-caloric effects by numerous external stimuli like pressure, voltage, etc. Their GMCE values were firstly reported in these references: Ni-Mn-Ga [30, 31]; Ni-Mn-Sn [29]; Ni-Mn-In ; Ni(Co-Mn-Ti all-*d*-metal [21]; MM'X [44, 45]; NiMnSi-Fe_2Ge [24]; HEA-FOMT [18] and related series [15, 17]. It should be noted that HEA-FOMT is at the ascent stage as earlier reports of magnetocaloric HEA are with values that are not competitive at all despite the claims (see relevant topical reviews in [13, 46]).

Last but not least are the RE-containing FOMT compounds, which are highly promising for cryogenic applications, with transition temperatures lower than 50 K. While the $RECo_2$ Laves phase was discovered long ago, it resurfaces today in the research community in particular due to the current interest in gas liquefaction resulting from increasing energy demands. A more recently found family of RE-containing cryogenic compounds that exhibit FOMT is $REIn_2$, whose first report stated that it has negligible hysteresis despite exhibiting FOMT [20]. Due to timely interest in cryogenic magnetocaloric materials arising from energy, sustainability, and criticality concerns, we will further discuss these RE-containing compounds together with others whose MCE values meet the GMCE threshold in the following sections of this chapter according to their chemical nature.

2 Modern relevant materials standing on "*giant* $Gd_5Si_2Ge_2$" – the shift to gas liquefaction

The transformation to a carbon-neutral society is on the horizon, and this greatly highlights hydrogen gas, a non-carbon-based fuel, as a viable alternative to fossil fuels. It can be used to power cars, trains, planes, and ships as well as to generate electricity. In addition, it can be stored for a long time, making it an ideal energy source during peak demand periods. Moreover, it does not generate any greenhouse gas emissions when burned, and its production is renewable – from primary sources through thermochemical, electrochemical, and biological conversion routes. Hence, it is an ideal way to support a low-carbon economy with a green and sustainable energy source. Based on the current usage statistics, it is projected to have a

massive hydrogen demand in the coming years, and this calls for massive development of energy efficient and effective technologies for hydrogen production, storage, and transportation systems.

Liquid hydrogen, among the hydrogen storage systems (compression, liquefaction, adsorption, hydrides and reformed fuels), is highly regarded as the most feasible method for storage and distribution due to its high gravimetric and volumetric energy densities, and high purity [47, 48]. Its demand is on the rise as it is a viable option for various hydrogen applications, such as electric vehicles, aerospace, fuel-based power generators etc. However, the process of liquefying hydrogen is energy-intensive, and it wastes about one third of the hydrogen's energy, rendering it largely uneconomical. Besides, the low liquid hydrogen temperature is another challenge that requires to be addressed appropriately and adequately, further raised in ref.[48]. This leads to the urgent call for high energy efficiency in hydrogen liquefaction processes.

And this is where emerging magnetocaloric refrigeration technology can be very useful for hydrogen liquefaction. In contrast to traditional cooling methods, magnetic refrigeration based on MCE uses a solid magnetic material as the refrigerant and a magnet to take the place of the compressor to achieve the low temperature range required for hydrogen liquefaction. This will enable its incorporation into industrial hydrogen liquefaction to greatly benefit from the advantages of MCE – environmentally friendliness and energy efficiency. The design and development of materials and prototypes, of which the former is the first roadblock to overcome, are all that is needed to bring this idea into reality. As the magnetocaloric materials falling within this target cryogenic temperature range (100 K and below) with solid performance tend to be primarily based on lanthanide metals, generally referred to as RE elements in related literature, a key component for the advance of this technology is material criticality (which we will further discuss in this chapter). One key issue with material design is the balance between performance, material criticality, supply risks, and economic importance, as we struggle to keep up with the rapid pace of advanced technology while keeping a sustainable modern way of life.

Though there is a wide library of diverse magnetocaloric materials found and reported, many of them are for room temperature applications. As for those for cryogenic applications, the common tendency is to associate compositions with lanthanides. However, large MCE values in pure RE elements were not achieved in the early years, and this includes Pr, Nd Er, and Tm [4] despite their high intrinsic magnetic properties at low temperatures. This is due to their antiferromagnetic and ferrimagnetic phases where much of their entropy is involved with flipping their spins to ferromagnetic alignment instead. While many intermetallic compounds containing lanthanide metals exhibit large MCE in this target temperature range, many of them also pose a significant economic risk and may not perform well enough to be considered promising candidates.

Published in Handbook on the Physics and Chemistry of Rare Earths, Volume 64 (2023) Pages 175-246
https://doi.org/10.1016/bs.hpcre.2023.10.004

Unlike other authoritative reviews related to MCE (fundamental concepts and underlying thermodynamic properties, devices and prototypes in ref. [11, 49], composite systems focused on performance optimization in [41], MCE characterization protocols, devices and measurements, and their analysis [11, 50, 51], latest trends in the magnetocaloric materials and analysis in [12, 14] (current), emergent magnetocaloric high-entropy alloys or materials in [13, 46], and more recently, a comprehensive catalog of magnetocaloric materials for cryogenic applications in [52]), in this chapter we focus on RE-containing cryogenic magnetocaloric compounds standing on the shoulders of "*giant* $Gd_5Si_2Ge_2$", i.e., exhibiting MCE values that meet the GMCE threshold, and the assessment of their performance versus criticality. As a result of this approach, high-performance materials are identified from a massive library of literature and their criticality assessment provides insights into potential compositions that balance critical with less critical elements while maintaining high MCE values. Additionally, we include the recent breakthroughs related to FOMT and magnetocalorics: the quantitative criteria to identify FOMT and the critical point of FOMT where it crossovers to SOMT, as well as the directed search strategy for multi-principal elements alloys with FOMT and GMCE. The latter design concept has the potential to balance criticality in significant amounts if it is appropriately applied to design high-performance cryogenic magnetocaloric materials. Furthermore, it is well-regarded to enable a combination of properties with mechanical stability, and this is in line with optimizing the performance of magnetocaloric materials, in terms of tunable criticality and transition temperatures, as well as good mechanical properties.

We will examine the massive magnetocaloric material library in this chapter based on the following material classifications: lanthanide metals, binary lanthanide-metalloid compounds, binary lanthanides-transition metals (non-magnetic and magnetic), ternary intermetallics of lanthanides with metalloids and/or transitional metals, RE oxides, and upcoming alloys with multiple principal elements. An assessment of performance and criticality is then presented, followed by an epilogue and future outlook on designing high-performance magnetocaloric materials with tunable criticality.

2.1 Lanthanide metals

Several lanthanide elements exhibit intrinsic large magnetic moment values as well as different magnetic structures and transitions, making them a popular choice for magnetic investigations, including for magnetocaloric. They were more intensively studied in the past, especially before the breakthrough of GMCE, than they are today for their pure states, as seen in reports on Nd, Gd, Tb, Dy, Ho, Er, and Tm. Their intensive reviews can be found in [9, 53]. In general, their magnetic properties can vary greatly depending on their magnetic crystalline structures, as well as the order of phase transitions and MCE at certain critical magnetic fields and

Published in Handbook on the Physics and Chemistry of Rare Earths, Volume 64 (2023) Pages 175-246
https://doi.org/10.1016/bs.hpcre.2023.10.004

temperature intervals. Their crystals have hexagonal closed-packed (hcp) structures; however, Nd displays double hcp structures with two distinct crystallographic sites [53, 54], resulting in a double MCE peak behavior upon cooling at 19 and 8 K (combination of two caret-shaped peaks located at the ordering temperatures mentioned) [9, 55]. For Tb, Dy and Ho, within the temperature range between T_C and T_N, they exhibit helicoidal antiferromagnetic (HAFM) structures that, at a critical magnetic field (H_{CR}), undergo a field-induced transition into "fan" structures. With increasing magnetic fields above H_{CR}, they reach the full completion of ferromagnetic (FM) ordering. As a result, the MCE arising from the HAFM→fan structure by the magnetic field is of first order at H_{CR} while the fan→FM is of second order. On the other hand, the magnetic structure of Er is more complicated: in decreasing temperatures from 85 to <18 K, it displays a longitudinal spin wave along the c-axis, transforming into a cycloid in which the spin wave was superimposed on a basal plane spiral structure, and finally into a FM cone (conical phase) with the *c*-axis FM ordered and the basal planes retaining the spiral ordering. During the AFM-FM transformation of Tm, its longitudinal spin wave phase changes into a FM structure involving four basal plane layers with magnetic moments parallel to *c*-axis, followed by three layers whose moments aligned antiparallel.

Among earlier MCE reports, only Gd stood out as the best magnetic refrigerant out of the seven pure lanthanide metals though Tb→Tm exhibits FOMT at certain temperature intervals and at magnetic fields below H_{CR}, due to their magnetic structure complexity. As an example, the MCE of Dy presented in **Figure 3 (A)** illustrates its different MCE behavior below and above H_{CR}[56]. It was highlighted in [4] that the low MCE values in these metals could be due to loss in entropy as the spins flip from AFM to FM alignment. Only recently, Ho has demonstrated the ability to induce a significant MCE for cryogenic applications using only low magnetic fields, as shown in **Figure 3 (B)**. This is due to the metamagnetic phase transition arising from the magnetic structure change at various temperatures occurring within a narrow field region. Hence, at the metamagnetic transition field (H_{CR}), the isothermal entropy change varies significantly as seen in **Figure 3 (C)**, while away from it, it remains constant. Authors reported a maximum $\Delta S_{isothermal}$ of −10 J $kg^{-1}K^{-1}$ ($\mu_0 H$ = 2 T), which can be deemed as GMCE (Gd has about −5 J $kg^{-1}K^{-1}$ for the same magnetic field change).

Published in Handbook on the Physics and Chemistry of Rare Earths, Volume 64 (2023) Pages 175-246
https://doi.org/10.1016/bs.hpcre.2023.10.004

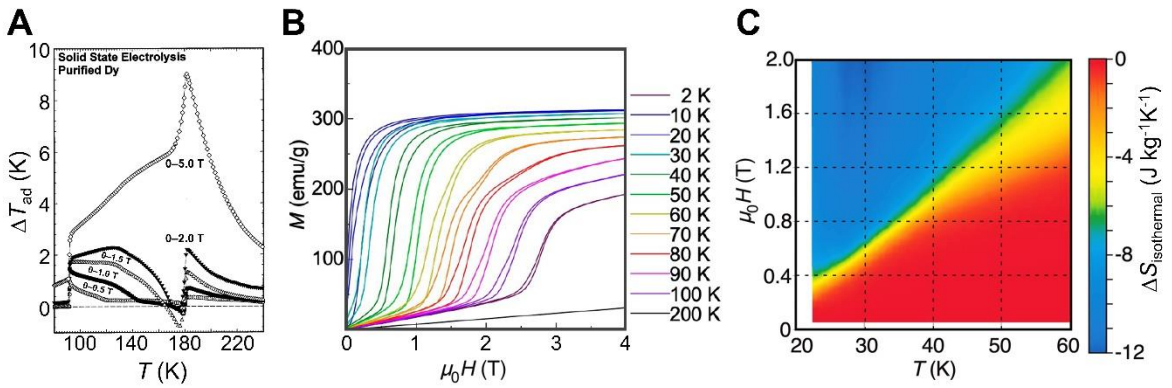

Figure 3. (A) Magnetocaloric reports on dysprosium from ref.[56]. Recent investigations of Ho single crystal: (b) its isothermal magnetization curves with the application of magnetic field along the hexagonal $[10\bar{1}0]$ direction, and **(C)** corresponding isothermal entropy change. *Figure **(A)** is reproduced with permission from K.A. Gschneidner, V.K. Pecharsky, The influence of magnetic field on the thermal properties of solids, Mat. Sci. Eng. a-Struct. 287 (2) (2000) 301–310, © (2000) Elsevier [56]. Figures **(B)** and **(C)** are reproduced from N. Terada, H. Mamiya, High-efficiency magnetic refrigeration using holmium, Nat. Commun. **12**(1), , 1212, © (2021) [57], licensed under an open access Creative Commons Attribution 4.0 International License.*

There were early works on introduction of RE alloying additions to Gd, Tb, Dy, and Er, which typically lowers the magnetic ordering temperatures. These intra-lanthanide compositions include Gd-RE (where RE = Tb, Dy, Ho, Er or Y), Gd-RE(1)-RE(2) (where RE(1)= Tb or Dy, and RE(2)=Nd), Tb-RE (RE = Dy, Y), Er-RE (RE = La, Pr). Their reports were as early as 1979 and largely discussed in many early review papers. As there are no further breakthroughs (i.e., MCE values that can be considered as large as GMCE) or recent reports, the MCE of early studied intra-lanthanides will not be further elaborated here; readers can refer to refs. [9, 53, 58] for further information.

2.2 Binary lanthanides-metalloid-based compounds

As we move away from compositions that only contain lanthanides, we will find the notable group composed of RE alloyed with metalloids, as in $Gd_5Si_2Ge_2$, the big-bang material crowned with the "GMCE" appellative.

Metalloids are referred to elements that combine both characteristics or exhibit characteristics that fall in between those of metals and nonmetals. The common ones alloyed to RE elements for MCE studies include B, Si, Ge, As and Sb. Alloying metalloids to RE can bring upon various types of magnetic ordering as well as thermomagnetic phase transitions. For instance, by changing the Si:Ge ratio in the $Gd_5Si_2Ge_2$ compound within a specific range, it can induce FOMT and reversible structural transition with essential change in the lattice parameters and thereby optimize the MCE values. In this section, we mainly focus on RE germanides, silicides, and

antimonides and highlight those compositions that meet the GMCE threshold while a separate section on magnetocaloric RE borides is covered in **Section 2.5**.

Figure 4 (A) shows the MCE performance of RE-metalloids, where it can be noticed that the $RE_5(Si_xGe_{1-x})_4$ pseudobinary alloys dominate and prioritize the compliance region for GMCE. Many of the studies examined on this system are reported with magnetic fields as high as 5 T, but as permanent magnets can only reach up to 2 T, we will keep our performance evaluation on MCE values at 2 T. Furthermore, this can efficiently identify compounds with performance that meet the GMCE threshold without requiring large magnetic fields. The $RE_5(Si_xGe_{1-x})_4$ phases result in a wide range of solid solutions, and **Figure 4 (B)** (taken from ref. [59]) summarizes the current understanding of their formation and crystal structures (at room temperature) for all RE. It should be noted that Pm (not studied) and Eu (does not exist in silicide or germanide at the 5:4 stoichiometry) are the exceptions. The $RE_5(Si_xGe_{1-x})_4$ family, stemming from the GMCE breakthrough reported in ref. [3], exhibits a complex interplay between their magnetic and crystallographic properties, depending largely on their compositions and preparation methods. For the $Gd_5(Si_xGe_{1-x})_4$ pseudobinary system, binary Gd_5Si_4 has orthorhombic Gd_5Si_4-type structure while binary Gd_5Ge_4 exhibits orthorhombic Sm_5Ge_4-type as shown as O(I)-Gd_5Si_4 and O(II)-Sm_5Ge_4 structures in **Figure 4 (C)**. As for $Gd_5Si_2Ge_2$ that started the GMCE appellation, it undergoes a magnetostructural transformation from O(I) to a monoclinic structure (M-$Gd_5Si_2Ge_2$ structure in **Figure 4 (C)**). Apart from the space group (SG) symmetry, their main characteristic that differentiates them in their distinctive slab structures is whether there are interslab Ge-Ge bonds [60]. Despite that their phase diagram as shown in **Figure 4 (D)** (taken from ref.[60]) clearly illustrates a strong compositional dependence on the magnetic ordering temperatures for varying Si content, it is still important to note that GMCE can also be produced in $Gd_5Si_xGe_{4-x}$ compositions other than x=2. However, in Si-rich compositions, which exhibit the highest magnetic ordering temperatures, the MCE values are moderate compared to the GMCE magnitude. A topical and comprehensive review discussing their composition-crystallography-property relationship as well as the magnetostructural transformation kinetics can be found in another dedicated chapter in volume 44 of this handbook series [59]. An extensive MCE review published later includes summaries of the transition temperatures reported for this system [11]. In the following, we discuss those compositions, other than the giant $Gd_5Si_2Ge_2$ of ref. [3], prioritizing the GMCE-compliant region shown in **Figure 4 (A)**.

Published in Handbook on the Physics and Chemistry of Rare Earths, Volume 64 (2023) Pages 175-246
https://doi.org/10.1016/bs.hpcre.2023.10.004

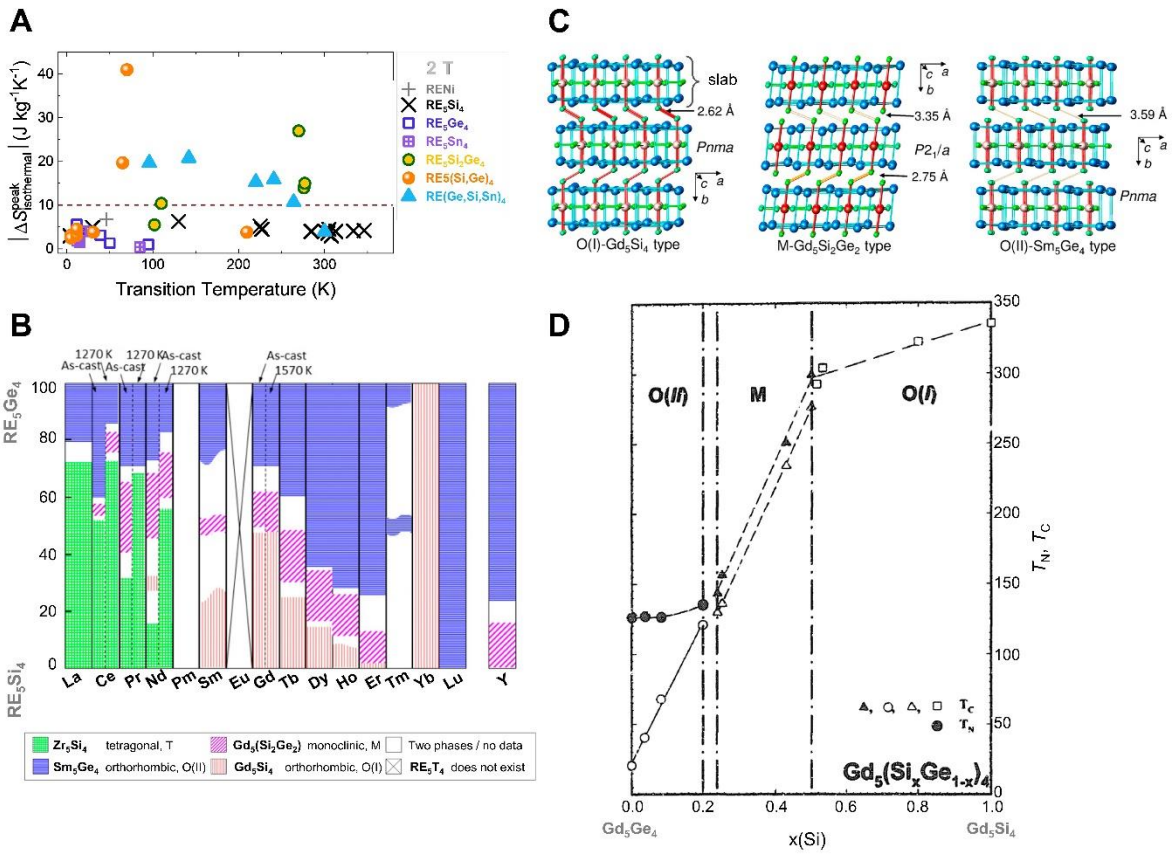

Figure 4. (A) MCE comparison of several families of RE-metalloids for 2 T shows those that fall in the GMCE threshold are mainly $RE_5(Si,Ge)_4$ compositions that could form a wide variety of crystal structures (at room temperature) depending on their RE **(B)**. The main crystal structures of $Gd_5(Si_xGe_{1-x})_4$ are further presented in panel **(C)** and the magnetic phase diagram of its pseudobinary system in panel **(D)**. Data in panel **(A)** are taken from [3, 8, 61-74]. *Figures in panels **(B)** and **(C)** are reproduced with permission from Y. Mudryk, V.K. Pecharsky, K.A. Gschneidner, Chapter 262—R5T4 Compounds: an extraordinary versatile model system for the solid state science, in: Handbook on the Physics and Chemistry of Rare Earths, Elsevier, 44 (2014) 283–449* [59]. *https://doi.org/10.1016/B978-0-444-62711-7.00262-0, © (2004) Elsevier. Figure **(D)** with permission from V.K. Pecharsky, K.A. Gschneidner, Phase relationships and crystallography in the pseudobinary system Gd_5Si_4 - Gd_5Ge_4, J. Alloy. Compd. 260 (1) (1997) 98–106,* © (1997) Elsevier [60].

Within the $Gd_5(Si_xGe_{1-x})_4$ pseudobinary system, one particularly intriguing feature is the observation of GMCE plateau spanning up to ~20 K for magnetic fields above 2 T, while also providing very impressive GMCE values at 2 T. The observed spikes could arise from measurement artifacts but the constant plateau $\Delta S_{isothermal}$ values evidently meet the GMCE threshold in the temperature range from ~70 to ~90 K [67]. This is remarkable since MCE values arising from FOMT usually suffer from narrow temperature spans. The wide temperature span was found for Ge-rich compositions described in refs. [67, 75, 76]. Another

system, $Dy_5(Si_xGe_{1-x})_4$, was also found displaying great MCE that meets the GMCE threshold: for x=0.75, maximum $\Delta S_{isothermal}$ = -19.7 J $kg^{-1}K^{-1}$ (2 T) with transition temperatures of 65 K [62]. These MCE results are presented in **Figure 5**. It was found to have a monoclinic crystal structure, similar to that of M-$Gd_5Si_2Ge_2$. Other $RE_5Si_2Ge_2$ data points observed in the GMCE-compliant region correspond to RE=Gd that had undergone appropriate heat treatment to optimize their GMCE values: from -15 (as arc-melted) to -27 J $kg^{-1}K^{-1}$ (annealed at 1570 K for 1 h) for 2 T [3].

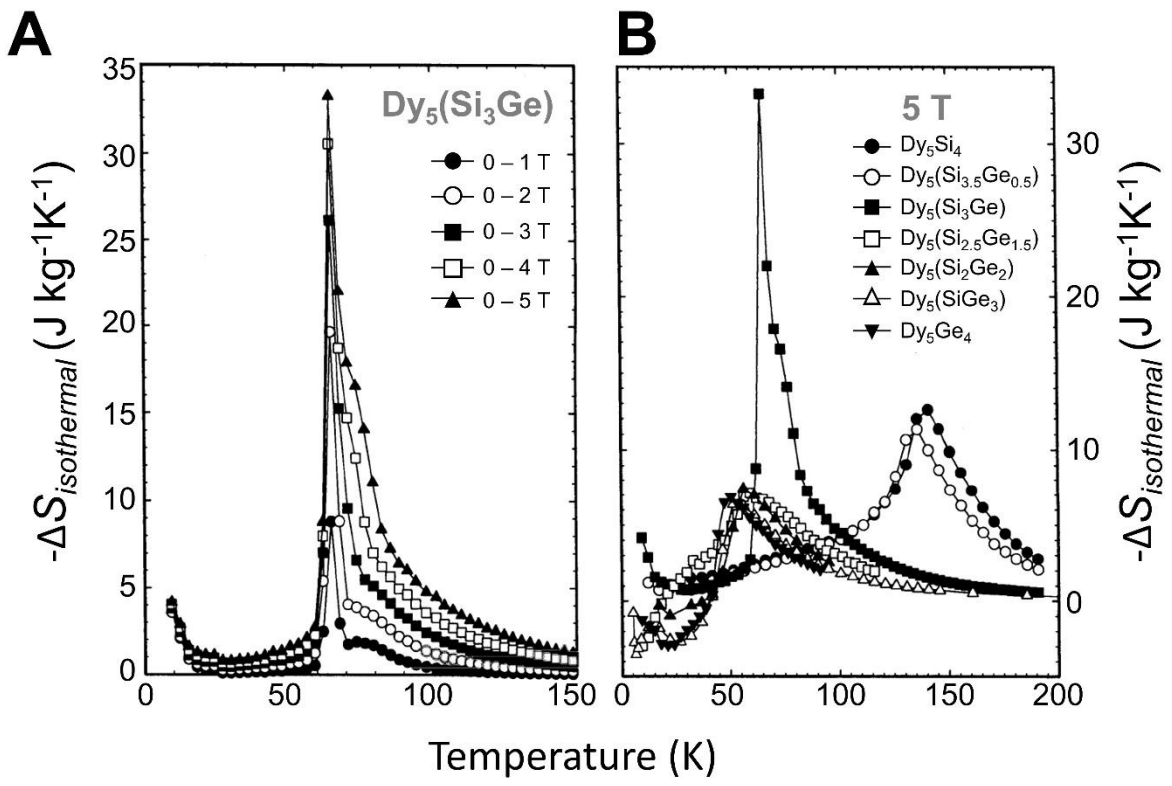

Figure 5. Temperature dependence of isothermal entropy change curves of **(A)** $Dy_5(Si_3Ge)$ and **(B)** $Dy_5(Si_xGe_{1-x})_4$ pseudobinary systems. *Reproduced with permission from V.V. Ivtchenko, V.K. Pecharsky, K.A. Gschneidner, Magnetothermal properties of $Dy_5(Si_xGe_{1-x})_4$ alloys, in: Advances in Cryogenic Engineering Materials, vol. 46, Part A, Springer US, 2000, pp. 405–412. https://doi.org/10.1007/978-1-4615-4293-3_52* [62].

Other remarkable RE-metalloids compounds include as-cast $Gd_5Ge_2Si_{2-x}Sn_x$: -10.7, -15.9, -15.3, -20.8, and -19.7 J $kg^{-1}K^{-1}$ for x = 0.1, 0.2, 0.4, 1.0 and 1.5, respectively, for 2 T [73] as shown in **Figure 6 (A)**. These compositions stemmed from the GMCE motivation reported in Gd_5Sn_4 [66]. Its ^{119}Sn Mössbauer spectroscopy results confirmed that it underwent a FOMT at 82 K, presenting GMCE values even for very low magnetic fields, as shown in **Figure 6 (B)**.

Published in Handbook on the Physics and Chemistry of Rare Earths, Volume 64 (2023) Pages 175-246
https://doi.org/10.1016/bs.hpcre.2023.10.004

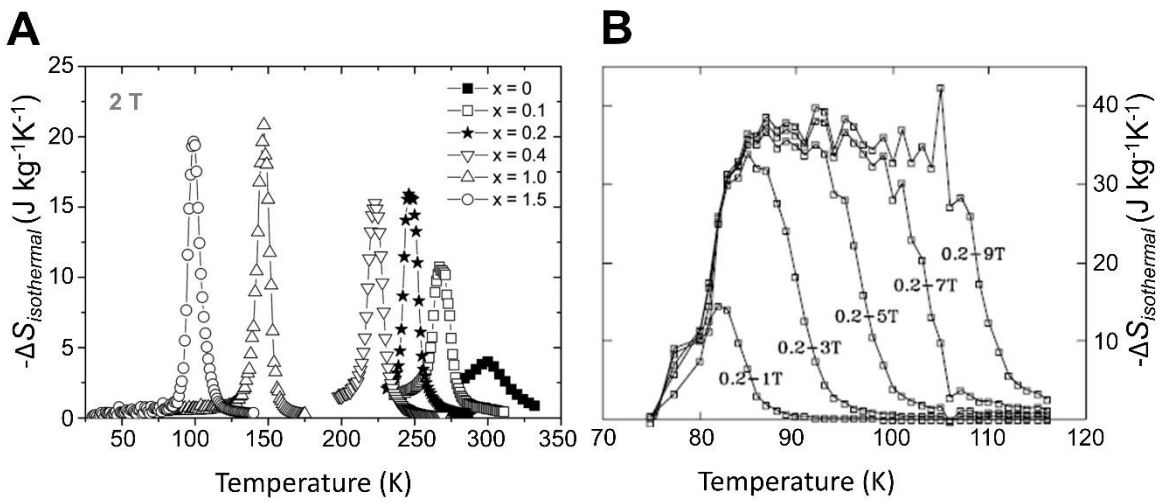

Figure 6. Temperature dependence of isothermal entropy change curves of **(A)** $Gd_5Ge_2Si_{2-x}Sn_x$ and **(B)** Gd_5Sn_4 systems. *Figure **(A)** is reproduced with permission from A.M.G. Carvalho, J.C.G. Tedesco, M.J.M. Pires, M.E. Soffner, A.O. Guimaraes, A.M. Mansanares, A.A. Coelho, Large magnetocaloric effect and refrigerant capacity near room temperature in as-cast $Gd_5Ge_2Si_{2-x}Sn_x$ compounds, Appl. Phys. Lett. **102**(19), 192410, © (2013) [73]. Figure **(B)** is reproduced with permission from D.H. Ryan, M. Elouneg-Jamroz, J. van Lierop, Z. Altounian, H.B. Wang, Field and temperature induced magnetic transition in Gd_5Sn_4: a giant magnetocaloric material, Phys Rev Lett **90**(11), 117202 (2003) [66]. © 2003 by the American Physical Society*.

2.3 Binary lanthanides-transition metal compounds

Besides metalloid additions to RE alloys, transition metals (TM) alloyed with lanthanides form another large group of magnetocaloric materials as well. They may come in the following stoichiometric compositions: RETM, $RETM_2$, RE_3TM, RE_3TM_2, and $RETM_5$, including those that are less common, such as RE_5TM_4, RE_2TM_7, or RE_7TM_{12}. Hence, in view of the wide and diverse range of stoichiometric compositions reported, we will focus on those meeting the GMCE threshold in the following order: RE with nonmagnetic TM, followed by RE with *3d* transition metal elements.

2.3.1 RE-non-magnetic TM

Magnetocaloric studies usually use nonmagnetic TM elements, such as Cu, Rh, Pd, Ag, Zn, Al, Ga, or In (including post-transition metals as well), combined with RE elements. As seen from their MCE performance for 2 T depicted in **Figure 7 (A)**, the top performers in the GMCE-compliant region are RE_2In, RE_3Ru, $REAl_2$, REGa, REZn, RERh, RE_3Rh_2, REAl and RE_7Pd_3.

Published in Handbook on the Physics and Chemistry of Rare Earths, Volume 64 (2023) Pages 175-246
https://doi.org/10.1016/bs.hpcre.2023.10.004

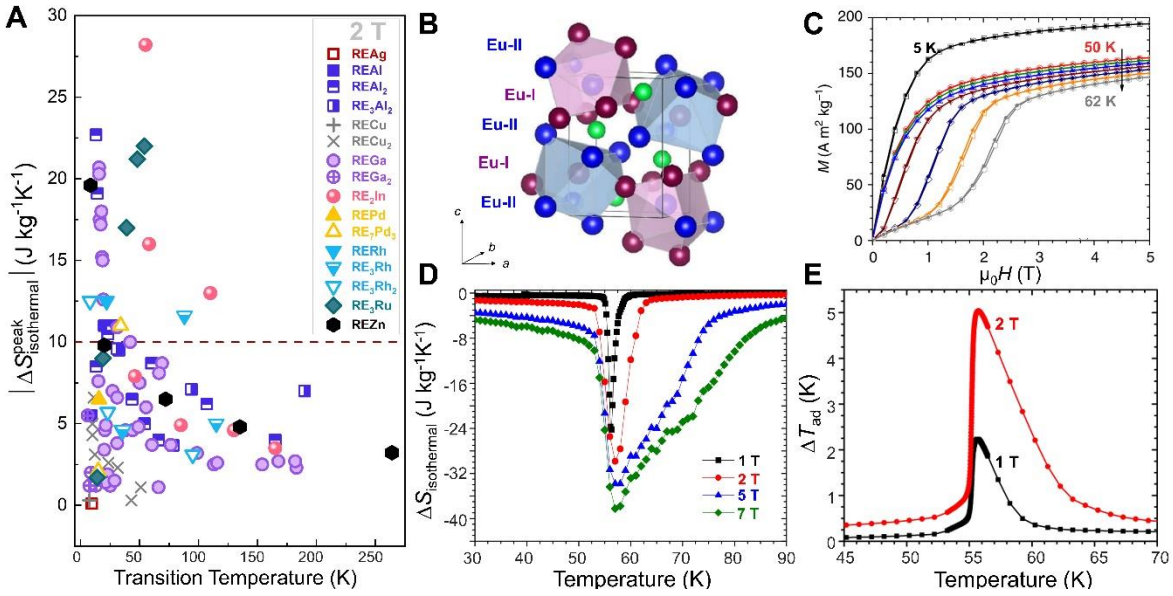

Figure 7. (A) MCE comparison of several families of RE-non-magnetic TM for 2 T. Eu_2In, **(B)** crystallizing in orthorhombic Co_2Si-type structure, emerges as the best performer in the GMCE-compliant region, and is weakly hysteretic (thermal hysteresis ~0.07 K from the magnetization measurements shown in **(C)**). Their excellent MCE can be observed from their temperature dependence of **(D)** isothermal entropy change and **(E)** adiabatic temperature change. Data in panel **(A)** are taken from [16, 19, 20, 25, 27, 77-119]. *Images **(B)** – **(E)** are reproduced from F. Guillou, A.K. Pathak, D. Paudyal, Y. Mudryk, F. Wilhelm, A. Rogalev, V.K. Pecharsky, Non-hysteretic first-order phase transition with large latent heat and giant low-field magnetocaloric effect, Nat. Commun. **9** (1) (2018) 2925 [20], licensed under an open access Creative Commons Attribution 4.0 International License.*

Among the RE_2In compounds, RE=Eu emerges with the largest MCE. **Figure 7 (B)** shows its orthorhombic Co_2Si-type structure (SG *Pnma*) as well as weak thermal hysteresis (~0.07 K from the magnetization measurements) [20]. It undergoes a FOMT at 55 K with very large MCE values of -28.2 J $kg^{-1}K^{-1}$ and 5 K, both for 2 T (presented in **Figure 7 (C)** and **(D)**). Compositions with RE = Pr, Nd, Tb, Dy, Ho and Er are also investigated for MCE, where those undergoing SOMT, such as RE = Tb, Dy, Ho and Er, do not meet the GMCE threshold. Before the discovery of Eu_2In, the MCE of RE_2In compounds with RE = Tb, Dy, Ho, and Er were already reported (their T_C = 165 [117], 130 [116], 85 [115] and 46 K [120], respectively). It is till the GMCE found in Eu_2In that led to further investigations on the RE_2In family in the opposite direction along the lanthanide row in the periodic table. In general, all RE_2In exhibit the hexagonal Ni_2-type crystal structure (SG $P6_3/mmc$), except for RE = Eu and Yb [121]. It is surprising to find GMCE values with RE = Pr, Nd and Eu in the RE_2In family, especially since Pr_2In and Nd_2In have a different structure from Eu_2In. The GMCE found in Pr_2In undergoing FOMT are: for 2 T, -15 J $kg^{-1}K^{-1}$ (T_C = 57 K) [19]; -16 J $kg^{-1}K^{-1}$ (T_C = 57 K) [122]. Additionally, Nd_2In exhibits a GMCE value of -13 J $kg^{-1}K^{-1}$ (2 T) at T_C = 110 K [16]. It is noteworthy that there is a discrepancy in the order of the thermomagnetic phase transition experienced by this compound. While ref.[16] suggests

it is a borderline case between FOMT and SOMT, ref.[118] indicates that it undergoes a FOMT (it should be noted that the latter reports a smaller MCE value: for 2 T, -7.42 J $kg^{-1}K^{-1}$ at T_C = 109 K).

Next on the list that falls in the GMCE-compliant region is the $REAl_2$ family. These Laves phase compounds have a cubic $MgCu_2$-type structure. The largest MCE reported among the binary $REAl_2$ family is found for $ErAl_2$: maximum $\Delta S_{isothermal}$ values for 2 T are approximately -19.1 [94] and -22.7 J $kg^{-1}K^{-1}$ [119] at T_C = 14 and 13 K, respectively. Note that these values were taken from the arc-melted states in the two reports. Therefore, the discrepancy could arise from the different protocols taken to prepare the samples. The MCE results of $REAl_2$ series with RE= Gd, Tb, Dy, Ho and Er from [119] are further presented in **Figure 8 (A)** and **(B)**. A further melt-spinning step of the sample in ref.[94] results in approximately -15.1 J $kg^{-1}K^{-1}$ (2 T) at T_C = 10 K. Ref.[95] reports the use of light RE elements in $REAl_2$ for magnetocaloric hydrogen liquefaction, in which the largest value obtained for $Pr_{0.75}Ce_{0.25}Al_2$ meets the GMCE threshold: -10.48 J kg^{-1} K^{-1} (2 T) at T_C = 23 K. Its MCE results are shown in **Figure 8 (C)** and **(D)**. Another candidate of this family of compounds falling in the GMCE threshold is reported for $HoAl_2$: -11 J $kg^{-1}K^{-1}$ (2 T) at T_C = 26 K [119].

Published in Handbook on the Physics and Chemistry of Rare Earths, Volume 64 (2023) Pages 175-246
https://doi.org/10.1016/bs.hpcre.2023.10.004

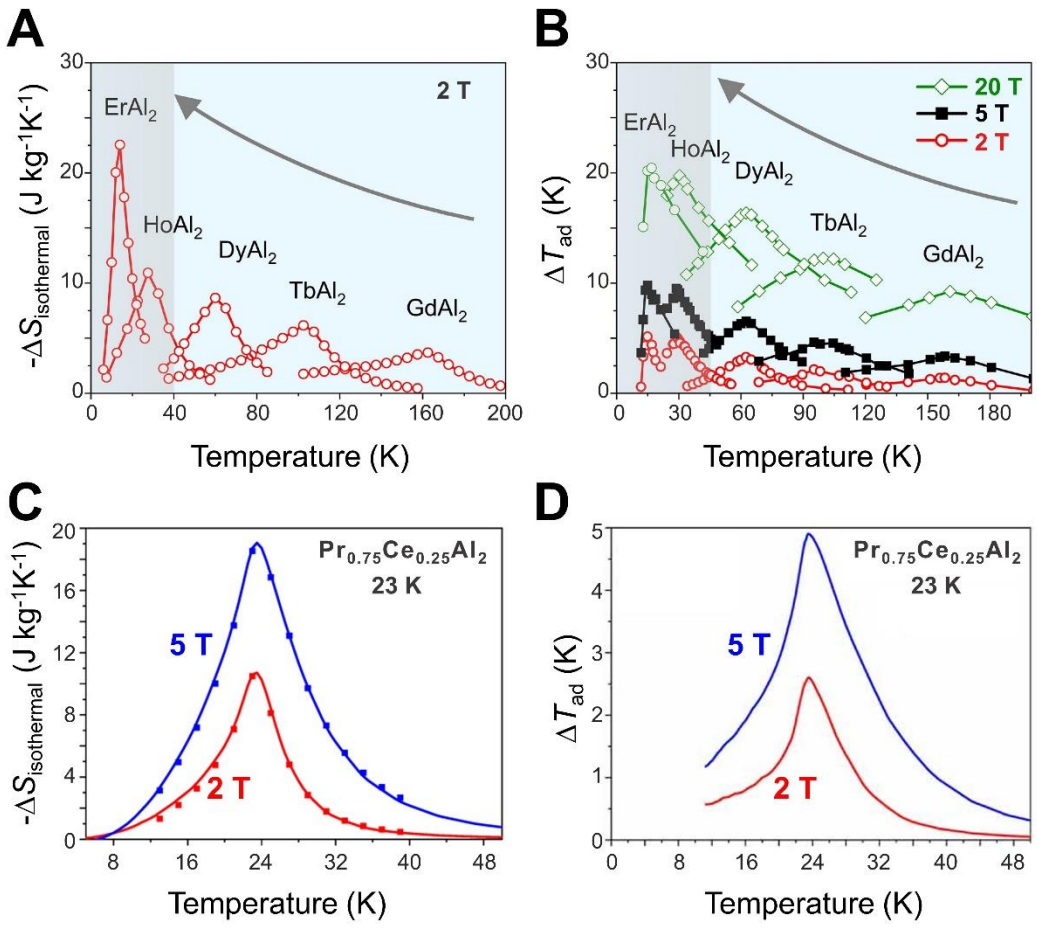

Figure 8. MCE of binary $REAl_2$ series: temperature dependence of **(A)** $\Delta S_{isothermal}$ and **(B)** ΔT_{ad}. The MCE results of $Pr_{0.75}Ce_{0.25}Al_2$ compound: temperature dependence of **(C)** $\Delta S_{isothermal}$ and **(D)** ΔT_{ad}. *Images **(A)** and **(B)** are reproduced with permission from W. Liu, E. Bykov, S. Taskaev, M. Bogush, V. Khovaylo, N. Fortunato, et al., A study on rare-earth Laves phases for magnetocaloric liquefaction of hydrogen, Appl. Mater. Today **29** (2022) 101624, © (2022) Elsevier [119]. Images **(C)** and **(D)** are reproduced from W. Liu, T. Gottschall, F. Scheibel, E. Bykov, N. Fortunato, A. Aubert, et al., Designing magnetocaloric materials for hydrogen liquefaction with light rare-earth Laves phases, J. Phys. Energy **5** (3) (2023) 034001 [95], licensed under an open access Creative Commons Attribution 4.0 license.*

Moving on to the next item on the list, we have the RE_3Ru family. However, there is still a lack of systematic studies on its potential use for magnetocaloric applications. Despite this, there are some encouraging examples, such as Gd_3Ru, which has a T_C = 54 K and exhibits an impressive MCE of -22 J $kg^{-1}K^{-1}$ (2 T) [25]. Their solid solutions, which involve using RE = Er, can adjust the T_C to lower temperatures while still meeting the GMCE threshold values up to x = 0.3 in $Gd_{3-x}Er_xRu$, as shown in **Figure 9 (A)** [100]. The crystal structure of these compounds is orthorhombic Fe_3C-type (SG *Pnma*), which is also reported for the RE_3Rh family. Among them, Tb_3Rh exhibits MCE that meets the GMCE threshold: -11.6 J $kg^{-1}K^{-1}$ (2 T) at ordering temperature of 88 K [27]. Together with another report [123], both works indicate that this

Published in Handbook on the Physics and Chemistry of Rare Earths, Volume 64 (2023) Pages 175-246
https://doi.org/10.1016/bs.hpcre.2023.10.004

compound undergoes FOMT (but the latter shows lower MCE values). Though Tb_3Ru [123], Ho_3Ru [101], and Ho_3Rh [101] are studied, their reported MCE values do not fulfill the GMCE threshold.

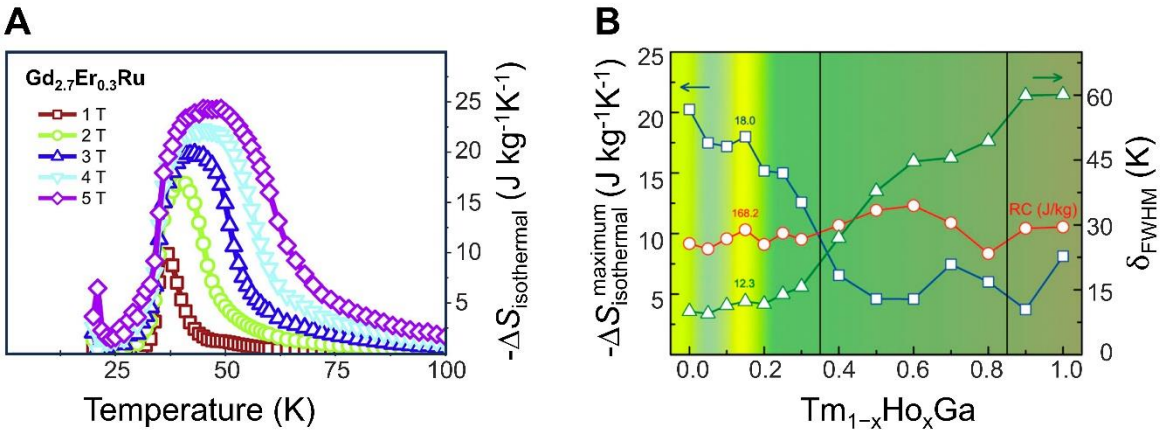

Figure 9. (A) The MCE of $Gd_{2.7}Er_{0.3}Ru$ fulfills the GMCE threshold. **(B)** The MCE parameters of $Tm_{1-x}Ho_xGa$ for 2 T: maximum $\Delta S_{isothermal}$, refrigerant capacity (RC) and temperature span at full-width half maximum. *Image **(A)** is reproduced with permission from J.C.B. Monteiro, F.G. Gandra, Magnetocaloric properties of $(Gd_{1-x}Er_x)_3Ru$ alloys and their composites, J. Alloy. Compd. **803** (2019) 1178–1183, © (2019) Elsevier [100]. Image **(B)** is reproduced with permission from S.X. Yang, X.Q. Zheng, W.Y. Yang, J.W. Xu, J. Liu, L. Xi, et al., Tunable magnetic properties and magnetocaloric effect of TmGa by Ho substitution, Phys. Rev. B **102** (17) (2020) 174441 [111]. © 2020 by the American Physical Society.*

Next on the list is the REGa family, in which those compositions consisting of RE = Nd, Tm, and Er, have the potential to produce high MCE values that are within the GMCE-compliant region. NdGa exhibits spin-reorientation (SR) transition temperature (T_{SR}) of 20 K and a T_C = 42 K, where the MCE that meets the GMCE threshold is found at the T_C: -10 J $kg^{-1}K^{-1}$ (2 T) [114]. TmGa was reported to show two successive transitions: FM-AFM at 12 K followed by AFM-PM at 15 K [110]. With increasing magnetic field, its behavior becomes FM-PM, and the MCE peaks broaden toward higher temperatures. Their low-field MCE values meet the GMCE threshold: for 2 T, maximum $\Delta S_{isothermal}$ and ΔT_{ad} values are -20.7 J $kg^{-1}K^{-1}$ and 5 K at 14.5 K. Another study that replaces Ho for Tm in $Tm_{1-x}Ho_xGa$ discovers MCE values that satisfy the GMCE-compliant region for x≤0.3 (as shown in **Figure 9 (B)**) [111]. While MCE decreases with Ho content, the two MCE peaks become more obvious with increasing Ho content even with selectively shown curves. The GMCE threshold can be reached with x ≤ 0.3: - 12.6 J $kg^{-1}K^{-1}$ (2 T) for x = 0.3 (note that the MCE curves were not presented in the report; these values are taken from the tabulated results). For ErGa, it exhibits dual MCE peaks, with a T_{SR} around 15 K and a FM-PM at T_C = 30 K: around -7.6 and -10.9 J $kg^{-1}K^{-1}$ (2 T) based on their magnetization data [106]. In general, binary REGa compounds and their solid solutions crystallize within the orthorhombic

CrB-type structure (SG *Cmcm*), and undergo two magnetic transitions, leading to reports on T_{SR} and T_C. In the order of RE = Gd, Tb, Dy, Ho and Er, T_C decreases with the increase in the atomic number of the RE elements, while the trend of T_{SR} is not as clear cut. Further details are provided in [124], which contains a comprehensive review of structures, transition temperatures, magnetic properties, and MCE of this family of compounds.

Another equiatomic binary RE-nonmagnetic TM compound found with MCE that fulfills the GMCE threshold is TmZn. It forms a cubic CsCl-type structure (SG $Pm\bar{3}m$) and is found exhibiting T_C = 8.4 K [79]. The authors observed a field-induced metamagnetic transition in the isothermal magnetization data over a wide temperature range, which led them to deduce that TmZn undergoes FOMT at temperatures above 8 K. They have suggested that the compound is likely an itinerant electron metamagnetic (IEM) material belonging to Zn-based intermetallic compounds. Despite the impressive MCE of -19.6 J kg^{-1}K^{-1} (2 T), there are no similar reports for other REZn [82, 83] or other isostructural compounds, such as TmCu or TmAg [77]. A theoretical report, however, did find remarkable MCE values predicted for HoZn and ErZn [78] though not found in the experimental reports [80, 81, 84].

An isostructural equiatomic binary compound whose MCE also fulfills the GMCE threshold is found in GdRh. It is interesting to note that its MCE report [85] was specifically targeted to the Gd_5Rh_4 system owing to its Gd_5Si_4-type structure, and a minor impurity phase was detected as GdRh. Nevertheless, the researchers carried out a comprehensive investigation of both compounds and unearthed that GdRh, which exists as a minor impurity in Gd_5Rh_4 samples, crystallizes in the CsCl-type structure (SG $Pm\bar{3}m$) and exhibits a MCE value of -12.5 J kg^{-1}K^{-1} (2 T) at T_C = 22 K, satisfying the GMCE threshold.

There are also RE_3TM_2 intermetallic compounds that contain non-magnetic TM elements and still exhibit MCE values within the GMCE-compliant region. One example of such a compound is Er_3Rh_2. Depending on the RE selection, two crystal structures of RE_3TM_2 family were reported: rhombohedral Er_3Ni_2-type structure (SG $R\bar{3}$) for RE = La – Nd [125], tetragonal Y_3Rh_2-type crystal structure (SG $I4/mcm$) for RE = Gd – Er and Y [126]. Their MCE investigations are scarce, but ref. [87] provides information on the RE = Nd, Ho, and Er systems. The authors found that the MCE of these compounds are of the SOMT nature, with Nd_3Rh_2 having the lowest value. Er_3Rh_2 is the only one that meets the GMCE threshold, with a value of -12.5 J kg^{-1}K^{-1} (2 T) at T_C = 8 K.

Other RE intermetallics with nonmagnetic TM elements whose MCE fulfills the GMCE threshold are found in: HoAl (orthorhombic DyAl-type structure with SG *Pbcm*) with a maximum $\Delta S_{isothermal}$ of -11 J kg^{-1}K^{-1} (2 T) at T_C = 20 K [89], and Nd_7Pd_3 whose maximum $\Delta S_{isothermal}$ is -11 J kg^{-1}K^{-1} (2 T) at T_C = 34 K [98].

Published in Handbook on the Physics and Chemistry of Rare Earths, Volume 64 (2023) Pages 175-246
https://doi.org/10.1016/bs.hpcre.2023.10.004

2.3.2 RE-magnetic TM

The MCE performance of RE-magnetic TM for 2 T is depicted in **Figure 10 (A)**, with most $RECo_2$ compounds emerging as the top performers, followed by RENi, $RENi_2$, $REMn_2$, RE_3Co, and RE_3Ni_2. Another family that dominates the GMCE-compliant region is $RE(Fe,Si)_{13}$, which has a wide range of tunable transition temperatures due to its diverse composition (as shown in **Figure 10 (B)**). In this section, we will start with the binary RE-magnetic TM compounds that meet the GMCE threshold, then move on to $RE(Fe,Si)_{13}$, which, while a TM-based compound, is a highly regarded magnetocaloric material to date.

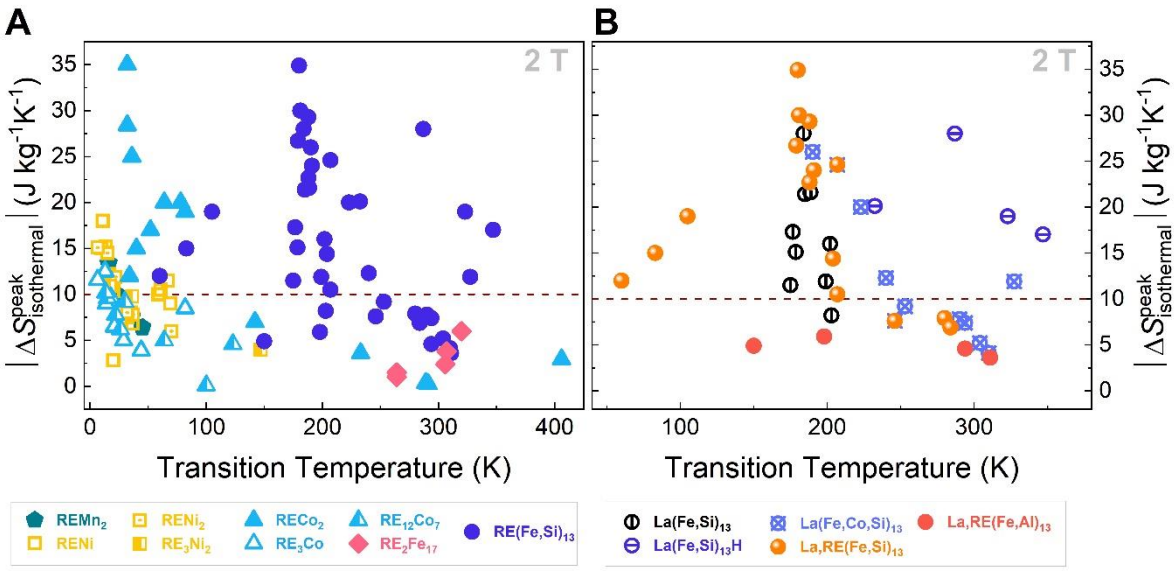

Figure 10. (A) MCE comparison of several families of RE-magnetic TM for 2 T shows that $RE(Fe,Si)_{13}$ family prioritizes the GMCE-compliant region. It can exhibit wide tunable transition temperatures depending on their extensive variety of compositions as magnified in panel **(B)**. *Data for drawing panel **(A)** are taken from [11, 22, 32, 38, 88, 127-163] and those for **(B)** from [11, 32, 38, 160-163].*

2.3.2.1 RE-Co

The $RECo_2$ compounds falling in the GMCE-compliant region are RE=Ho and Er: -19 and -35 J kg^{-1} K^{-1} at 82 and 32 K for 2 T [12, 22, 164]. Later reports found different values whilst fulfilling the GMCE threshold: -20 [145] and -28.4 J kg^{-1} K^{-1} [149] at 78 and 32 K for 2 T. Their $\Delta S_{isothermal}$ curves are presented in **Figure 11** while ΔT_{ad} values reported for 2 T are 2 [53] and ~3.8 K [22] for RE = Ho and Er, respectively. $RECo_2$, in spite of crystallizing within the same crystal structure for all RE (cubic $MgCu_2$-type structure, also commonly referred to as the C15-type or Laves phase), only showed very large MCE values for Ho and Er, while all the other RE elements in this compound family did not. Furthermore, alloying two different rare-earth elements finely tune the transition temperatures [148] while the partial substitution of Co by Ni [143, 145], lowered the transition temperatures.

Published in Handbook on the Physics and Chemistry of Rare Earths, Volume 64 (2023) Pages 175-246
https://doi.org/10.1016/bs.hpcre.2023.10.004

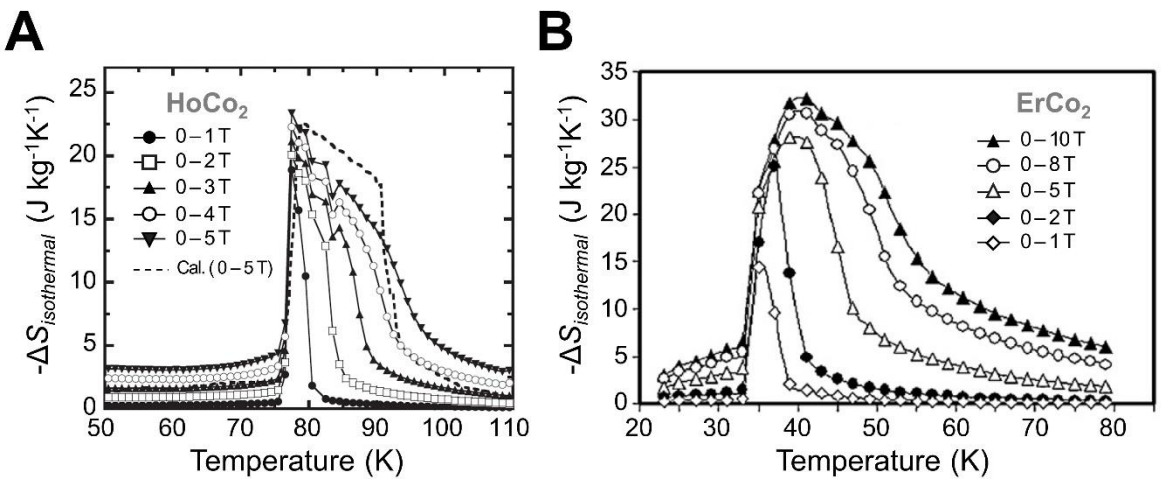

Figure 11. Temperature dependence of isothermal entropy change curves of $RECo_2$ compounds falling in the GMCE-compliant region: RE = **(A)** Ho and **(B)** Er. *Reproduced with permission from T. Tohei, H. Wada, Change in the character of magnetocaloric effect with Ni substitution in $Ho(Co_{1-x}Ni_x)_2$, J. Magn. Magn. Mater.* ***280****(1), 101-107, © (2004) Elsevier [145] and M. Balli, D. Fruchart, D. Gignoux, Magnetic behaviour and experimental study of the magnetocaloric effect in the pseudobinary Laves phase $Er_{1-x}Dy_xCo_2$, J. Alloy Compd* ***509****(9), 3907-3912, © (2011) Elsevier [149].*

One of the mechanisms behind the large MCE values found in $RECo_2$ was linked to the order of thermomagnetic phase transition that they undergo. Earlier works reported that their thermomagnetic transition changes from SOMT for RE = Gd and Tb to FOMT for RE = Dy, Ho, Er. Although it has been an ongoing controversial issue regarding the order of the thermomagnetic phase transition of $TbCo_2$, those looking for a large MCE from FOMT should be aware that it will require coupling both magnetic and structural transitions together. Furthermore, the order of thermomagnetic phase transitions of these compounds cannot be solely determined by the Banerjee´s criterion [165] based on the Arrott plots, which has been found giving erroneous interpretations to other complementary techniques [166]. A more recently discovered quantitative criterion [38] to determine the order of thermomagnetic phase transitions will be covered later in this section. It is not restricted to any model yet could be applicable to evaluate complicated scenarios, such as weak FOMT, minimal hysteresis or concurrent phase transitions.

Among the RE_3Co family, cases where RE= Er and Tm exhibit MCE values fulfilling the GMCE threshold: -12.5 [153] and -11.6 J kg^{-1} K^{-1} [155] (2 T) at 13 and 6.5 K, respectively. This family of compounds, as well as RE_3Ni compositions, exhibit the same crystallographic structure,

orthorhombic Fe_3C-type structure (SG *Pnma*), yet complex magnetic structures with different magnetic phase transitions [124] (between RE=Gd to Tm, T_N= 128 [167] and 4.5 K [155]). RE elements carry the magnetic moment in these systems, while Co acts as non-magnetic element and, at the same time, stabilizes the AFM ordering. Er_3Co, unlike the other compounds in this family, only displays one FM-like transition at 13 K. The others exhibit two consecutive phase transitions caused by different magnetic orderings that occur closely to each other, leading to two peaks or a table-like MCE observed in their data, as in cases with RE=Tb, Dy and Ho [124].

The occupied *f*-orbitals of lanthanides could result in intermetallic formation with unusually high stoichiometric coefficients. The $RE_{12}Co_7$ series is one example of such a case and studied for their MCE. They form a complicated monoclinic $Ho_{12}Co_7$-type structure (SG $P2_1/c$) containing four types of coordination polyhedra for the RE sites [168]. Depending on the RE element, the compounds could undergo one FM-PM transition (for RE = Gd, Tb and Dy) or multiple phase transitions at low temperatures with RE=Ho and Er. However, among them, the one meeting the GMCE threshold is $Er_{12}Co_{17}$: -10.2 J kg^{-1} K^{-1} (2 T) at 13.5 K [159].

2.3.2.2 RE-Ni

Among the RE-Ni compounds, the largest MCE values fulfilling the GMCE threshold are found for the RENi family, where RE=Tb, Dy, and Er: -11.5 [134], -10.5 [133] and -15 J $kg^{-1}K^{-1}$ (2 T) [129] with T_C = 67, 61, 10 K, respectively. The RENi compounds could crystallize within the CrB- (RE = Ce, Pr, Nd, Sm, Gd and Tb) or FeB-type structures (RE = Dy, Ho, Er, Tm and Y). Most of these have been studied for their MCE, with the exception of NdNi and TmNi. **Figure 12 (A)** presents the MCE results of TbNi as an example showcasing the significant MCE of this family. Furthermore, the MCE of the $Ho_xEr_{1-x}Ni$ pseudobinary system meets the GMCE threshold for $x \leq 0.4$ [124].

Published in Handbook on the Physics and Chemistry of Rare Earths, Volume 64 (2023) Pages 175-246
https://doi.org/10.1016/bs.hpcre.2023.10.004

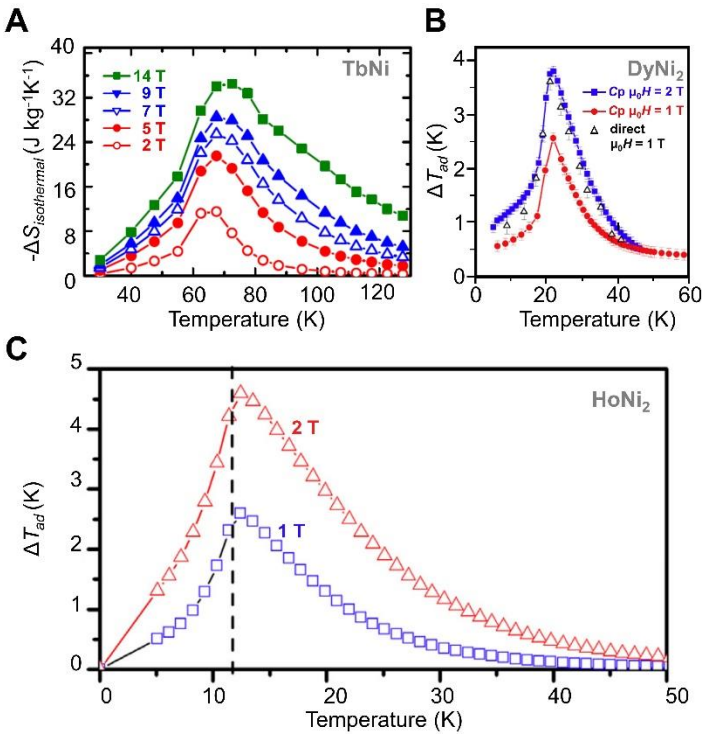

Figure 12. Temperature dependence of **(A)** isothermal entropy change curves of TbNi compound and adiabatic temperature change of $RENi_2$ systems with RE= **(B)** Dy and **(C)** Ho. The dashed line in panel **(c)** indicates the T_C. *Reproduced with permission from R. Rajivgandhi, J. Arout Chelvane, S. Quezado, S.K. Malik, R. Nirmala, Effect of rapid quenching on the magnetism and magnetocaloric effect of equiatomic rare earth intermetallic compounds RNi (R = Gd, Tb and Ho), J. Magn. Magn. Mater.* ***433****, 169-177, © (2017) Elsevier [134]; J. Cwik, Y. Koshkid'ko, N.A. de Oliveira, K. Nenkov, A. Hackemer, E. Dilmieva, et al., Magnetocaloric effect in Laves-phase rare-earth compounds with the second-order magnetic phase transition: Estimation of the high-field properties, Acta Mater* ***133****, 230-239, © (2017) Elsevier [136]; J. Ćwik, Y. Koshkid'ko, K. Nenkov, E.A. Tereshina, K. Rogacki, Structural, magnetic and magnetocaloric properties of $HoNi_2$ and $ErNi_2$ compounds ordered at low temperatures, J. Alloy Compd* ***735****, 1088-1095, © (2018) Elsevier [137].*

The next RE-Ni intermetallics that fall in the GMCE-compliant region is the $RENi_2$ family, in particular RE=Dy, Ho and Er: -11.9 [136], -14.5 [137, 138] and -15.1 J kg^{-1} K^{-1} [137] (2 T) at T_C= 22, 15, 6.5 K, respectively. Moreover, their directly characterized ΔT_{ad} amount to ~3.6, ~4.7 and ~3.8 K (2 T) for RE = Dy, Ho and Er, respectively (the results of $DyNi_2$ and $HoNi_2$ are presented in **Figure 12 (B)** and **(C)**). The RE_3Ni_2 family whose MCE meets the GMCE threshold is with RE=Er, with maximum $\Delta S_{isothermal}$ of -10.9 J kg^{-1} K^{-1} and calculated ΔT_{ad} = 3.3 K (both for 2 T) at T_C = 17 K [141]. On the other hand, Ho_3Ni_2 barely scratch the GMCE threshold: -9.8 J kg^{-1} K^{-1} and calculated ΔT_{ad} = 3.2 K (both for 2 T) at T_C = 36 K.

2.3.2.3 RE-Mn

RE-Mn compounds conforming to the GMCE threshold can be found in the $REMn_2$ family where they crystallize in different Laves phase structure, depending on the RE element as well as the annealing temperature [169, 170]. While RE = Tb and Dy crystallize in the cubic Laves phase structure (C15 type), $HoMn_2$ and $ErMn_2$ crystallize in the hexagonal Laves phase structure (C14 type). Yet, their magnetic structures and local magnetic moments are governed by the lattice constants (i.e., the distance of Mn–Mn, RE–R and RE–Mn bonds), not the type of Laves phase structures they form [131]. Their MCE values that meet the GMCE threshold are found for $HoMn_2$ and $ErMn_2$: -10 and -13.4 J $kg^{-1}K^{-1}$ (2 T) at magnetic ordering temperatures of 23 and 16 K, respectively.

2.3.2.4 RE-Fe

Several RE-Fe compositions have been studied for MCE, including $REFe_2$, $REFe_3$, RE_2Fe_{17}, and $RE(Fe,Si)_{13}$, but only the latter performs best and meets the GMCE threshold.

Since the first report on $RE(Fe,Si)_{13}$ with RE=La in 2001 [34] and their hydrides near room temperature by Fujita et al [32], the $La(Fe,Si)_{13}$ compounds have become a phenomenon. They crystallize in $NaZn_{13}$-type structure and could be tuned from FOMT to SOMT simply by varying the Si content. Recent studies on $La(Fe,Si)_{13}$ focus on hysteresis tuning and mechanical stability [39, 43, 171] (one of these reports is presented in **Figure 13 (A)**), which has been a concern for high-performing magnetocaloric materials. While these efforts deserve praise, interpretations of their results can often be challenging, especially regarding the order of thermomagnetic phase transitions. We developed two quantitative criteria to assist the community in resolving these issues: calculating the critical compositional point [37] where FOMT crosses over to SOMT, and evaluating the order of the thermomagnetic phase transition appropriately using the FOMT fingerprint [38]. Neither of them requires further fitting or is limited to thermodynamic models. The same magnetic data measured for MCE calculations is all what is needed for these evaluations.

Published in Handbook on the Physics and Chemistry of Rare Earths, Volume 64 (2023) Pages 175-246
https://doi.org/10.1016/bs.hpcre.2023.10.004

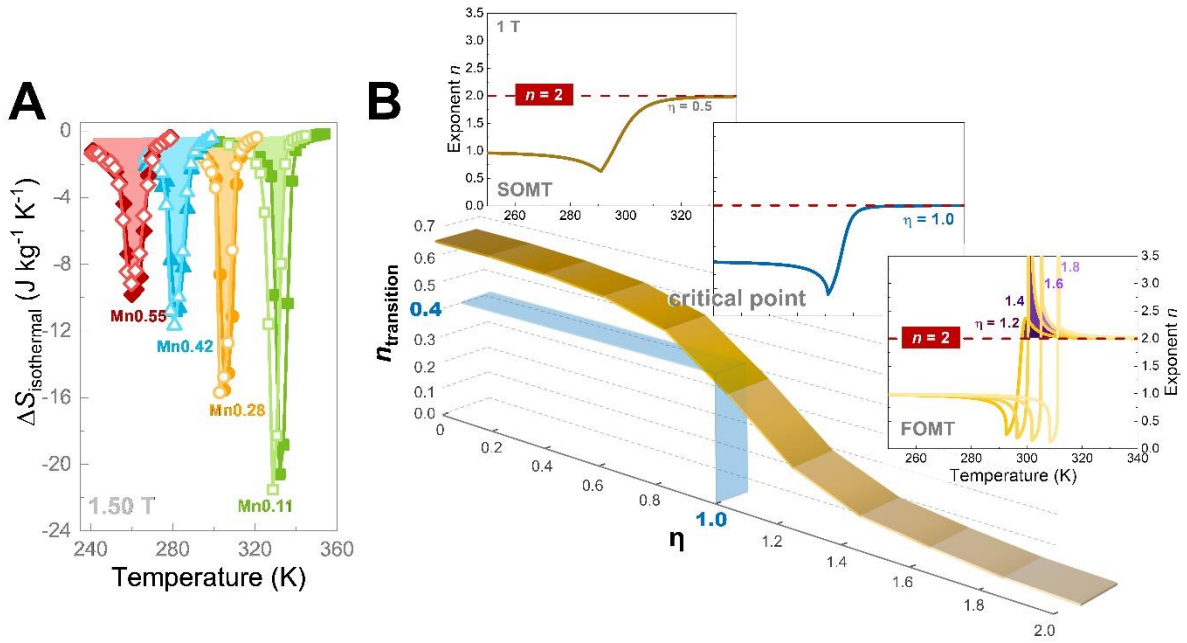

Figure 13. (A) Temperature dependence of isothermal entropy change curves of $La(Fe,Mn,Si)_{13}H$ compounds with varying Mn content and hysteresis. **(B)** The exponent *n* criterion to determine for SOMT (η < 1), critical point (η = 1), and FOMT (η > 1). It is illustrated in the main panel that the minimum of exponent n, at transition temperatures, yields 0.4 as a criterion for evaluating the critical point of FOMT crossover to SOMT. The FOMT fingerprint can be seen in overshoots of *n*>2, which are further color-shaded. *Figure **(A)** is reproduced from L.M. Moreno-Ramirez, J.Y. Law, J.M. Borrego, A. Barcza, J.-M. Greneche, V. Franco, First-order phase transition in high-performance $La(Fe,Mn,Si)_{13}H$ despite negligible hysteresis, J. Alloy Compd **950** (2023) 169883 [39] of © 2023 Author(s), licensed under an open access Creative Commons Attribution 4.0 International License.*

These criteria utilize the exponent *n* of the magnetic field dependence of $|\Delta S_{\text{isothermal}}|$ and is calculated as:

$$n(T,H) = {\mathrm{d}\ln|\Delta S_{\text{isothermal}}|}/{\mathrm{d}\ln H}$$

where *T* is temperature and *H* is the magnetic field. Ref. [38] reports the discovery of the FOMT fingerprint using this exponent *n* criterion: it is a FOMT if the field dependence exponent n overshoots above 2 near the transition temperature; on the contrary, the lack of overshoot indicates either a SOMT or the critical point at which FOMT crosses over to SOMT. **Figure 13 (B)** summarizes the *n* criteria identifying these different regimes using Bean and Rodbell model [172] simulations via the variation of the η parameter, as η < 1 for SOMT; η = 1 for critical point; and η > 1 for FOMT. Due to the initial FM states, the exponent *n* shows a value of 1 at low temperatures for all cases. It then reaches a minimum at the transition temperatures, and for η > 1, overshoots of *n* > 2 are seen near the minima (color-shaded in the figure). The FOMT has a unique fingerprint in this regard. As the temperatures increase, exponent *n* reaches the value of 2 in all cases, indicating that the sample has reached its PM state. In ref[38], we used

both theoretical calculations and experimental case studies to validate our discovery for magnetoelastic phase transitions (including the crossover encountered in $La(Fe,Si)_{13}$ compounds), distributed transition temperatures in FOMT systems, magnetostructural phase transformation as well as AFM-FM phase transitions.

The other *n* criterion, for the determination of the critical point where FOMT crossovers to SOMT, is illustrated in the main panel of **Figure 13 (B)**: when η = 1 (the critical point), the minimum of exponent *n* at the transition temperatures ($n_{transition}$) is 0.4. This criterion breakthrough is reported in [37].

It has been a few years since these criteria were discovered, and the community has applied and expanded them to observing exponent *n* values beginning at 2 during the AFM state at low temperatures [173], as well as validating its capability in a wide range of materials[16-18, 36, 40, 160, 161, 174, 175] and complex scenarios such as concurrent phase transitions of multiphase materials [176].

As many researchers rely on the overshoot of FOMT fingerprint to evaluate their materials, one should appropriately determine $\Delta S_{isothermal}(T, H)$ to avoid evaluating artifacts or noisy *n* results as they would compromise the criterion. The first step is to consider the demagnetizing effect on $\Delta S_{isothermal}(T, H)$ measurements, which can greatly aid interpretation at low magnetic fields. Impurities affecting the MCE and phase transition order can be revealed by the low magnetic field behavior. Similarly, the $n(T, H)$ results should be verified with the original $\Delta S_{isothermal}(T, H)$ results on the same temperature scale axis, as illustrated in **Figure 14** (the appropriate overshoot is shaded in purplish color). This is because FOMT overshoot may be mistaken when the $\Delta S_{isothermal}(T, H)$ switches from a negative to a positive sign or vice versa (shaded in pattern-filled style in **Figure 14 (B)** while the appropriate overshoot is colored purple). Hence, determining $\Delta S_{isothermal}(T, H)$ properly before *n* calculations is crucial to avoiding artifacts.

Published in Handbook on the Physics and Chemistry of Rare Earths, Volume 64 (2023) Pages 175-246
https://doi.org/10.1016/bs.hpcre.2023.10.004

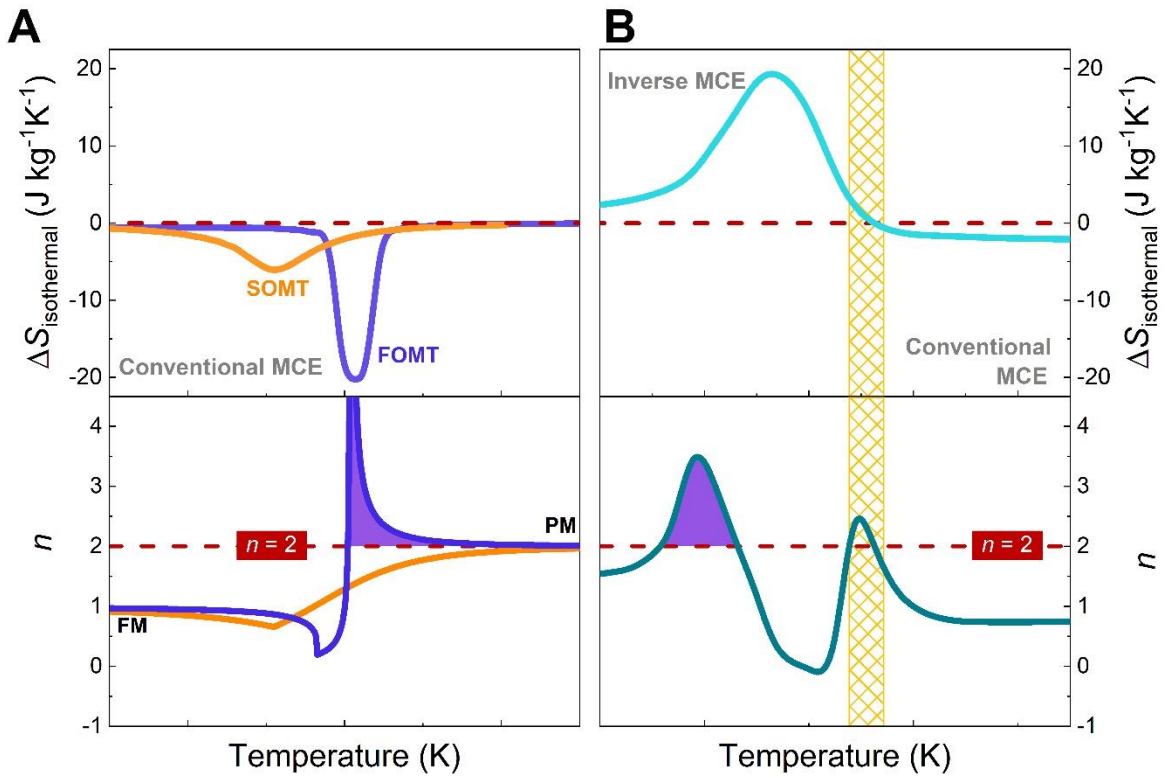

Figure 14. The FOMT fingerprint is shown schematically in **(A)** a direct MCE example and **(B)** an inverse MCE example (both shaded in purple). In the latter, switching signs of isothermal entropy change (pattern-filled region) are present along with both inverse and direct MCE types, which should not be confused with the overshoot in FOMT *n* criterion. *Image adapted from J.Y. Law, V. Franco, Review on magnetocaloric high-entropy alloys: Design and analysis methods, J. Mater. Res.* ***38****(1) (2023) 37-51 [13], © 2023 Author(s), licensed under an open access Creative Commons Attribution 4.0 International License.*

Considering how extensively the $La(Fe,Si)_{13}$ family has been studied, in our discussion, we will focus on the substitutions that can greatly enhance their MCE performance. Impressive maximum $\Delta S_{isothermal}$ values of -16 to -28 J $kg^{-1}K^{-1}$ (2 T) and ΔT_{ad} of 6.5 – 8.1 K (2 T) at magnetic ordering temperatures of 208 – 184 K can be obtained for $La(Fe_xSi_{1-x})_{13}$ with x = 0.877 – 0.900 [32]. Hydrogenation of these samples further enhanced their MCE: magnetic ordering temperature increases to 233 – 323 K with maximum $\Delta S_{isothermal}$ values of -19 to -28 J $kg^{-1}K^{-1}$ (2 T) and ΔT_{ad} of 6.0 – 7.1 K (2 T). Minor Ni [160] and Cr substitutions [161] into the $LaFe_{11.6-x}M_xSi_{1.6}$ compound family (M = Ni or Cr) also gave MCE values that meet the GMCE threshold (-21.4 J $kg^{-1}K^{-1}$ at 2 T, obtained for up to x=0.21 for $LaFe_{11.6-x}Cr_xSi_{1.6}$. Mn substitutions in the $La(Fe,Mn,Si)_{13}H$ series could yield MCE values as large as -9.2 to -21.5 J $kg^{-1}K^{-1}$ (note that these are measured up to 1.5 T) and, at the same time, tune for a smaller thermal hysteresis (as shown in **Figure 13 (A)**) [39]. Minor Co substitutions in $LaFe_{11.7-x}Co_xSi_{1.3}$ series could give

MCE values meeting the GMCE threshold (for 2 T, -20 to -12.3 J $kg^{-1}K^{-1}$ obtained up to x = 0.4) [11].

There are excellent MCE values reported in each of the works for Ce doping at the La-site, with the largest reported in each series being: -19 J $kg^{-1}K^{-1}$ (2 T) for $La_{1-z}Ce_z(Fe_{x-}Mn_ySi_{1-x})_{13}$ [177], -28.9 J $kg^{-1}K^{-1}$ (2 T) for $La_{1-x}Ce_x(Fe_{0.86}Si_{0.14})_{13}$ [178], and -26.7 J $kg^{-1}K^{-1}$ (2 T) for $La_{1-x}Ce_xFe_{11.5}Si_{1.5}C_y$ [179]. Although $La_{1-z}Pr_z(Fe_{0.88}Si_{0.12})_{13}$ and their hydrides had very high MCE values, their MCE decreased with increasing Pr additions (MCE values for 2 T are not provided) [180]. Upon varying Si content in $La_{0.7}Nd_{0.3}Fe_{13-x}Si_x$, MCE as large as -21 to -13.2 J $kg^{-1}K^{-1}$ (2 T) were found for x = 1.2 to 1.6 [181]. Ref.[182] reported MCE as large as -29.3 and -10.5 J $kg^{-1}K^{-1}$ (2 T) for $La_{0.7}Nd_{0.3}Fe_{11.5}Si_{1.5}$ and $La_{0.7}Nd_{0.3}Fe_{11.2}Si_{1.8}$, respectively. In the same work, authors found that the large MCE value was unfortunately reduced when Co was added. Likewise, increasing Co substitutions to $La_{0.8}Ce_{0.2}Fe_{11.5-x}Co_xSi_{1.5}$ inevitably reduces the MCE values especially when their FOMT crossovers to SOMT [183].

RE doping of the $La(Fe,Si)_{13}$ family generally lowers the transition temperature, which was related to the lattice contraction when RE substitutes for La, reported in [184] for $La_{1-x}RE_xFe_{11.5}Si_{1.5}$ with RE=Ce, Pr and Nd. The authors also show that maximum $\Delta S_{isothermal}$ values increase with RE up to $La_{0.7}Nd_{0.3}Fe_{11.5}Si_{1.5}$ and $La_{0.5}Pr_{0.5}Fe_{11.5}Si_{1.5}$ compositions. If one wishes to use substitutions to enhance MCE performance, it is critical to note that one should only design minor substitutions with starting parent compositions that undergo FOMT, while SOMT-starting compositions defeat the purpose.

2.4 Ternary intermetallics of lanthanides with metalloids and/or transition metals

In this section, we include ternary combinations of RE elements with TM and/or a main group element. Similarly to previously discussed binary compounds, ternary intermetallics exhibit a wide variety of possible composition combinations, which is evidenced from the MCE performance comparison plot shown in **Figure 15**. Moreover, this plot helps filter out the combinations fulfilling the GMCE threshold quickly as shown in the inset. Combinations that include non-metal elements of the second period, such as B, C, N or S, will be discussed separately in the next section.

Published in Handbook on the Physics and Chemistry of Rare Earths, Volume 64 (2023) Pages 175-246
https://doi.org/10.1016/bs.hpcre.2023.10.004

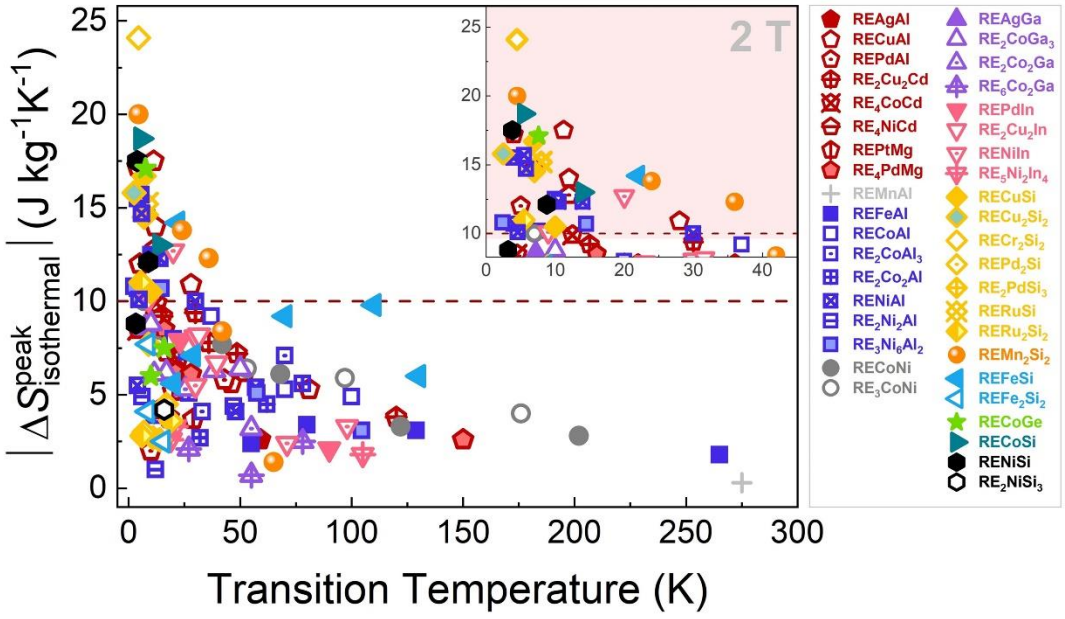

Figure 15. Main panel: MCE comparison of the ternary intermetallics for 2 T. Inset: A magnified subplot showing compounds in the GMCE-compliant region. Dash line represents the lower limit of the GMCE threshold. *Data taken from [11, 53, 174, 185-243].*

$RECr_2Si_2$ can be noticed standing out among the ternary RE-containing intermetallics (**Figure 15**) with the largest maximum $\Delta S_{isothermal}$ value of -24.1 J $kg^{-1}K^{-1}$ (2 T) at ~4.5 K (just above the boiling point of helium) for RE = Er [190]. It crystallizes into a body-centered tetragonal $ThCr_2Si_2$-type structure. It is a promising magnetocaloric material candidate, especially for helium liquefaction given that its ΔT_{ad} (calculated from heat capacity data) reaches the large value of 8.4 K for 2 T in addition to the absence of thermal or field hysteresis. It is not clear how the maxima in the $\Delta T_{ad}(T, H)$ curves shift to higher temperatures not matching the corresponding temperatures of $\Delta S_{isothermal}(T, H)$ but a ΔT_{ad} value of at least 8 K (2 T) can be found for a span of ~11 – 15 K.

The next family of ternary intermetallics with very large maximum values falling in the GMCE compliance region is $REMn_2Si_2$. $ErMn_2Si_2$ stood out among them with maximum $\Delta S_{isothermal}$ value of -20 J $kg^{-1}K^{-1}$ (2 T) and underwent a FM-PM (of SOMT-type) at ~4.5 K, which is just above the boiling point of helium [198]. Similarly to $ErCr_2Si_2$, it crystallizes in $ThCr_2Si_2$-type structure and shows $\Delta T_{ad}(T, H)$ curves (calculated from heat capacity data) displaced to higher temperatures not matching the corresponding temperatures of $\Delta S_{isothermal}(T, H)$. It gives a maximum ΔT_{ad} of 5.4 K (2 T) and at least 5 K can be observed for a span of ~11 – 15.5 K. Authors attributed the observed large MCE value to both the field sensitive magnetic transition and large moment of the intermetallic. In fact, this work was inspired by the findings of

$NdMn_2Ge_{0.4}Si_{1.6}$ compound: it undergoes a field-induced AFM-FM (FOMT) giving a GMCE of 12.3 J $kg^{-1}K^{-1}$ (2 T) [197]. The selection of $NdMn_2Si_2$ was inspired by the interesting interplay between the *3d* and *4f* magnetism of $REMn_2X_2$, and the fact that its Mn-Mn interatomic distance has a significant effect on both the magnitude of Mn magnetic moments and the magnetic state of the Mn sublattice. Therefore, authors selected Nd for its FM ordering while simultaneously offering FM ordering of the Mn lattice as well as the fact that the large atomic radii difference between Si (1.32 Å) and Ge (1.37 Å) can significantly alter the magnetic states of both Nd and Mn sublattices. The tetragonal $ThCr_2Si_2$-type structure (SG *I*4/*mmm*), from neutron diffraction, reveals its PM state above T_N~360 K, with canted AFM magnetic structure (AF*mc*) in the temperature range of 36 < *T* < 360 K. The authors reported that the compound underwent a FOMT from AF*mc* to canted ferromagnetism (F*mc* (Mn) + FM (Nd)) from the neutron diffraction results upon cooling to $<T_C$~36 K. However, further information about the magnetic structure was cited in unpublished results during the publication time and is currently difficult to trace in the literature. The same co-authors reported large maximum $\Delta S_{isothermal}$ values for other members of the family: $NdMn_{1.9}V_{0.1}Si_2$ and $NdMn_{1.7}Cr_{0.3}Si_2$ with -13.8 [244] and ~-8.4 J $kg^{-1}K^{-1}$ [201] (both for 2 T) undergoing FOMT at T_C~24 and 42 K, respectively. The latter shows a ΔT_{ad}~2.4 K (2 T) at T_C~42 K [201]. These compounds could both be potential candidates for hydrogen liquefaction as they exhibit extremely low hysteresis (thermal ≤0.8 K and magnetic <0.1 T). As an example, the low thermal hysteresis and large MCE of $NdMn_{1.7}Cr_{0.3}Si_2$ is presented in **Figure 16**. Another isostructural ternary compound whose MCE falls in the GMCE compliance region is $EuCu_2Si_2$ with maximum $\Delta S_{isothermal}$ (2 T) = -15.8 J $kg^{-1}K^{-1}$ at T_N= 2.5 K [241].

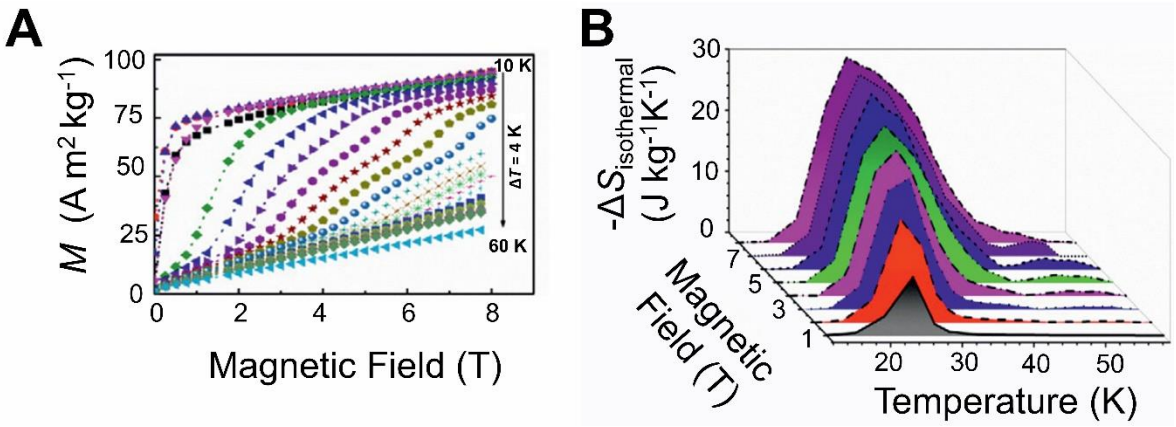

Figure 16. $NdMn_{1.9}V_{0.1}Si_2$ with thermal hysteresis of 0.8 K based on their isothermal magnetization curves **(A)**. Corresponding temperature dependence of isothermal entropy change curves for up to 8 T **(B)**. *Images from M.F.M. Din, J.L. Wang, R. Zeng, S.J. Kennedy, S.J. Campbell, S.X. Dou, Magnetic properties and magnetocaloric effect in layered $NdMn_{1.9}V_{0.1}Si_2$, EPJ Web of Conferences **75** (2014) 04001 [244], licensed under an open access Creative Commons Attribution License 2.0.*

The RECo(Ge/Si) family comes next; according to refs. [202, 210, 211, 245-248], the type of RE element has a significant impact on the crystal structures and magnetic properties of these compounds. For RE = La – Sm, Gd and Tb in RECoSi, the compounds crystallize in tetragonal CeFeSi-type structure (SG *P*4/*nmm*) that is closely related to the $ThCr_2Si_2$ structure and is said to be composed of separate "$ThCr_2Si_2$ blocks" ("$BaAl_4$ slab") connected by RE-RE contacts [248]. The authors reported LaCoSi as Pauli paramagnet and CeCoSi and PrCoSi as Curie-Weiss paramagnets down to 1.6 K. For RECoSi compounds with RE = Nd, Sm, Gd and Tb , AFM ordering is detected below T_N = 7(1), 15(3), 175(3) and 140(3) K respectively. For RE=Dy, Ho and Er, the compounds crystallize in orthorhombic TiNiSi-type structure (SG *Pnma*, no.62) and exhibit FM-PM instead [202, 245, 246]. In general, this family of compounds, RECo(Ge/Si), crystallizes in TiNiSi-type structure for RE=Tb onwards down to the heavy lanthanides (also applicable to substitutions of Ni on the Co-site) [247]. In this family of stoichiometry, RE = Ho exhibits the largest MCE regardless of whether the metalloid is Ge or Si. Both undergo SOMT and exhibit reversible GMCE of -17.1 and -13 J $kg^{-1}K^{-1}$ (2 T) at T_C of 7.6 and ~14 K for HoCoGe [210] and HoCoSi [205], respectively. The latter is reported from evaluations using magnetization data while those from heat capacity data give a smaller value (about -9 J $kg^{-1}K^{-1}$ for 2 T). For the maximum ΔT_{ad} (2 T), HoCoGe and HoCoSi were found with 6 and ~3 K. Other compounds of this family reported for MCE are reviewed in ref. [202], in which ErCoSi shows a GMCE of -18.7 J $kg^{-1}K^{-1}$ (2 T) at T_C of 5.5 K; moreover, the composite $(Ho_{1-x}Er_x)CoSi$ was reported, spanning across 15 to 5.5 K, with GMCE of -17.9, -17.9, -18.2, -18.0, -18.5, and -18.7 J $kg^{-1}K^{-1}$ (2 T) for x = 0, 0.2, 0.4, 0.6, 0.8, and 1, respectively. The related citation is included in the review paper, which originated from the PhD thesis of Z.Y. Xu [249].

Next in line is the RENiSi compounds, which also crystallize in orthorhombic TiNiSi-type crystal structure. For RE=Tb-Er, the compounds were found exhibiting AFM ordering with strong magnetocrystalline anisotropy at low temperatures [202], and among them, HoNiSi presented the largest MCE of -17.5 J $kg^{-1}K^{-1}$ (2 T) at a corresponding temperature of ~4.5 K (T_N = 3.8 K) [206]. Another dedicated work reported its giant anisotropic MCE where its rotational isothermal entropy change values, $\left|\Delta S^{\mathrm{R}}_{\mathrm{isothermal}}\right|$, ~18.6 and 26.7 J $kg^{-1}K^{-1}$ for 2 and 5 T, respectively [250]. These results, including $-\Delta S^{\mathrm{R}}_{\mathrm{isothermal}}$, $\Delta T^{\mathrm{R}}_{\mathrm{ad}}$, and calculated rotational isothermal entropy change results, $-\Delta S_{\mathrm{R,cal.}}$, for 5 T as a function of the rotation angle, are presented in **Figure 17 (A)**, **(B)** and **(C)**, respectively. Exploiting the textured behavior of DyNiSi, measurements were made with different directions with respect to the magnetic field (**Figure 17 (D)**): the resulting $\Delta T_{ad,difference}$ between the different directions amounted to 4.4 and 10.5 K (**Figure 17 (E)** and $\Delta S_{isothermal,difference}$ reached -11 (at 8.5 K) and -17.6 (at 13 K) J $kg^{-1}K^{-1}$ (**Figure 17 (F)**) for 2 and 5 T, respectively [207]. The report also included the rotational $\Delta S_{isothermal}$ of the polycrystalline material measured at 8.5 K as a function of rotation angle for various

magnetic field changes: $\Delta S^{\mathrm{R}}_{\mathrm{isothermal}}(\theta, H)$. The enhancement of magnetic moments in the AFM lattice at the beginning of rotation causes the positive $\Delta S^{\mathrm{R}}_{\mathrm{isothermal}}(\theta)$ values found for low fields close to the perpendicular direction (90°) of its columnar grains is parallel to the magnetic field. Since most of the moments in the AFM sublattice would align with the field direction as the sample was rotated towards the parallel direction (0°), the moment ordering increased, and resulted in negative $\Delta S^{\mathrm{R}}_{\mathrm{isothermal}}(\theta)$ values. They gradually rose to a maximum of $\Delta S^{\mathrm{R}}_{\mathrm{isothermal}}(\theta) = -7.9\ \mathrm{J\,kg^{-1}K^{-1}}$ as the sample was rotated from 90° to 0° during the application of 2 T. For comparison, the MCE of ErNiSi was reported in ref.[202], showing T_N = 4 K and a maximum $\Delta S_{\mathrm{isothermal}}$ of -8.8 J kg^{-1}K^{-1} for 2 T.

Published in Handbook on the Physics and Chemistry of Rare Earths, Volume 64 (2023) Pages 175-246
https://doi.org/10.1016/bs.hpcre.2023.10.004

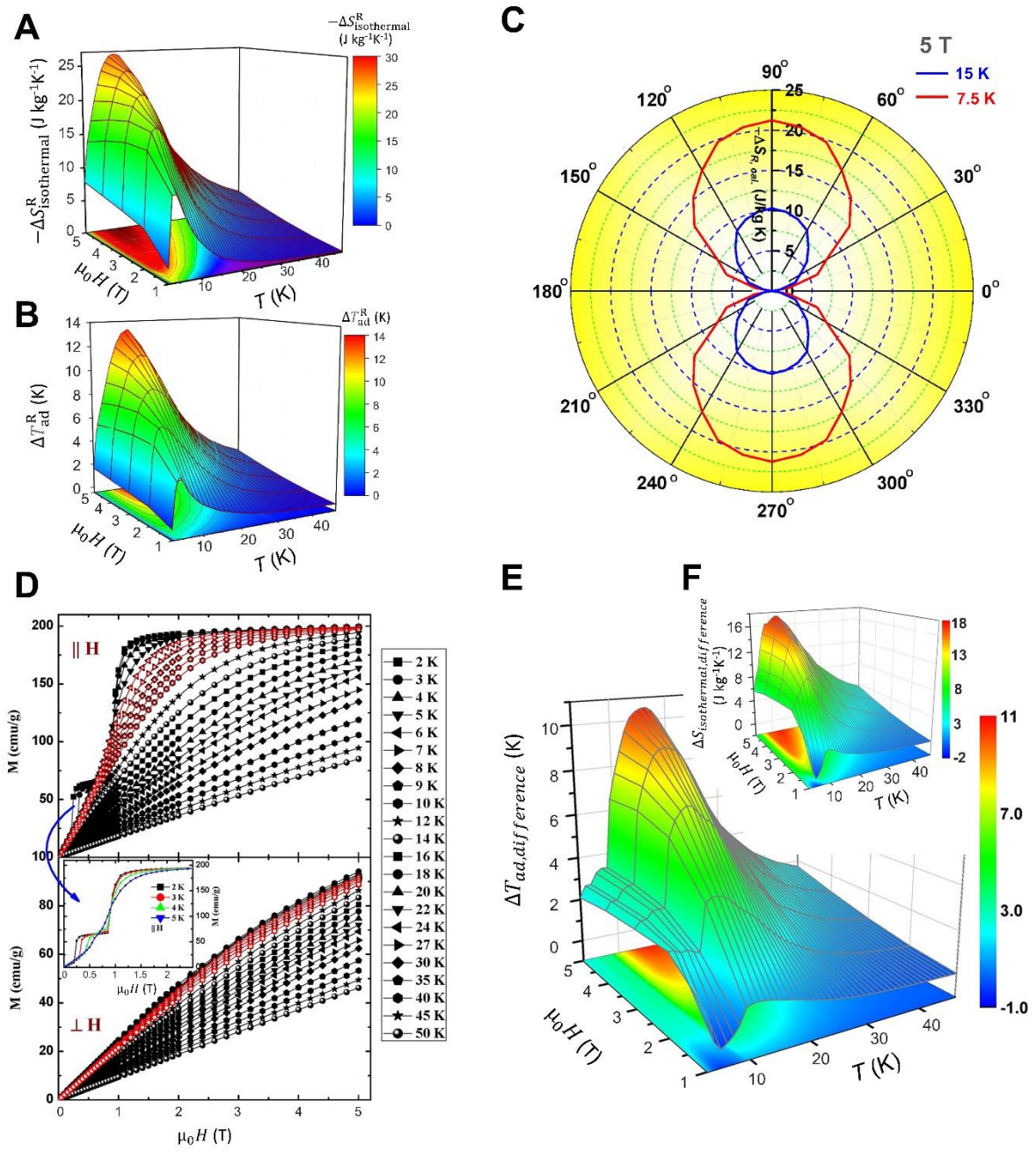

Figure 17. MCE results for HoNiSi: **(A)** $-\Delta S^{R}_{isothermal}$, **(B)** ΔT^{R}_{ad}, and **(C)** $-\Delta S_{R,cal.}$ (5 T) as a function of the rotation angle measured with the perpendicular direction (hard axis) as the starting direction. The calculations were made at temperatures just below and after the $-\Delta S^{R}_{isothermal}$ peak: 7.5 and 15 K, respectively. The second example of textured behavior and MCE is represented by DyNiSi: **(D)** Magnetization isotherms measured along parallel (top panel) and perpendicular (bottom panel) directions. Red highlighted curves indicate measurements performed in decreasing fields near T_N. Inset: Isotherms measured along parallel direction in temperature of 2–5 K for low magnetic fields. The rotational MCE results of DyNiSi: **(E)** $\Delta T_{ad,difference}$ and **(F)** $\Delta S_{isothermal,difference}$. *Images **(A)** – **(C)** are reproduced from H. Zhang, C. Xing, H. Zhou, X. Zheng, X. Miao, L. He, et al., Giant rotating*

magnetocaloric effect induced by highly texturing in polycrystalline DyNiSi compound, Acta Mater. ***193****, 210-220, © (2020) Elsevier [250]. Images* ***(D)*** *–* ***(F)*** *from H. Zhang, Y.W. Li, E.K. Liu, Y.J. Ke, J.L. Jin, Y. Long, B. Shen, Giant rotating magnetocaloric effect induced by highly texturing in polycrystalline DyNiSi compound, Sci. Rep.* ***5*** *(2015) 11929 [207], licensed under an open access Creative Commons Attribution 4.0 International License.*

Next on the list are the RECuAl compounds with RE = Gd, Tb, Dy, Ho or Er. The polycrystalline materials crystallize in hexagonal ZrNiAl-type structure. Two types of basal plane layers are distributed along their *c* axis: one with all the RE atoms and ⅓ of the Cu atoms, and the other comprised of a non-magnetic layer formed by the remaining ⅔ of the Cu atoms and all the Al atoms. Consequently, uniaxial magnetic anisotropies are observed in RE=Gd, Dy, and Er, while basal-plane magnetic anisotropy is observed in HoCuAl. For TmCuAl, neutron diffraction studies revealed a very complex magnetic structure: a longitudinal spin wave structure with a propagation vector **k** = (½ 0 q) in the range 2-1.2 K and Tm magnetic moments aligned along the *c*-axis; below 1.2 K, a commensurate basal-plane AFM component with **k** = (½ 0 ½) develops resulting in a canted magnetic structure [251]. MCE reports show a typical FM–PM transition with a monotonic decrease in T_C as RE evolves from Gd to Er. Their maximum $\Delta S_{isothermal}$ values (for 2 T) that fall in the GMCE compliance region are -10.9 [218], -17.5[220], -14.7[219], and -17.2 J kg^{-1}K^{-1} [221] for RE=Dy, Ho, Er and Tm, respectively. With transition temperatures ranging from 28 to 4 K, their large MCE values (for RE = Dy – Tm in RECuAl) suggest that they could be promising candidates for low temperature applications, especially gas liquefaction.

ReNiAl intermetallics, also crystallizing within hexagonal ZrNiAl-type structure (SG $P\bar{6}2m$) same as for RECuAl compounds, have been reported with coexistence of FM and AFM states. Among them, the MCE of DyNiAl and HoNiAl meet the GMCE threshold: -10 (at 30 K) [252] and -12.3 J kg^{-1}K^{-1} [253] for 2 T. Their corresponding maximum ΔT_{ad} (2 T) were 3.5 and 4 K, respectively. The fact that Cu doping at the Ni-site can significantly increase $\Delta S_{isothermal}$ values is another intriguing discovery for this family of compounds. An example is the Tm($Ni_{0.7}Cu_{0.3}$)Al compound, whose maximum $\Delta S_{isothermal}$ (2 T) is -10.7 J kg^{-1}K^{-1}, which is nearly twice as large as for TmNiAl (-5.5 J kg^{-1}K^{-1} for 2 T) while maintained at the same corresponding peak temperature near 4 K [254]. While $ErNi_{1-x}Cu_xAl$ compounds with x = 0.2, 0.5, and 0.8 fall within the GMCE compliance region, i.e., -10.1, -14.7, and -15.7 J kg^{-1}K^{-1} (2 T) [255], the Ho($Ni_{0.7}Cu_{0.3}$)Al compound exhibits the same maximum $\Delta S_{isothermal}$ (2 T) as HoNiAl [256].

In the RECuSi family, compounds with RE=Dy, Ho, and Er meet the GMCE threshold: -10.5 [187], -16.7 [186], and -14.5 J kg^{-1}K^{-1} (2 T) [185]. It has been reported that they undergo an AFM–PM transition at T_N = 14 [185], 11 [185], 10 [187], 7 [186], and 7 K [185] when RE = Gd, Tb, Dy, Ho, and Er. The large MCE found in HoCuSi was attributed to its field-induced AFM-FM metamagnetic transition, which was concurrently accompanied by a very large saturation

Published in Handbook on the Physics and Chemistry of Rare Earths, Volume 64 (2023) Pages 175-246
https://doi.org/10.1016/bs.hpcre.2023.10.004

magnetization and a substantial lattice volume change around T_N. **Figure 18** presents thermal expansion results, taken from ref. [202] based on a PhD thesis [185].

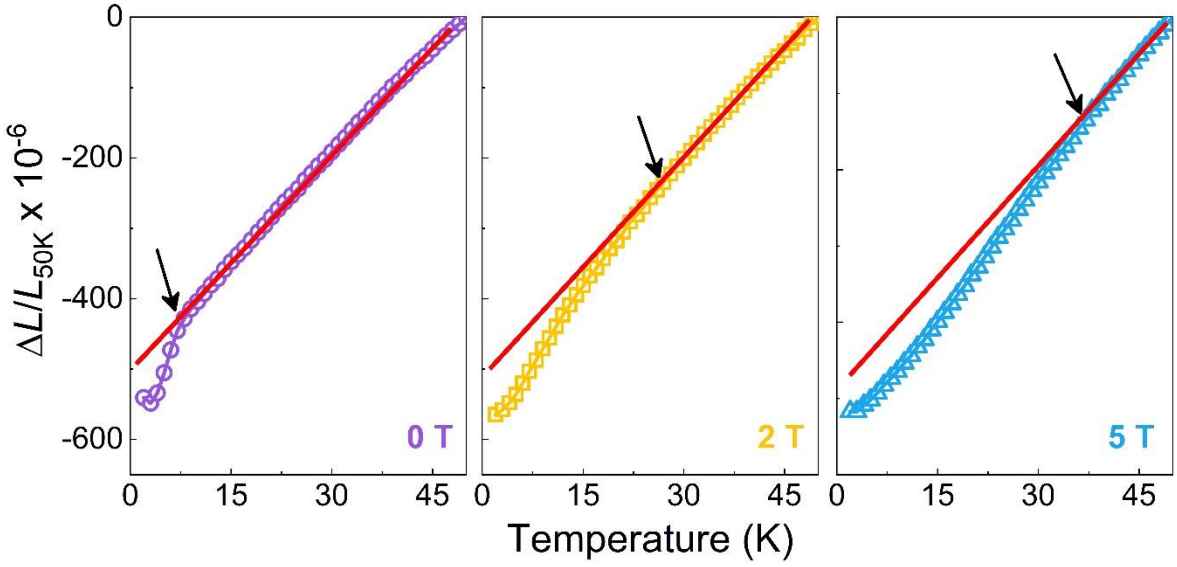

Figure 18. Temperature dependence of the thermal expansion results of HoCuSi shows an overall linear decreasing trend with decreasing temperature. There is a noticeable abrupt drop around T_N for 0 T, which suggests that there is sudden thermal expansion occurring near T_N due to a change in lattice constants. Additionally, with increasing magnetic fields, the abrupt thermal expansion shifts to higher temperatures, resulting in asymmetries observed in their $\Delta S_{isothermal}$ peaks. *Data courtesy from Hu Zhang, USTB, China.*

Next in line comes the ErRuSi compound, which features a maximum MCE of -15.2 J $kg^{-1}K^{-1}$ (2 T) [192], meeting the GMCE threshold. It was reported crystallizing in orthorhombic Co_2Si-type structure and undergoing a FOMT at 8 K. Its asymmetrical broadening of the $\Delta S_{isothermal}(T, H)$ peak towards high temperatures with increasing magnetic field changes leads to an enhanced cooling efficiency, which the authors attribute to the FOMT and the spin fluctuations caused by the Ru *4d* sublattice. Few studies have been performed on MCE for related RERuSi compounds; the most recent one reports a lower MCE in GuRuSi (5.6 J $kg^{-1}K^{-1}$ at T_C = 78.3 K for 2 T), which crystallizes in a tetragonal CeFeSi-type structure (SG *P*4/*nmm*) instead [257].

REFeSi intermetallics also crystallize within tetragonal CeFeSi-type structure, same as GdRuSi compound, and are more widely studied. Except for HoFeSi, this family of compounds exhibits FM ordering below their respective T_C for RE = Gd, Tb, Dy and Er. HoFeSi exhibits a complex magnetic structure with FM and AFM/ferrimagnetic (FIM) moments at low temperatures. It presents an inverse MCE of 5.6 J $kg^{-1}K^{-1}$ (2 T) at the FIM transition (20 K) and a direct MCE of -7.1 J $kg^{-1}K^{-1}$ (2 T) at T_C = 29 K) [258]. Yet, ErFeSi has the largest MCE among this family of compounds despite undergoing SOMT of FM-PM: -14.2 J $kg^{-1}K^{-1}$ (2 T) at T_C = 22 K, which falls

within the temperature range desirable for hydrogen liquefaction [200]. TbFeSi is up next with -9.8 J $kg^{-1}K^{-1}$ (2 T) and a T_C = 110 K [199].

The following compounds on the list are REPdAl; depending on the selection of heat treatment techniques, they crystallize into various crystal structures, affecting their magnetic properties [202, 259]: By annealing at high temperatures (~1050°C) and then cooling rapidly, the metastable high-temperature modification (HTM) forms hexagonal ZrNiAl-type structure, while annealing at low temperatures (~750 °C) the low-temperature modification (LTM) leads to orthorhombic TiNiSi-type structure. Among them, those whose MCE meets the GMCE threshold are HoPdAl (HTM) and ErPdAl (HTM): -12.8 and -12 J $kg^{-1}K^{-1}$ (2 T) at T_C = 12 and 5 K, respectively (values taken from ref. [202]). Ref. [260] reports that for 2 T, as-cast HoPdAl yields -11.4 J $kg^{-1}K^{-1}$, compared to -12.8 J $kg^{-1}K^{-1}$ for the hexagonal HTM analog (annealed at 1080°C for 12 days) while the orthorhombic LTM counterpart (annealed at 750°C for 50 days) has much smaller MCE of about -2.8 J $kg^{-1}K^{-1}$.

RENiIn compounds are reported to form the hexagonal ZrNiAl-type structures where their magnetic transition temperatures could vary from 96 K to 9 K for RE=Gd to Er [261]. According to early neutron diffraction works, RENiIn compounds with RE=Gd, Ho, and Er, are primarily FM, RE=Dy is predominantly AFM, and TbNiIn has a complex magnetic structure suggesting the presence of both FM and AFM components [261-263]. These are also reported in a later publication dedicated to a systematic MCE study for RE=Gd-Er [264] that also fills a gap for HoNiIn. The latter exhibits two successive magnetic transitions with increasing temperatures, of which the first at 7 K may be a change from collinear to non-collinear magnetic structure, while the second at 20 K is ascribed to FM-PM transition. Among the studied series, the MCE of HoNiIn and ErNiIn fall in the GMCE-compliance region: -12.7 and -10.1 J $kg^{-1}K^{-1}$ (2 T) at T_C=20 and 9 K, respectively.

Among the MCE reports for RECoAl compounds, those that meet the GMCE threshold are RE = Ho [222] and Tm [265]. They present -12.5 and -10.2 J $kg^{-1}K^{-1}$ (2 T) at T_C = 10 and 6 K for RE = Ho and Tm, respectively. The RECoAl compounds crystallize in hexagonal $MgZn_2$-type structure (SG $P6_3/mmc$) and authors mention that compounds with RE=Tb, Dy, Ho and Tm exhibit strong anisotropies. A related composite of this compound with composition (Gd,Dy,Er)CoAl was developed, revealing T_C = 45 K and MCE = -6.3 and -14.0 J $kg^{-1}K^{-1}$ for 2 and 5 T, respectively [222]. As the Steven factors of Dy and Er have opposite signs [266], the composition designed by the authors was motivated by the idea of using Er to cancel the anisotropy of Dy while Gd is making up for the effect of Er on the transition temperature. GdCoAl shows a table-like MCE with a relatively constant $|\Delta S_{isothermal}|$ over a large temperature range, ~4.6 to 4.9 J $kg^{-1}K^{-1}$ for 76-97 K, while DyCoAl shows -9.2 J $kg^{-1}K^{-1}$ (T_C=37 K). Furthermore, a dedicated study on DyCoAl reveals the compound having a commensurate FM structure with collinear Dy magnetic moments laying in the *ab* plane [267] (same MCE value as that reported in ref. [222])

and that ErCoAl exhibits a MCE of approximately 8 J $kg^{-1}K^{-1}$ (2 T) and T_C = 16 K [268]. The wide T_C separation among GdCoAl, DyCoAl, and ErCoAl, as well as the intricate magnetic structure of DyCoAl, unfortunately lead to a lower MCE value when combining them into a composite. Readers are recommended to consult the thorough review book chapter in ref. [41] for information on the proper steps to take when designing magnetocaloric composites for performance optimization.

Other ternary compositions found with MCE falling in the GMCE compliance region include $RE_3Ni_6Al_2$, $RERu_2Si_2$, RE_3CoNi, and RE_4CoCd. For $RE_3Ni_6Al_2$, the compounds with RE=Ho and Er exhibit -10.7 and -10.8 J $kg^{-1}K^{-1}$ (2 T) with T_C = 14.5 and 2.4 K, respectively [227]. They were found crystallizing in cubic Ca_3Ag_8-type structure (SG $Im\bar{3}m$) and underwent a FM-PM transition. Among the $RERu_2Si_2$ family, $ErRu_2Si_2$ exhibits a MCE that meets the GMCE threshold: -11 J $kg^{-1}K^{-1}$ (2 T) [193]. Authors reported that it underwent a FOMT at the transition temperature of 5.5 K with a maximum ΔT_{ad} (2 T) of approximately 5.6 K within a wide temperature span. For RE_3CoNi compounds, the MCE of Tm_3CoNi fulfills the GMCE threshold: -10 J $kg^{-1}K^{-1}$ (2 T) with T_C = 6 K [242]. Among RE_4CoCd compounds, we would consider that Er_4CoCd, crystallizing in cubic Gd_4RhIn-type structure, meets the GMCE threshold: its maximum $\Delta S_{isothermal}$ (2 T) = -9.9 J $kg^{-1}K^{-1}$ and T_C= 12.5 K [239].

2.5 Lanthanides-non-metals-based compounds

Aside from combining lanthanides with metallic elements for magnetocalorics, lanthanide compounds with nonmetallic elements, such as B, C, N, S, or O, as one of the major constituents have also been reported. Those with minor nonmetal additions to RE, such as up to 15 atomic percent of B, C, or H to Gd, only resulted in a reduction in the MCE that Gd is capable of. For those containing oxygen, they will be discussed in the next section as there are wide variations in compositions and characteristics among magnetocaloric RE oxides. This section is therefore primarily on RE borides, carbides, sulfides, and nitrides, especially highlighting the compositions meeting the GMCE threshold.

In **Figure 19**, we compare the magnetocaloric properties of RE borides, carbides, sulfides, and nitrides. The GMCE-compliant region appears to be dominated by REB_2, $RECoC_2$, $RECo_2B_2C$, EuS, EuSe, and REN, where REB_2 is clearly the most prominent in terms of the MCE magnitude and transition temperature range.

Published in Handbook on the Physics and Chemistry of Rare Earths, Volume 64 (2023) Pages 175-246
https://doi.org/10.1016/bs.hpcre.2023.10.004

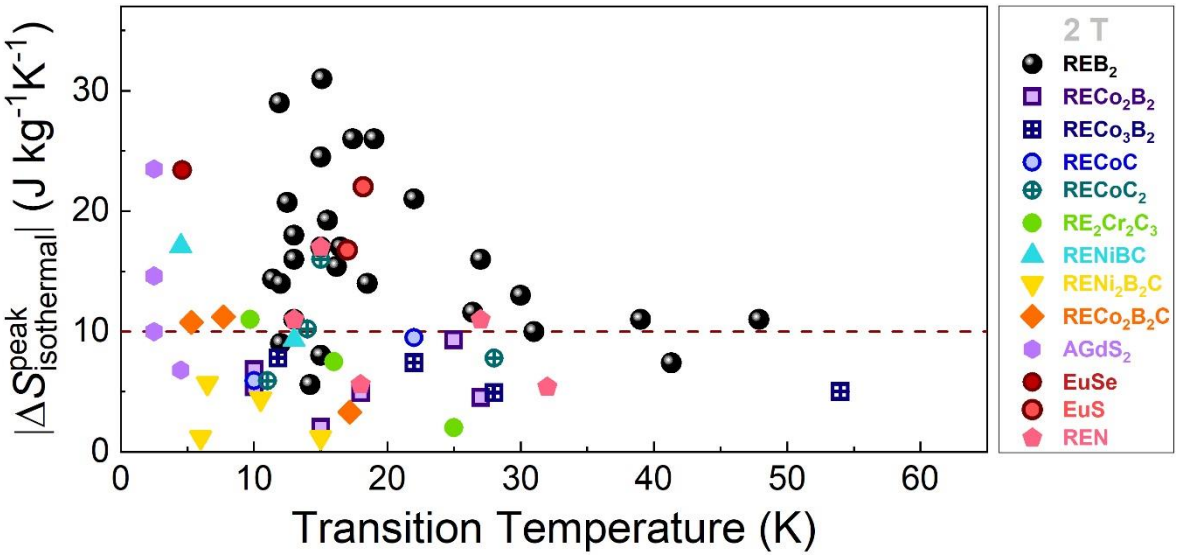

Figure 19. MCE comparison of the RE borides, carbides, sulfides, and nitrides for 2 T. The dash line represents the lower limit of the GMCE threshold. Among the GMCE-compliant region, REB_2 stood out in terms of the MCE magnitude and transition temperature range. *Data are taken from [26, 269-280].*

The heightened interest in these compounds is sparked by the promising MCE found in HoB_2. It is to be highlighted that this composition was sought by machine learning (ML) approach (outlined in **Figure 20 (A)**) and experimentally verified: HoB_2 undergoes SOMT yet shows a very large reversible MCE at 15 K (presented in **Figure 20 (B)** and **(C)**) [269]. Its SOMT is verified from the positive slopes observed in the Arrott plots (**Figure 20 (D)**) and excellent collapse of their magnetocaloric curves from the universal curve approach developed by Victorino Franco [50, 51] (**Figure 20 (E)**). According to the authors, the additional contribution from the SR transition and the large FM fluctuation above T_C both contributed to the large MCE obtained in HoB_2 [281].

Published in Handbook on the Physics and Chemistry of Rare Earths, Volume 64 (2023) Pages 175-246
https://doi.org/10.1016/bs.hpcre.2023.10.004

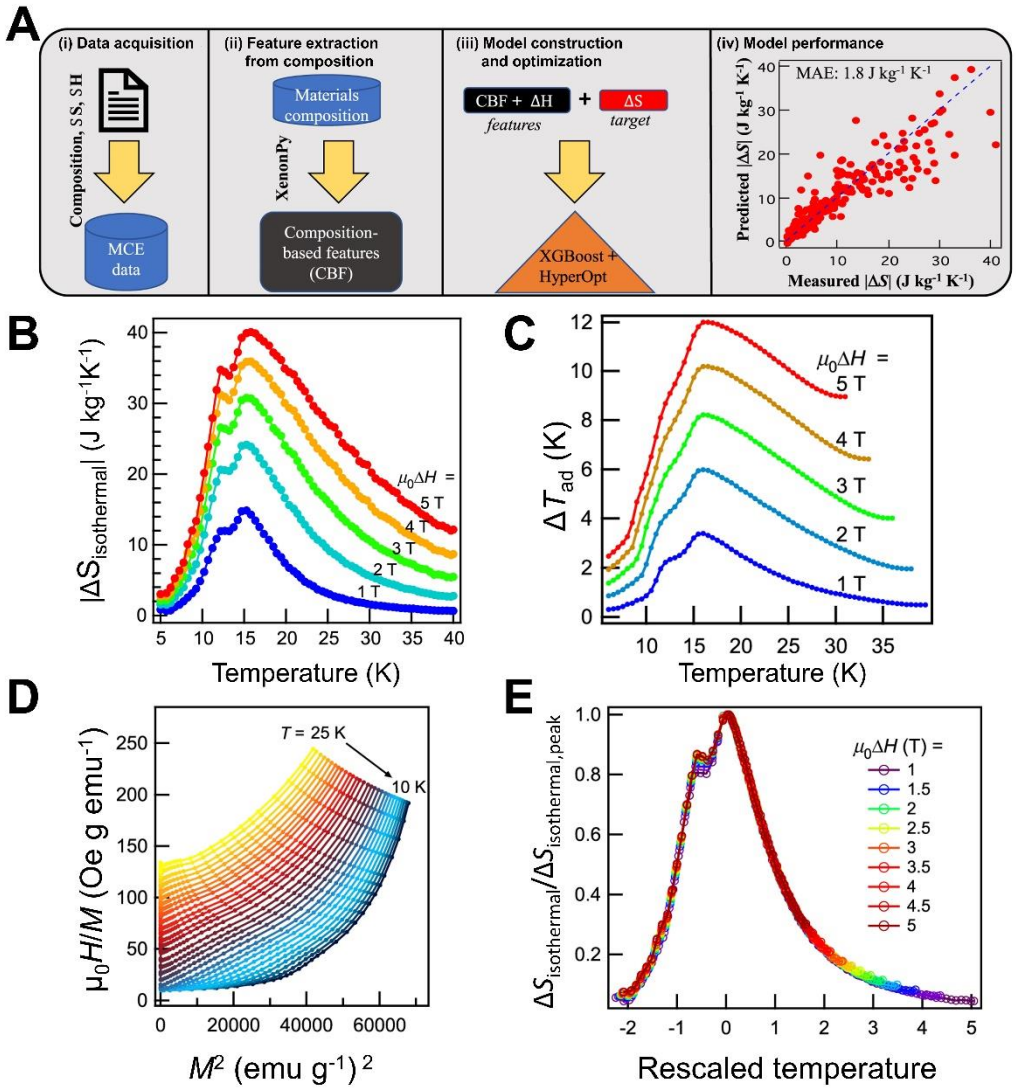

Figure 20. The first report of REB_2 was the ML-sought HoB_2, whose model construction process is outlined in **(A)**: Step (i) reviewing literature and extracting data; step (ii) includes extracting compositional-based features using XenonPy30 python package and using them along with their reported field change values; step (iii) involves optimizing the model using HyperOpt package by minimizing the mean absolute error (MAE) score; and step (iv) evaluation of the performance of the constructed model by comparing predicted and reported $\Delta S_{isothermal}$ values for a validation set of ~300 compositions. The found HoB_2 composition exhibits large **(B)** $\Delta S_{isothermal}$ and **(C)** ΔT_{ad} at temperatures near the boiling point of hydrogen. It undergoes SOMT as shown in the **(D)** Arrott plots and **(E)** universal curve scaling. *Images are reproduced from P. Bd Castro, K. Terashima, T.D. Yamamoto, Z. Hou, S. Iwasaki, R. Matsumoto, et al., Machine-learning-guided discovery of the gigantic magnetocaloric effect in HoB_2 near the hydrogen liquefaction temperature, NPG Asia Materials* ***12****(1) (2020) 35 [269], under an open access Creative Commons Attribution 4.0 International License.*

Based on the advantages of HoB_2 as described in ref. [269], a number of substitutions to the AlB_2-type crystal structure are investigated to expand its operating temperature of 10–30 K to directly cool hydrogen gas from 77 to 22 K, in an effort to optimize the design of a high-efficiency refrigeration system for hydrogen liquefaction via a three-stage magnetic refrigerator [282, 283]. The substitution efforts include Dy or Gd and Al at the RE and B sites, respectively. The motivation of Dy substitution stems from the fact that it also behaves as a standard ferromagnet (T_C = 50 – 55 K) with additional SR transitions (20 and 12 K) similar to HoB_2. Its first MCE report displayed two MCE peaks of approximately -4.3 and -7.6 J $kg^{-1}K^{-1}$ at 20 and 48 K (2 T) respectively (for 5 T, the approximate values are -10.4 and -17 $kg^{-1}K^{-1}$ at 25 and 50 K respectively) [284]. When Dy is added to the Ho site in the pseudobinary $Ho_xDy_{1-x}B_2$ system, the working temperature expanded (11 – 50 K) at the expense of $\Delta S_{isothermal}$ decreasing (half the value for HoB_2 for x > 0.5), but this could also result in a table-like MCE with very high *RC* values over 600 J kg^{-1} (5 T) [270, 285]. The overall broadening of the MCE behavior to a table-like feature with expanded working temperature is also found for $Ho_xGd_{1-x}B_2$ system with x = 0.2, 0.3 and 0.4 [271]. Phase segregation instead of solid solution formation is reported when Al substitutions were made to the B-site in the $HoB_{2-x}Al_x$ system: stoichiometric HoB_2 and B-substituted $HoAl_2$ [286]. Even though the system still exhibits double MCE peaks (at T_{C1} of 15 K and T_{C2} above 32 K), the lower HoB_2 phase fraction regrettably results in a lower MCE: T_{C1} is the same as HoB_2, while T_{C2} resembles $HoAl_2$. TbB_2 was reported to undergo a SOMT at 144 K with -5.2 J $kg^{-1}K^{-1}$ (2 T)[287]. Authors estimated that it could give a large ΔT_{ad} of 14.7 K (2 T). If the latter is proven true, this magnitude would substantially allow the compound to comply the GMCE threshold despite its moderate $\Delta S_{isothermal}$ values.

While HoB_2 maintains the best MCE among this family of compounds, substitutions of $x \leqslant 0.7$ in the $Ho_xRE_{1-x}B_2$ or $HoB_{2-x}Al_x$ systems yield $\Delta S_{isothermal}$ values that could meet the GMCE threshold. However, there is room for improvement in the low field ΔT_{ad} of HoB_2 (12 K for 5 T; 6 K for 2 T) to satisfy the GMCE threshold for both $\Delta S_{isothermal}$ and ΔT_{ad} parameters. Other REB_2 and their MCE have not been reported. The MCE is also frequently reported for $RECo_2B_2$ and $RECo_3B_2$, but they fall short of the GMCE cutoff, and thus will not be further discussed.

When it comes to RE carbides, those whose compositions include TM could exhibit $\Delta S_{isothermal}$ values that satisfy the GMCE criteria when RE = Gd and Er in $RECoC_2$, RE = Er in $RE_2Cr_2C_3$, RE = Er in RENiBC, and RE = Tb and Dy in $RECo_2B_2C$.

Both $GdCoC_2$ and $ErCoC_2$ crystallize in the $CeNiC_2$-type structure (SG *Amm*2), each with a FM-PM transition at T_C of about 15 and 14 K respectively [288, 289]. Both reports demonstrate that the magnetocaloric curves collapse onto a universal curve, indicating they undergo SOMT. Yet they still manage to provide a significant MCE value of -16 [288] and -10.2 J $kg^{-1}K^{-1}$ (2 T)[289] each, which is sufficient to meet the GMCE threshold. $Er_2Cr_2C_3$ was reported to exhibit an

orthorhombic structure of SG *C*12/*m*1, a FM-PM transition at T_C = 9.7 K and displaying a maximum $\Delta S_{isothermal}$ value of approximately -11 J kg^{-1}K^{-1} (2 T) [290]. In this family of compounds, the magnetic ordering differs depending on the RE selection: FM-PM for RE = Er (T_C = 9.7 K) while PM-AFM for RE = Ho (T_N = 15.8 K) and Dy (T_N = 25.2 K). Moving to the next family of compounds, the RE nickel boron carbides, RENiBC, the compound with RE = Er undergoes a SOMT at transition temperature of 4.5 K, presenting $\Delta S_{isothermal}$ values that satisfy the GMCE threshold: -10 and -17.1 J kg^{-1}K^{-1} for 1 and 2 T respectively [291]. Other closely related quaternary RE nickel boron carbides are the $RENi_2B_2C$ compounds, which were reported to crystallize in $ThCr_2Si_2$-type crystal structure with alternating RE-C and Ni_2B_2 layers along the *c*-axis. However, none of their MCE reports fall in the GMCE-compliance region. When Co replaces Ni in $RECo_2B_2C$, the compounds crystallize in a $LuNi_2B_2C$-type crystal structure with *I*4/*mmm* space group, as reported in ref.[292] for RE=Gd, Tb or Dy. Another obvious distinction between them and the $RENi_2B_2C$ compounds is that they exhibit FM-PM transition (T_C ~17.2, 5.3 and 7.7 K for Gd, Tb and Dy) while the presence of nickel in the latter stabilizes the AFM ordering associated to FOMT for low magnetic fields. Among them, the $\Delta S_{isothermal}$ values of $TbCo_2B_2C$ and $DyCo_2B_2C$ falls in the GMCE-compliance region: -10.75 and -11.20 J kg^{-1}K^{-1} (2 T) respectively.

Among the magnetocaloric sulfides reported, EuS was the first one: Bredy and Seyfert reported in 1988 an estimated MCE value of -22.7 J kg^{-1}K^{-1} (3 T) from the heat flux measurements of a flat sintered polycrystalline sample [293]. A later study on an EuS single crystal revealed that it undergoes a SOMT from FM–PM (T_C = 18.2 K) with very large and isotropic MCE of -22.7 J kg^{-1}K^{-1} (**Figure 21 (A)**) and relative cooling power (*RCP*) of 284 J kg^{-1} (2 T) [272]. The exceptional MCE of EuS, -16.76 J kg^{-1}K^{-1} (2 T), was also found for polycrystalline powders synthesized from different batches of the Eu_2O_3 precursor and sulfurization conditions [273]. This compound, an ordinary FM semiconductor, crystallized in a NaCl-type structure and is expected to exhibit relatively weak crystalline field effect and magnetic anisotropy. Despite this, the sizeable, reversible, and isotropic MCE discovered suggests that it may be worthwhile to explore europium monochalcogenides. Having said that, this is also reflected in the remarkable and isotropic MCE reported for EuSe and EuO where the former undergoes a FOMT while the latter a SOMT from FM-PM at T_C = 69 K (further covered in the next section). EuSe single crystals were reported to exhibit a large MCE of -23.4 J kg^{-1}K^{-1} (2 T) with a T_N = 4.6 K (**Figure 21 (B)**) [26]. In this report, the isotropic MCE is revealed by measuring its isothermal magnetization curves with magnetic field applied along the [100] and [110] directions, where they perfectly coincide at temperatures above T_N and with very slight difference below T_N. Its large MCE (which falls in the GMCE threshold) is resulted from the FOMT it undergoes at T_N. Although a notable isotropic MCE is found for EuS and EuSe, reports on related families are scarce.

Published in Handbook on the Physics and Chemistry of Rare Earths, Volume 64 (2023) Pages 175-246
https://doi.org/10.1016/bs.hpcre.2023.10.004

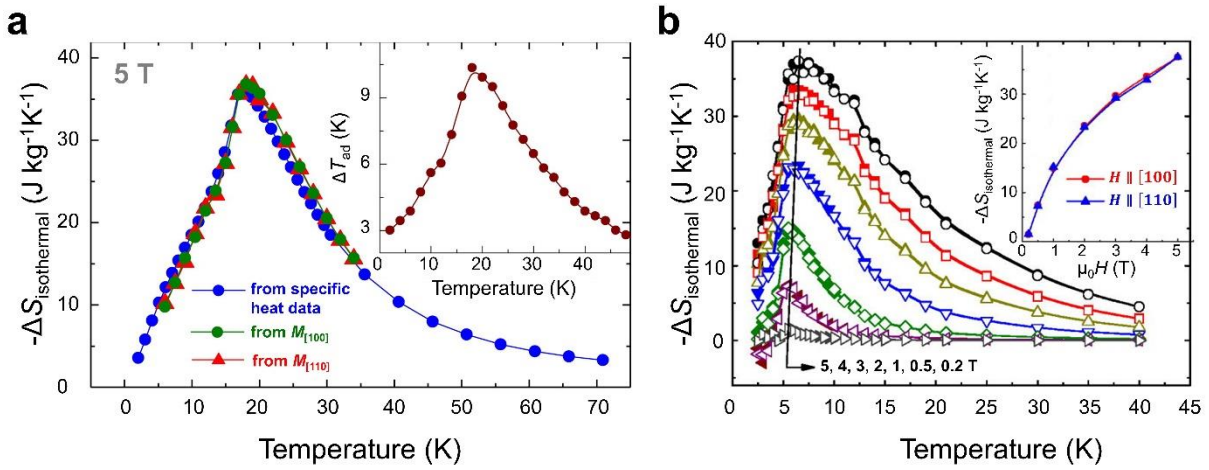

Figure 21. Large, reversible isotropic MCE obtained for **(A)** EuS and **(B)** EuSe. *Image **(A)** reproduced with permission from D.X. Li, T. Yamamura, S. Nimori, Y. Homma, F. Honda, Y. Haga, et al., Large reversible magnetocaloric effect in ferromagnetic semiconductor EuS, Solid State Commun. **193**, 6-10, © (2014) Elsevier [272]. Image **(B)** with permission from D.X. Li, T. Yamamura, S. Nimori, Y. Homma, F. Honda, D. Aoki, Giant and isotropic low temperature magnetocaloric effect in magnetic semiconductor EuSe, Appl. Phy.s Lett. **102**(15), 152409 (2013) [26].*

Another group of GMCE-qualified candidates that stands out in **Figure 19** is the RE nitrides. Crystallizing in the NaCl-type crystal structure, they are dense materials, yet have high thermal conductivity. They are chemically stable and do not react with hydrogen gas. Their MCE investigations began with mononitrides with formula REN, RE = Gd, Tb, Dy, Ho or Er, and then evolved to binary RE nitrides. They undergo SOMT of FM-PM with decreasing T_c along the Gd < Tb < Dy < Ho < Er as shown in **Figure 22 (A)**. Among these, ErN and HoN show very large $|\Delta S_{\text{isothermal}}|$ values above the GMCE threshold as seen from their MCE results in **Figure 22 (B)**. Their ΔT_{ad}(5 T) were found to be -8.5 and -10.3 K [294], which are comparable to the Gd value(-11.6 K for 5 T from ref. [58]). In addition, their nanoparticles have been reported with unparalleled magnetocaloric properties [295, 296]. Though one can find the combination of all these factors makes them magnetocaloric materials with excellent performance for hydrogen liquefaction, it would be worthwhile to investigate their ΔT_{ad} performance for smaller magnetic field changes, such as 2 T. In this way, their suitability for liquefaction applications without large magnetic fields could be evaluated further.

Published in Handbook on the Physics and Chemistry of Rare Earths, Volume 64 (2023) Pages 175-246
https://doi.org/10.1016/bs.hpcre.2023.10.004

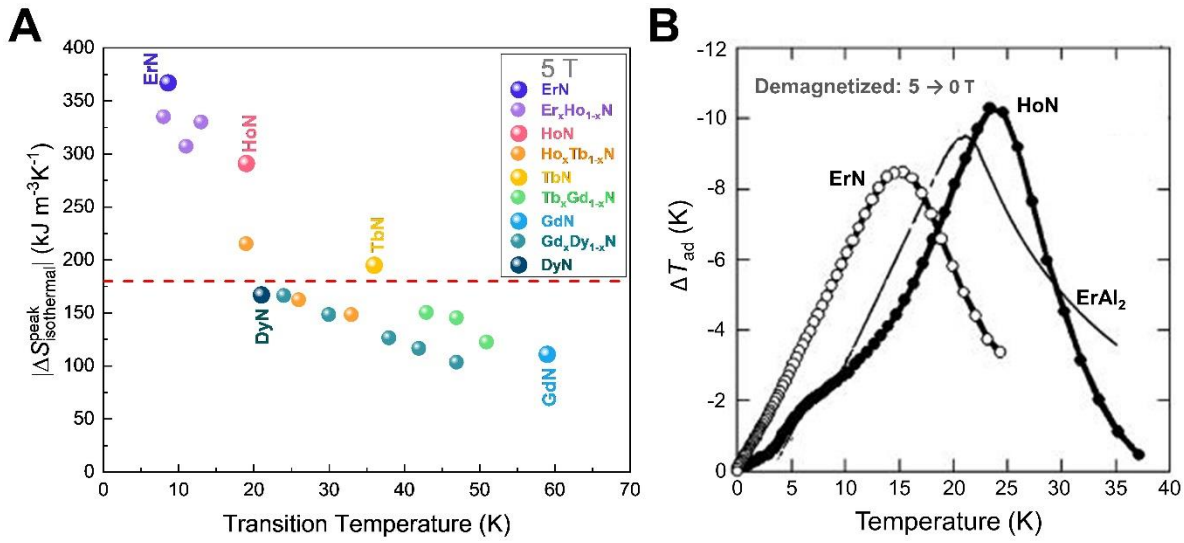

Figure 22. (A) MCE comparison of the RE nitrides for 5 T. Dash lines represent the lower limit of the GMCE threshold. **(B)** The temperature dependence of ΔT_{ad} (5 T) of ErN and HoN published in ref.[294] shows they are promising magnetocaloric refrigerants for cryogenic applications (note: ΔT_{ad} of Gd is ~11.6 K for the same magnetic field change, whose data is taken from ref. [58]). *Data from panel **(A)** are taken from [276-279]. Image **(B)** reproduced with permission from S. Nishio, T. Nakagawa, T. Arakawa, N. Tomioka, T.A. Yamamoto, T. Kusunose, et al., Specific heat and thermal conductivity of HoN and ErN at cryogenic temperatures, J. Appl. Phys. **99**(8), 08K901 (2006) [294].*

2.6 Rare-Earth Oxides

Magnetic oxides crystallize in a wide range of structures and exhibit diverse yet complex behavior that may involve non-collinear magnetism, ferrimagnetism, or multiple phase transitions along with structural changes. The presence of multiple magnetic atoms in the structures further results in distinct orderings for each species. For example, it is very common to include a transition metal (Mn, Cr, Fe, etc.) in the RE oxides, where the interaction between 3*d* and 4*f* electrons will significantly impact on the magnetic properties, and thus MCE, of the compounds, giving rise to distinctive features.

The wide tunable transition temperatures of RE oxides span from a few K to more than 1000 K; many of them are found at extremely low temperatures, typically below 10 K, while several others, including manganites, ferrites, spinels, etc., are at higher temperatures. For gas liquefaction using the MCE, we emphasize in this section the compounds with transition temperatures within our desired range, starting with simple oxides made up of one TM at the anion site (e.g., $RECrO_4$, $RETiO_3$, $REVO_4$, etc.), followed by double TM in the anion site, then garnets and other complex oxides.

2.6.1 RE oxides with a single TM at the anion-site

The simple RE oxides studied for MCE are typically of $RETMO_3$ and $RETMO_4$ stoichiometries, which exhibit the perovskite- and tetragonal zircon-type structures respectively. For the former, outstanding MCE values found in the GMCE-compliant region as shown in **Figure 23 (A)** are with TM = Ti, while in the $RETMO_4$ stoichiometry, they can be found for $RECrO_4$ or $REVO_4$ as well as for some of the spinel oxides. There is no other known simpler oxide that exhibits remarkable MCE besides the well-known EuO. With a Curie temperature of 69 K, this ferromagnetic binary oxide crystallizes in a NaCl-type structure and displays MCE of -17.5 J $kg^{-1}K^{-1}$, 6.8 K, and *RCP* of 665 J kg^{-1} for 5 T (-8.5 J $kg^{-1}K^{-1}$ and 3.2 K for 2 T) [297]. Even though it undergoes SOMT, its ΔT_{ad} values make it a promising SOMT refrigerant in this temperature range (despite having lower MCE values than the cryogenic compounds undergoing FOMT).

Rare-earth titanates ($RETiO_3$) are among the reported magnetocaloric oxides that exhibit simple FM ordering whose transition temperatures can be tuned within 30-70 K. $DyTiO_3$ single crystal was reported with a Curie temperature of 65 K, displaying -9.64 J $kg^{-1}K^{-1}$ (2 T) as shown in **Figure 23 (B)** [298], which scratches the lower limit of the GMCE threshold. This compound also stood out among the systematic studies of $RETiO_3$ family where RE = Dy, Ho, Er, Tm, or Yb described in ref. [299]. Although the MCE reported for a single $GdTiO_3$ crystal is not even close to the cutoff, it is interesting to note that as we advance away from the heavy RE, the table is reversed for $EuTiO_3$: both its single crystal and polycrystalline forms showed reversible GMCE values. Ref.[300] reports maximum $\Delta S_{isothermal}$ values of -11 (1 T) and -22.3 J kg^{-1} K^{-1} (2 T) at 5.5 K with negligible magnetic and thermal hysteresis. This was attributed to field-induced AFM-FM and FM-PM transitions. Larger $\Delta S_{isothermal}$ values are reported for $EuTiO_3$ compounds, for both single crystal and polycrystalline samples as shown in **Figure 23 (C)** and **(D)** [301]. This exceptional titanate was further investigated as $EuTi_{0.85}Nb_{0.15}O_3$ single crystal [302], in which the small Nb substitution at the Ti site enables the compound to reach FM metallic state. The reported parameters are T_C = 9.5 K and GMCE values (2 T) as high as -23.8 J kg^{-1} K^{-1} and 9.8 K in the absence of thermal and field hysteresis.

Published in Handbook on the Physics and Chemistry of Rare Earths, Volume 64 (2023) Pages 175-246
https://doi.org/10.1016/bs.hpcre.2023.10.004

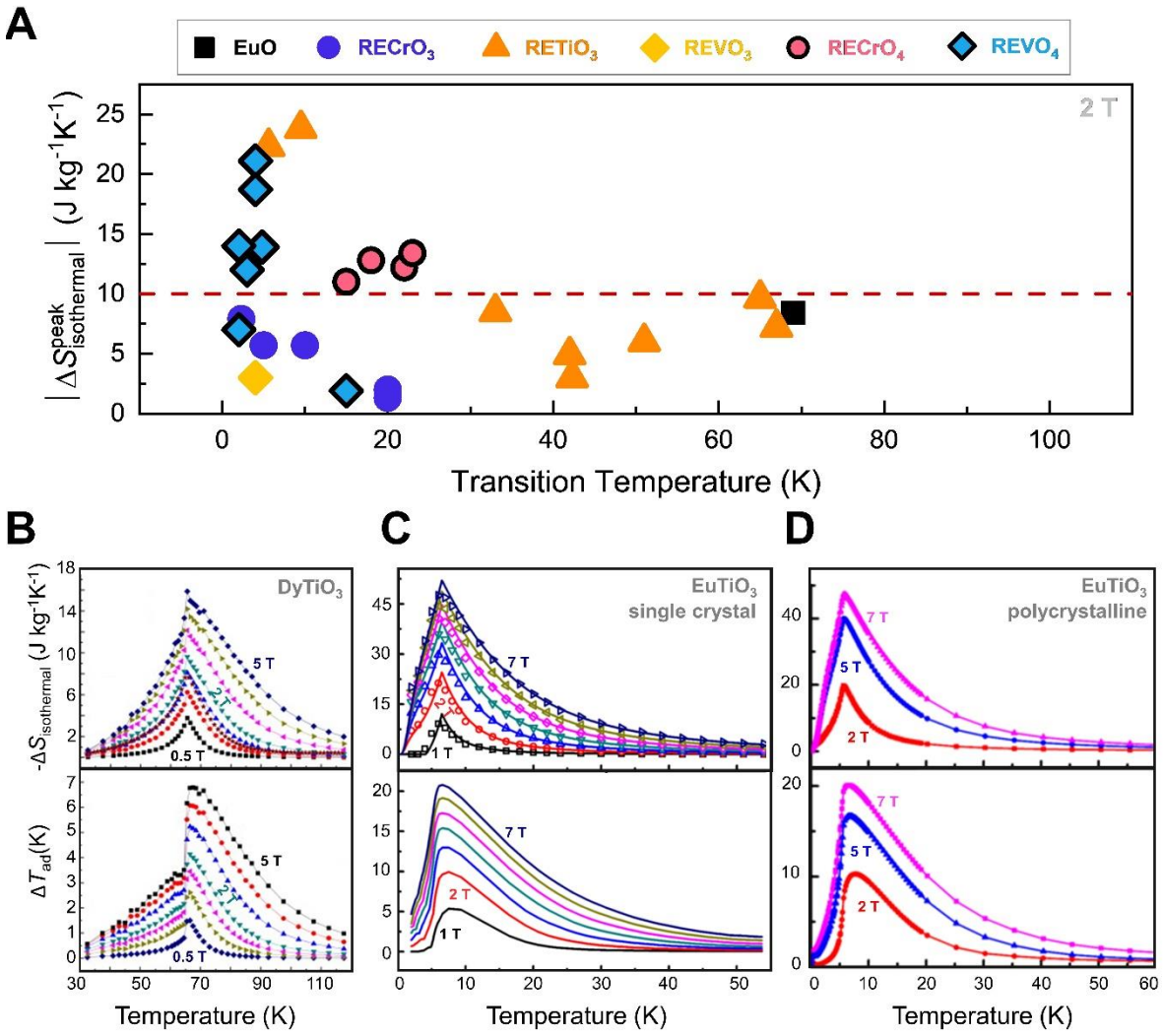

Figure 23. (A) MCE comparison of simple RE oxides for 2 T. Exceptional MCE meeting the GMCE threshold are found in $RETiO_3$ compounds: their temperature dependence of isothermal entropy change (top panels) and adiabatic temperature change (bottom panels) of **(B)** $DyTiO_3$ single crystal [298], **(C)** $EuTiO_3$ single crystal, and **(D)** $EuTiO_3$ polycrystalline samples. *Data from panel **(A)** are taken from [297, 303-310]. Images **(B)** to **(D)** are reproduced with permission from Y.T. Su, Y. Sui, X.J. Wang, J.G. Cheng, Y. Wang, W.F. Liu, et al., Large magnetocaloric properties in single-crystal dysprosium titanate, Mater. Lett. **72**, 15-17, © (2012) Elsevier [298] and A. Midya, P. Mandal, K. Rubi, R.F. Chen, J.S. Wang, R. Mahendiran, et al., Large adiabatic temperature and magnetic entropy changes in $EuTiO_3$, Phys. Rev. B **93**(9) (2016) 094422 [301]. © (2016) by the American Physical Society.*

Several RE vanadates with $REVO_4$ stoichiometry have been reported to possess excellent magnetocaloric properties, meeting the GMCE threshold. However, these properties are only observed at very low temperatures (many of them show AFM ordering below 5 K). Vanadates with RE = Gd, Tb, Dy, Ho, Er or Yb, have been studied for their MCE, where $GdVO_4$ shows exceptional MCE that falls within the threshold of GMCE magnitude: about -24 J $kg^{-1}K^{-1}$ (3 T)

at around 3 K [311]. This has been reported in two works [311, 312], where the former focused on magnetic structure and MCE while the latter provided a systematic investigation of the magnetic structure, MCE, and heat capacity of the compounds with RE = Gd, Ho, Er or Yb. Among them, only $GdVO_4$ and $ErVO_4$ exhibit MCE values that fall in the GMCE magnitude: for 2 T, $\Delta S_{isothermal} \sim$ -12 and -14 J kg^{-1} K^{-1}, respectively. An exceptional case was found for $DyVO_4$ as presented in **Figure 24 (A)**: its MCE value is about -13.9 at ~4.8 K (2 T) [309]. In addition, its ΔT_{ad} behavior (**Figure 24 (B)**) shows double peaks, one resulting from the AFM ordering of Dy^{3+} moments and the other from the structural change connected to the *4f* ferroquadrupolar ordering of Dy^{3+} ions. The authors attribute this GMCE to a field-induced metamagnetic transition at low magnetic fields, making it a suitable potential candidate for gas liquefaction applications. In another case, $TbVO_4$ single crystals have been found with very broad MCE along the easy magnetization *a*-axis [313].

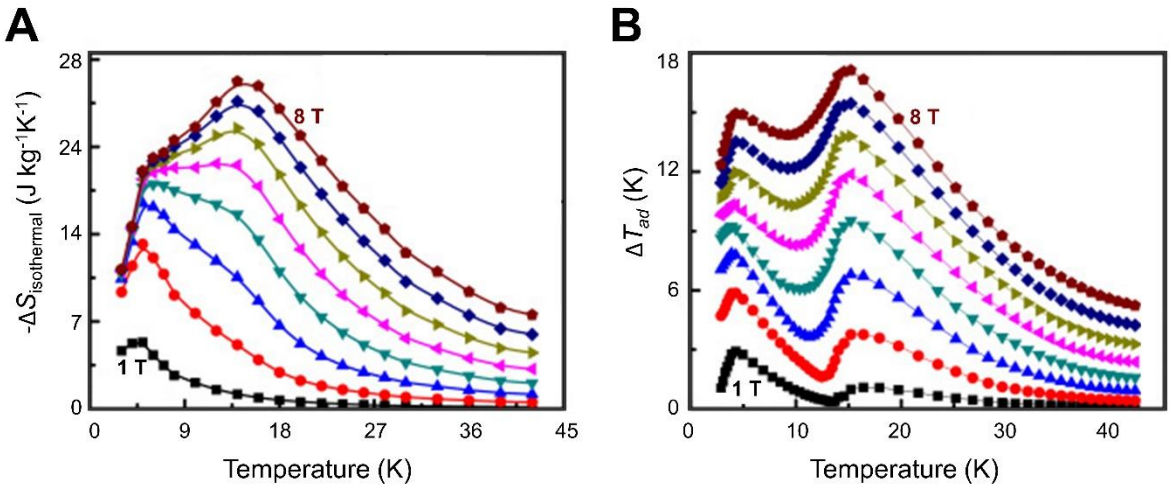

Figure 24. Remarkable MCE of $DyVO_4$ compound meeting the GMCE threshold: temperature dependence of **(A)** $\Delta S_{isothermal}$ and **(B)** ΔT_{ad}. *Reproduced with permission from A. Midya, N. Khan, D. Bhoi, P. Mandal, Giant magnetocaloric effect in antiferromagnetic $DyVO_4$ compound, Physica B **448**, 43-45, © (2014) Elsevier [309].*

There are mainly two groups of RE-Cr oxides studied for MCE: RE chromites, $RECrO_3$, and RE chromates, $RECrO_4$. The largest MCE found for the former is reported for $ErCrO_3$: -12.9 J $kg^{-1}K^{-1}$ for 5 T [314]. However, this magnitude cannot be considered large enough for a GMCE (although it is larger than 10 J kg^{-1} K^{-1}, the accepted threshold corresponds to a field of 2 T, which is not the case here), and we will advance the discussion to the second group – $RECrO_4$ family. Crystallizing in tetragonal zircon-type structure, $RECrO_4$ show complex magnetic properties caused by the competition between FM and AFM super exchange interactions of *3d* and *4f* spins. Typically, they behave as ferromagnets apart from RE = Gd, Ho, Dy, and Er, which have field-induced metamagnetic transitions. As a result, their MCE could reach at least -11 J kg^{-1} K^{-1} for 2 T, which meets the GMCE threshold [306-308]. Among them, $HoCrO_4$ shows

Published in Handbook on the Physics and Chemistry of Rare Earths, Volume 64 (2023) Pages 175-246
https://doi.org/10.1016/bs.hpcre.2023.10.004

a maximum $\Delta S_{isothermal}$ value of approximately -12.8 J kg^{-1} K^{-1} (2 T) with T_C = 18 K, and $DyCrO_4$ with approximately -13.4 J kg^{-1} K^{-1} (2 T) and T_C = 23 K [306]. **Figure 25** displays their reported MCE data, which show them to be a promising group of compounds for additional research.

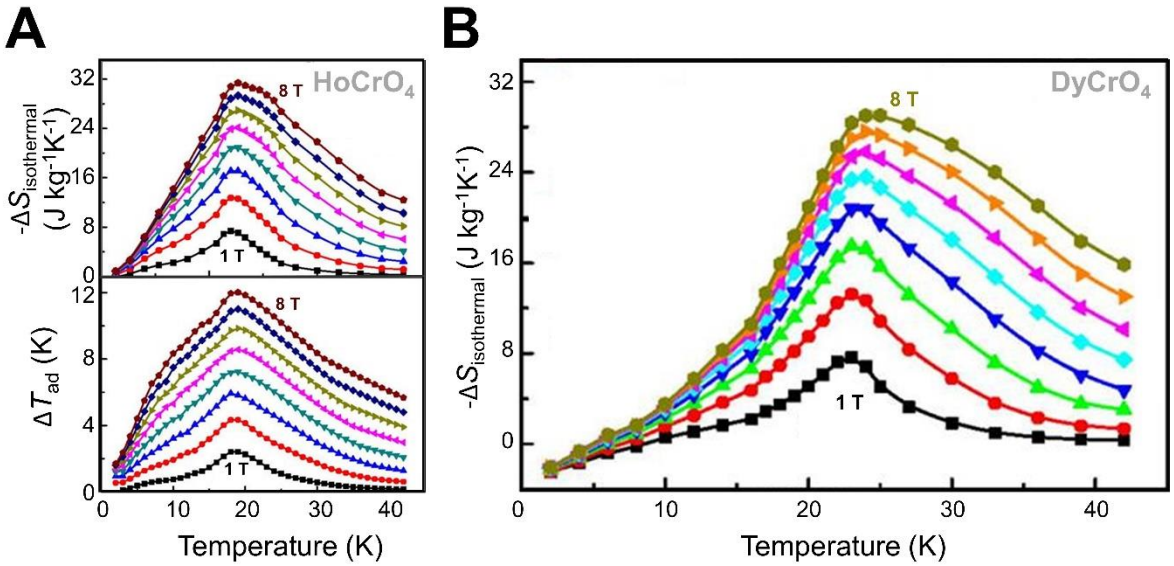

Figure 25. $RECrO_4$ compounds are one group of RE oxides that falls in the GMCE-compliant region where the MCE of **(A)** $HoCrO_4$ (top: $\Delta S_{isothermal}$; bottom: ΔT_{ad}) and **(B)** $DyCrO_4$ are a couple of examples. *Images are reproduced with permission from A. Midya, N. Khan, D. Bhoi, P. Mandal, 3d-4f spin interaction induced giant magnetocaloric effect in zircon-type $DyCrO_4$ and $HoCrO_4$ compounds, Appl. Phys. Lett.* ***103****(9) (2013) 092402 [306].*

In addition, very large $\Delta S^{R}_{isothermal}$ values were found for single crystals of rare-earth perovskites with $REFeO_3$ stoichiometry and exhibiting large anisotropy in various crystallographic directions [315-319]), reaching values as large as -11.9 to -16.62 J kg^{-1}K^{-1} (2 T) for RE = Tb[317], Dy[316] or Er [315]. These fall within the GMCE threshold and the rotational MCE data for $TbFeO_3$ are presented in **Figure 26** as an example.

The literature contains numerous magnetocaloric reports on manganites with $REMnO_3$ stoichiometry, including their single crystal investigations (for RE = Nd, Tb, Dy Ho or Tm). Their transition temperatures can be easily changed simply by modifying the elements or applying pressure (e.g., tunable transition temperature from ~100 to ~40 K for the $La_{0.65}Ca_{0.35}Ti_{1-x}Mn_xO_3$ system where x = 0 - 0.4 [320]). We will not go into further details on the MCE reported for the $REMnO_3$ family of compounds because, regrettably, they do not meet the GMCE threshold.

Published in Handbook on the Physics and Chemistry of Rare Earths, Volume 64 (2023) Pages 175-246
https://doi.org/10.1016/bs.hpcre.2023.10.004

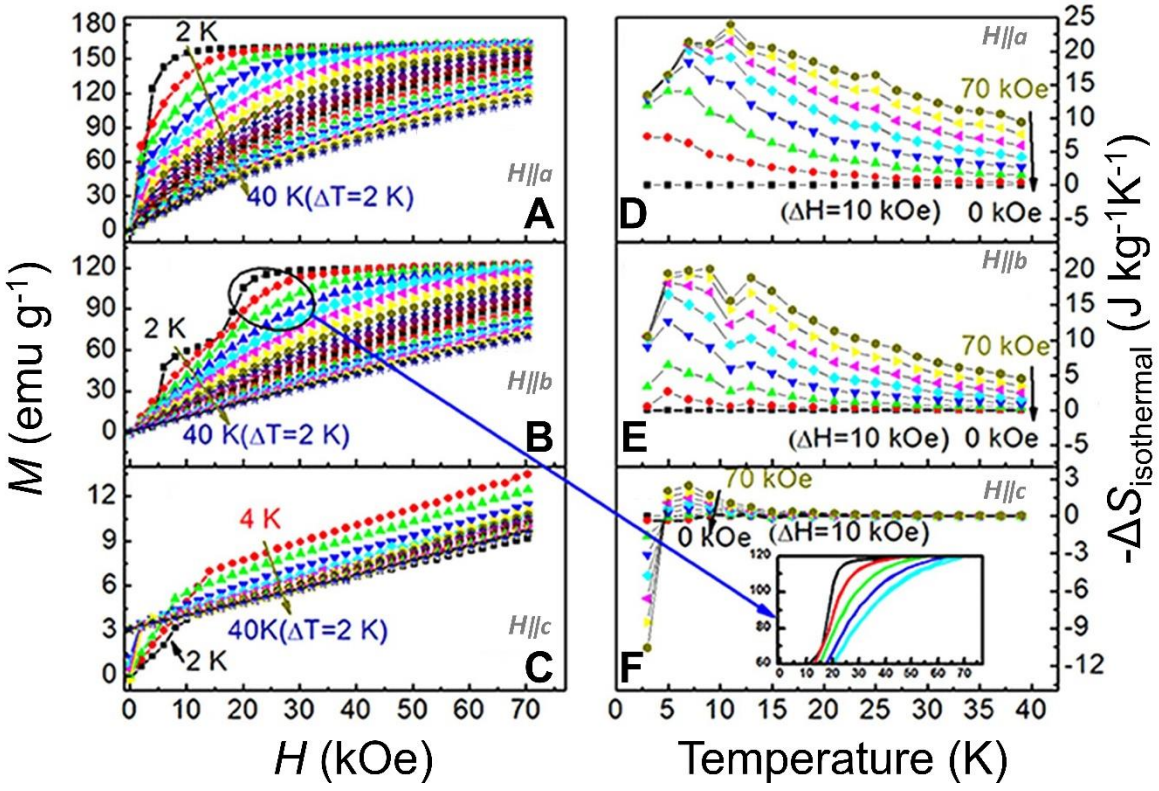

Figure 26. The magnetization isotherms of $TbFeO_3$ single crystal measured with increasing and decreasing magnetic fields within 2 – 10 K along the **(A)** *a*-, **(B)** *b*-, and **(C)** *c*-axes; Their corresponding isothermal entropy change along the **(D)** *a*-, **(E)** *b*-, and **(F)** *c*-axes, where the large anisotropic MCE along *a*-plane meets the GMCE threshold. The magnified subplot of the measurements along *b*-axis in panel **(F) s**hows minor hysteresis loss during the cycling process. *Images are reproduced from Y.J. Ke, X.Q. Zhang, Y. Ma, Z.H. Cheng, Anisotropic magnetic entropy change in $RFeO_3$ single crystals (R = Tb, Tm, or Y),, Sci. Rep.* ***6*** *(2016) 19775 [317] under an open access Creative Commons Attribution 4.0 International License.*

2.6.2 RE oxides with double TM at the anion-site

Furthermore, there are many MCE papers that report more complex stoichiometries of RE oxides, such as $RETM_2O_5$, $RE_2TM_2O_5$, $RETM_2O_6$, $RE_2TM_2O_6$ (sometimes classified as double perovskite) or $RE_2TM_2O_7$. During their systematic investigations, some of them were found to show large MCE values, but to display them, magnetic fields larger than 2 T were needed, so they do not meet the GMCE threshold. There are, however, others that meet this threshold as shown in the MCE performance comparison plot in **Figure 27 (a)**, and that will be further reviewed and discussed in this section.

Published in Handbook on the Physics and Chemistry of Rare Earths, Volume 64 (2023) Pages 175-246
https://doi.org/10.1016/bs.hpcre.2023.10.004

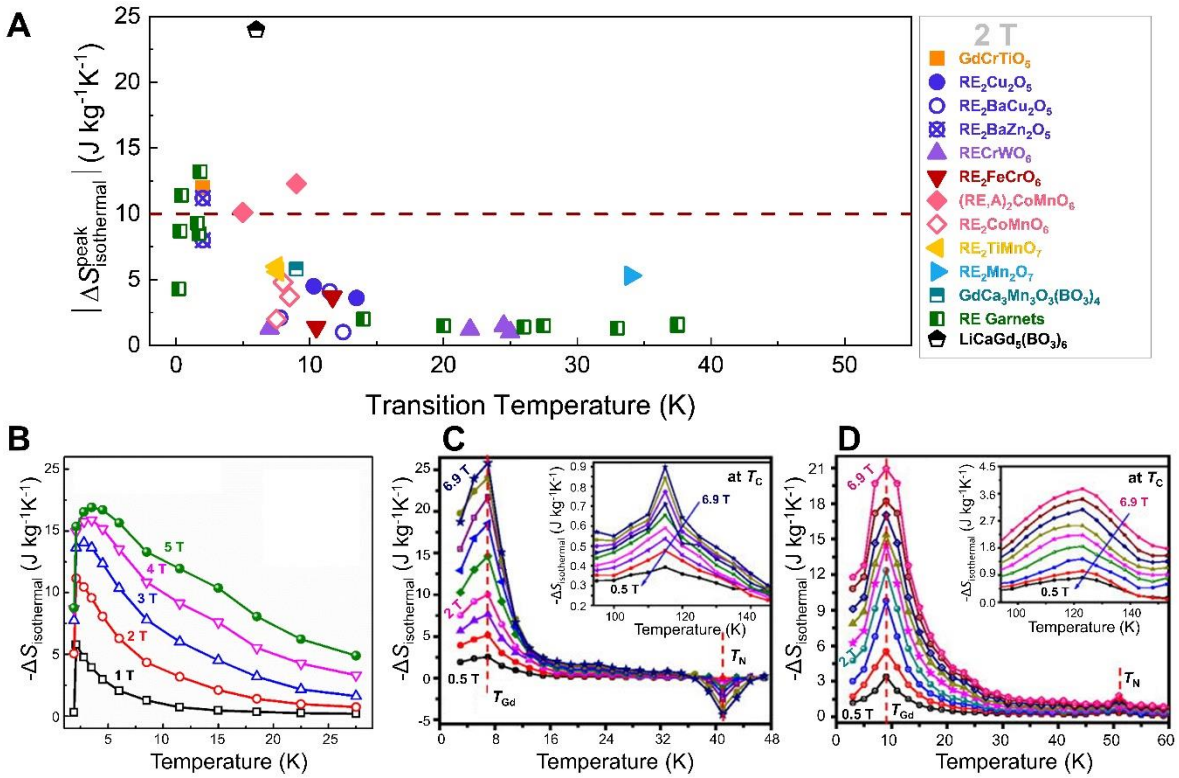

Figure 27. (A) MCE comparison (2 T) of complex RE oxides with double TM at the anion site. Those fulfilling the GMCE threshold are **(B)** $DyBaZnO_5$, **(C)** Gd_2CoMnO_6, and **(D)** $Gd_{2-x}Sr_xCoMnO_6$ (where x = 0.5). *Data from panel **(A)** are taken from [321-338]. The image in **(B)** is reproduced with permission from P. Xu, L. Hu, Z. Zhang, H. Wang, L. Li, Electronic structure, magnetic properties and magnetocaloric performance in rare earths (RE) based RE_2BaZnO_5 (RE = Gd, Dy, Ho, and Er) compounds, Acta Mater.* ***236****, 118114, © (2022) Elsevier [324]. Images **(C)** and **(D)** are reproduced with permission from R.C. Sahoo, S. Das, T.K. Nath, Role of Gd spin ordering on magnetocaloric effect and ferromagnetism in Sr-substituted Gd_2CoMnO_6 double perovskite, J. Appl. Phys.* ***124****(10) (2018) 103901 [328].*

Among the family of $RE_2TM_2O_5$, Dy_2BaZnO_5 was reported showing MCE of -11.2 J $kg^{-1}K^{-1}$ (2 T) at 2 K as depicted in **Figure 27 (B)** [324]. Experimental and computational results for RE = Gd, Ho or Er, were also reported. The RE_2BaZnO_5 compounds crystallize in two types of crystal structures depending on the RE selection: SG *I4/mcm* for RE = La, Nd; SG *Pnma* for RE = Eu, Gd, Tb, Dy, Ho, Er or Y.

In the $RE_2TM_2O_6$ family, Gd_2CoMnO_6 was found exhibiting MCE = -10.1 J $kg^{-1}K^{-1}$ (2 T), which could be improved to -12.3 J $kg^{-1}K^{-1}$ (2 T) by 25% Sr-substitution of Gd ions, resulting in $Gd_{1.5}Sr_{0.5}CoMnO_6$, both data being recorded at low temperatures [328]. These MCE results are presented in **Figure 27 (C)**. In this family of cobalt-manganese containing double perovskites, the GMCE observed at low temperature is attributed to 3*d* (Co^{2+}/Mn^{4+}) - O^{2-} and 4*f* (Gd^{3+}) exchange interaction. Meanwhile, at higher temperatures, the rock-salt like ordering of Co^{2+} and Mn^{4+} octahedra following a 180˚ super exchange contributes to a FM ordering. It is

interesting to note that doping divalent alkaline-earth metals (A') at the RE site will yield exciting phenomena, one of them being the change in the magnetic structure caused by the difference in the ionic radii between the RE^{3+} and A'^{2+} ions as the latter are bigger than the former, causing local distortion in the crystal structure. This will significantly affect the interactions of spins that are close to one another and cause the coupling strength to change. When RE is magnetic (e.g., Gd, Nd, etc.) while A is nonmagnetic (such as Sr, Ca, etc.), these effects are more pronounced. Thus, hole doping of Sr^{2+} at the Gd site of $(Gd_{1-x}Sr_x)_2CoMnO_6$ enhances ferromagnetism and in turn suppresses the inverse MCE without significantly affecting the overall magnetothermal response. The authors indicated that these facts can be best understood by the inverse Dzyaloshinskii-Moriya interaction mechanism.

2.6.3 RE garnets and other complex oxides

Since the earliest days of magnetocaloric studies, the MCE of RE garnets have been well understood [53]. Gadolinium gallium garnet, generally known as GGG, has long been recognized as the standard magnetocaloric material in cryogenic magnetic refrigeration because of the high $|\Delta S_{isothermal}|$ values it exhibits at 5 K [304]. $Dy_3Ga_5O_{12}$, $Dy_3CrGa_4O_{12}$ garnets also show MCE that meet the GMCE threshold: about -11.4 and -13.2 J $kg^{-1}K^{-1}$ (2 T) [335]. In addition, motivated by the enhanced magneto-optic characteristics found in $LiCaTb_5(BO_3)_6$ compared to the standard $Tb_3Ga_5O_{13}$ (TGG) crystal, due to the larger Tb concentration and the favorable site anisotropy of Tb^{3+} coordination environment [339], a theoretical analysis based on the single ion anisotropy found a significant MCE improvement over the notable GGG. This MCE enhancement was evidenced for both theoretical and experimental studies in $LiCaRE_5(BO_3)_6$ where RE = Gd or Tb: MCE values as large as -21.5 or -24 J $kg^{-1}K^{-1}$ (2 T) were measured [338]. For RE = Gd, measurements were performed on a powder sample, while for the other compound, studies were made on a single crystal. Another complex RE oxide displaying large MCE that meets the GMCE threshold is $KEr(MoO_4)_2$, which is an excellent candidate for cryogenic magnetic refrigeration [340]. The magnetic anisotropy of its single crystals gives a value of ~10 J $kg^{-1}K^{-1}$ (2 T) simply by rotating within the *ab* plane.

2.7 Upcoming systems that combine multiple properties for optimized performance: the high-entropy alloy concept

Despite the scarcity of reports, several magnetocaloric materials were developed using the high-entropy alloy (HEA) design concept. This concept emphasizes the central area of the phase diagram (represented as a ternary one in **Figure 28 (A)**), in which the configurational entropy of mixing, ΔS_{mix}, is greatly increased using a blend of several principal elements, rather than alloying elements to dilute a single base constituent (or two), as is the case with conventional alloy development. As a result, these new alloys are dubbed "high-entropy alloys."

HEA, by themselves, exhibit mechanical properties that outperform conventional alloys [341, 342], thereby underscoring the potential of HEA design in discovering new magnetocaloric materials with optimal mechanical stability. Their design concept was initially intended to produce single phase metallic solid solutions by using five or more principal elements in equimolar concentrations. It is important to note that HEA has evolved and now include both intermetallic and ceramic compounds, even with less than five principal elements and compositions that are not equimolar (for more information, readers may refer to [13, 46, 343]).

Most magnetocaloric HEA reports focus on amorphous structures, whose MCE values are within the range of conventional amorphous magnetocaloric materials that do not reach the GMCE threshold. It should be noted there were two milestones related to amorphous magnetocaloric alloys that sparked their investigation (presented in **Figure 28 (B)**): the MCE of Finemet-type alloy [344] and the discovery of universal curves for the magnetic field dependence of $\Delta S_{\text{isothermal}}$ [345, 346]. Unfortunately, the same applies to crystalline RE-HEA (their MCE does not meet the GMCE threshold). One of the primary reasons is their adhesion to the initial HEA design concept, which uses five or more principal elements in equiatomic amounts. For forming the amorphous phase in HEA, it is important to carefully select elements with different atomic radii and enthalpy of mixing (ΔH_{mix}) values, as is the case with RE-TM blend with stoichiometric compositions that fall within the predicted range for creating bulk metallic glass in the HEA space: atomic radius difference $\geq 9\%, -35 \leq \Delta H_{mix} \leq -8.5\ \text{kJ mol}^{-1}$ and $7 \leq \Delta S_{mix} \leq 14\ \text{J K}^{-1} \cdot \text{mol}^{-1}$ [347]. Gd, Tb, Dy, Ho, Er, and Tm, are the common choices for the RE site. Fe, Ni, Co, Cu, and Al are often selected as TM . Typically, in quinary HEAs, 60% of the principal elements are RE, resulting in properties similar to those found in amorphous RE-TM structures: broad magnetic ordering transitions and smeared-out MCE behavior. This also applies to quaternary RE-TM HEA. More principal elements in the HEA concept may result in dilution or complex interaction effects, though some of their MCE values are similar to those in amorphous RE-based alloys with high MCE values [348-353]. Therefore, when designing HEAs with only RE elements, it is essential to consider the effects of the composition on magnetic interactions and anisotropy.

Published in Handbook on the Physics and Chemistry of Rare Earths, Volume 64 (2023) Pages 175-246
https://doi.org/10.1016/bs.hpcre.2023.10.004

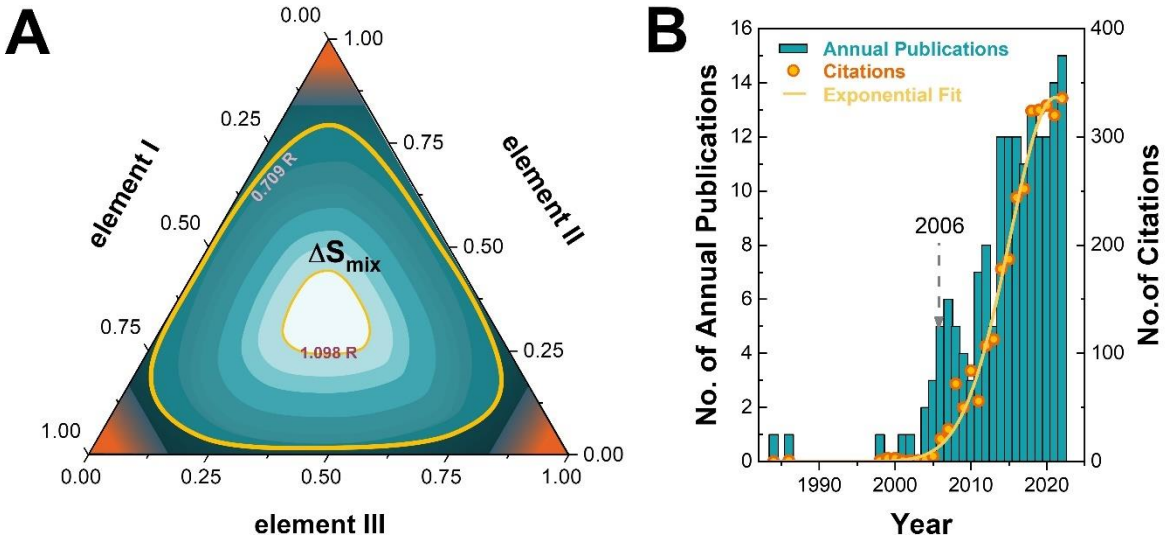

Figure 28. (A) Contour ΔS_{mix} plot of a model ternary alloy where the conventional alloy compositions are found at the corners and edges (*R* refers to the ideal gas constant). ΔS_{mix} values increase to maximum (at the center of the plot) where the elements are in equimolar concentrations. **(B)** Web of Science literature survey on the annual publications on amorphous magnetocaloric materials show a surge (left y-axis; bar graph) and an exponential fit to the citations (right y-axis; circles), both after the publication of refs. [344, 345] in 2006. Search terms include "amorphous" and "magnetocaloric" in the title field. *Under an open access Creative Commons Attribution 4.0 International License and © 2021 and 2023 Author(s), images **(A)** and **(B)** are reproduced from J.Y. Law, V. Franco, Review on magnetocaloric high-entropy alloys: Design and analysis methods, J. Mater. Res. **38**(1) (2023) 37-51 [13] and C. Romero-Muniz et al., Magnetocaloric materials for hydrogen liquefaction, The Innovations: Materials (2023) Accepted [52].*

Therefore, to fully take advantage of the HEA alloys characteristics, specifically their excellent mechanical properties, strategic approaches must be implemented to design high-quality magnetocaloric materials with a longer lifespan. This was recently tackled by targeted property search in the vast HEA space as it expands to non-equimolar concentrations (ΔS_{mix} threshold for HEA is at least 1.5 times of ideal gas constant, *R*, embracing the evolution of its definition). These studies have revealed that magnetocaloric HEA materials could perform similarly to high-performing conventional magnetocaloric materials (displayed in **Figure 29 (A)**): non-equiatomic $Fe_{0.222}Mn_{0.223}Ni_{0.222}(Ge,Si)_{0.333}$ HEA were tuned for undergoing FOMT, leading to MCE values as large as $\Delta S_{isothermal}$ = -10.2 J $kg^{-1}K^{-1}$ for the as-cast state [17, 18] and -18.0 J $kg^{-1}K^{-1}$ for the annealed counterparts [15] (2 T). They are the best performers among magnetocaloric HEA (**Figure 29 (B)**) and close the pre-existing gap between magnetocaloric HEA vs. conventional materials (**Figure 29 (C)**). They also meet the GMCE threshold; although HEA containing RE principal elements have not yet been reported, the targeted property search approach serves as a useful starting point. This topic has been recently discussed in a review on magnetocaloric HEA [13] regarding the potential of finding improved MCE in the non-

equiatomic HEA space. In addition, attempts have been made to apply the HEA concept to conventional high-performing magnetocaloric compounds. These include (Tb,Dy,Gd)$(Co,Fe)_2$ Laves phase [354-358], (Gd,Tb,Dy,Ho,Er)Al_2 Laves phase [359], and $(Ce,Pr,Nd)_2Fe_{17-x}Si_x$ compounds [360]. However, no reports have yet been made on adjusting their MCE to meet the GMCE threshold. Nevertheless, these findings offer valuable information on different ways of utilizing the revolutionary HEA concept to develop magnetocaloric materials that could ideally possess optimal magnetocaloric and mechanical properties.

Published in Handbook on the Physics and Chemistry of Rare Earths, Volume 64 (2023) Pages 175-246
https://doi.org/10.1016/bs.hpcre.2023.10.004

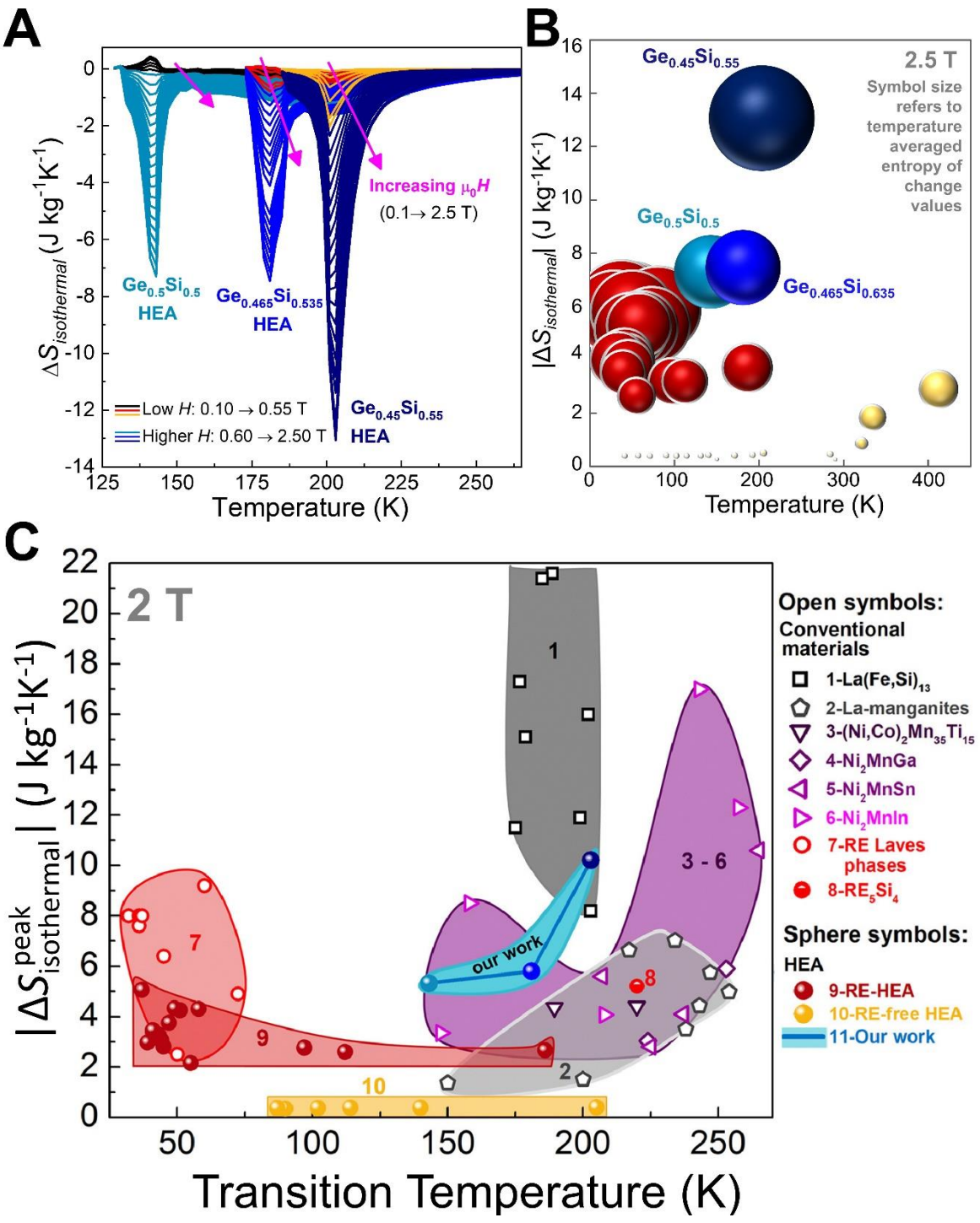

Figure 29. (A) The MCE results for FeMnSiGeSi HEA found by a targeted property strategic search meet the GMCE threshold and stand out as the best performer among magnetocaloric HEA **(B)**. **(C)** MCE comparison with conventional materials reveals they (bluish region) close the pre-existing gap between magnetocaloric HEA vs. notable $La(Fe,Si)_{13}$, Fe_2P and $Gd_5Si_2Ge_2$ systems. *Reproduced under an open access Creative Commons Attribution 4.0 International License and © 2021 and 2023 Author(s), images*

Published in Handbook on the Physics and Chemistry of Rare Earths, Volume 64 (2023) Pages 175-246
https://doi.org/10.1016/bs.hpcre.2023.10.004

***(A)**, **(B)** and **(C)** are adapted from J.Y. Law, Á. Díaz-García, L.M. Moreno-Ramírez, V. Franco, Increased magnetocaloric response of FeMnNiGeSi high-entropy alloys, Acta Mater. **212** (2021) 116931 [18].*

3 Performance and criticality

There is no doubt that it is important to have a good magnetocaloric response, however, economic factors are also crucial for the likelihood of practical technological applications being realized. It is particularly important to consider the material criticality for any application aiming to be implemented on a large scale, in order to ensure its long-term viability. We recently reviewed magnetocaloric materials for cryogenic applications and conducted a criticality assessment of all the materials we mentioned [52], which was usually disregarded in many other works. Based on the assessment of three crucial factors (supply risk, vulnerability to supply restrictions, and environmental implications), this concept, which was originally developed for metals, identifies which materials are most appropriate for a particular industrial production process. In this section, the assessment of performance and criticality will be focused on those materials with MCE standing on the shoulders of the "*giant* $Gd_5Si_2Ge_2$", including those highlighted in **Figure 2**.

Our evaluation employs the supply risk (*SRI*) and Economic Importance (*EI*) indices obtained from the "Study on Critical Raw Materials for the EU 2023" [361], by the European Commission, whose methodology has been established in cooperation with the Ad hoc Working Group on Defining Critical Raw Materials in 2017 [362]. The *SRI* calculates the likelihood that the supply chain will be disrupted by considering variables like supply concentration, import dependence, governance performance as measured by the World Governance Indicators, trade restrictions, and agreements, and the presence and importance of substitutes. The evolution of the criticality faced by RE elements from 2017 to 2023 is further highlighted in **Figure 30** for readers with further interest in evaluating their lanthanide-containing materials. For our assessment, we calculated the indices of the potential compound by taking the mass fraction of each element into account. In broad terms, the higher the indices, the more critical the material or element. Nevertheless, we follow the threshold of criticality zone recommended by the European Commission: $SRI \geqslant 1$ and $EI \geqslant 2.8$ (rounded to one decimal).

Published in Handbook on the Physics and Chemistry of Rare Earths, Volume 64 (2023) Pages 175-246
https://doi.org/10.1016/bs.hpcre.2023.10.004

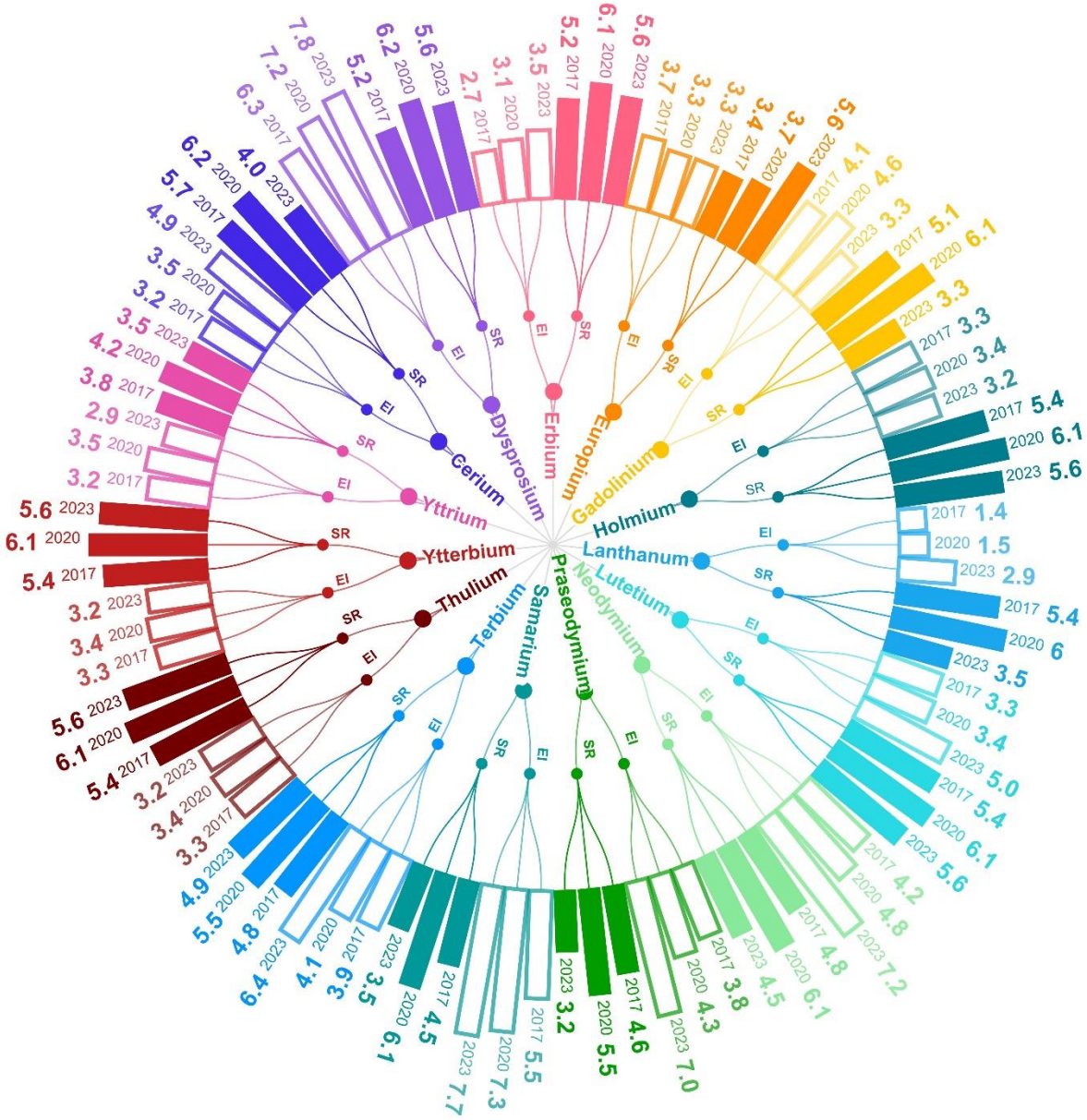

Figure 30. A radial chart illustrating the criticality faced by RE elements from 2017 to 2023. The criticality screening is based on Supply Risk (*SRI*) and Economic Importance (*EI*), whose values are calculated from a consolidated study on critical raw materials for European Union in ref. [361, 363, 364]. The cutoffs considered for criticality zone are $SRI \geqslant 1.0$ and $EI \geqslant 2.8$ rounded to one decimal.

Figure 31 maps the overall results for magnetocaloric performance (both $\Delta S_{isothermal}$ and transition temperature) versus the *SRI*, specifically for the materials standing on the "*giant* $Gd_5Si_2Ge_2$" (reviewed in earlier sections of this book chapter). Most of these compounds, which saturate at temperatures below 50 K, show medium to high *SRI*, implying their criticality at present. Among them, binary RE-metalloids based intermetallics exhibit a wide range of transition temperatures with excellent MCE while their *SRI* currently span between 2.5 and

Published in Handbook on the Physics and Chemistry of Rare Earths, Volume 64 (2023) Pages 175-246
https://doi.org/10.1016/bs.hpcre.2023.10.004

4.9. On the other hand, the compounds observed saturating at lower *SRI* (i.e., below 2) are mostly those highlighted in **Figure 2** and the binary RE intermetallics with magnetic TM elements, whose transition temperatures lie between 60 and 350 K.

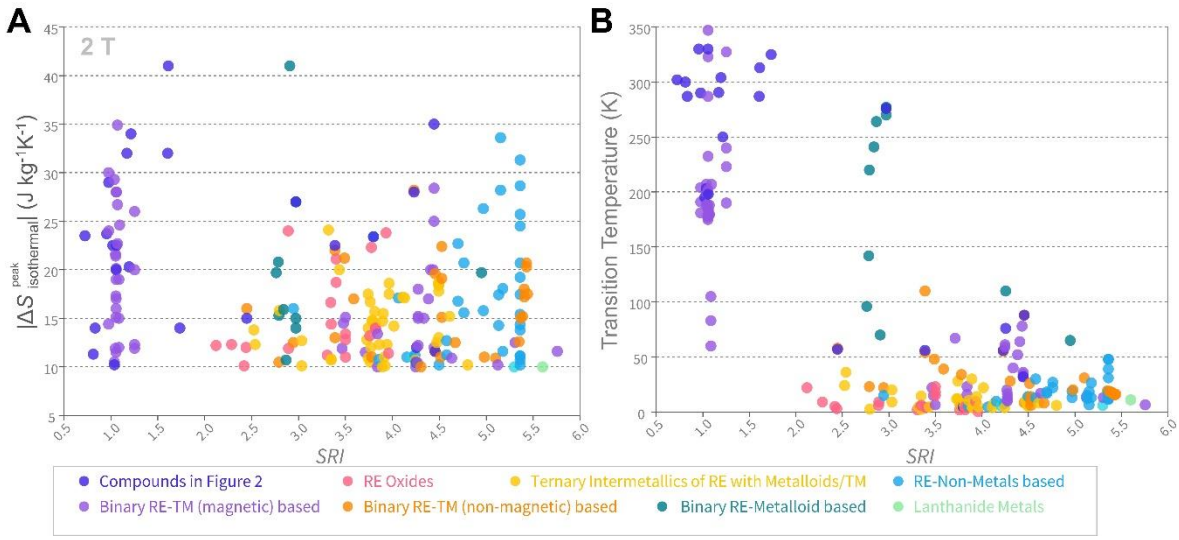

Figure 31. Performance comparison (2 T) of magnetocaloric materials standing on the "*giant* $Gd_5Si_2Ge_2$" including an assessment of their criticality supply risk index (*SRI*): **(A)** $\left|\Delta S^{\text{peak}}_{\text{isothermal}}\right|$ and **(B)** transition temperatures.

We present a further analysis of the compounds saturating below *SRI* < 2 in **Figure 32**. Several of them are RE-free compositions, while those containing RE elements belong to the $La(Fe,Si)_{13}$ family. The latter's *SRI* can range from 1.0 to 1.3 depending on their designed compositions, which shows that selecting and designing the right compositions is important for fine-tuning the material criticality. In this case, several critical elements, such as Ce, Nd, Pr, and/or Co, utilized in the substitutions contributed to the higher *SRI* of the $La(Fe,Si)_{13}$ family. Similarly, this is also true for compounds highlighted in **Figure 2**, such as HEA-FOMT, MM'X, NiMnSi-Fe_2Ge, whose material criticality is moderated by their less critical elements despite containing critical components. Therefore, the same strategy could be applied to low temperature magnetocaloric compounds that have high magnetocaloric performance, as shown in **Figure 31**. As a start, it might be a good idea to consider those with medium criticality: RE oxides, RE-metalloids-based intermetallics, RE with non-metals-based compounds, and even RE with metalloids/TM elements. For instance, HoCoGe and HoCoSi with $\left|\Delta S^{\text{peak}}_{\text{isothermal}}\right|$ (2 T) of 17.1 and 13 J kg^{-1}K^{-1} with transition temperatures of 7.6 and 14 K, show current *SRI* of 4.1 and 4.5 (rounded to one decimal), respectively. Other ternary systems, such as HoNiSi (-17.5 J kg^{-1}K^{-1}, 4.5 K, 4.0), HoCuSi (-16.7 J kg^{-1}K^{-1}, 7 K, 3.8), HoCuAl (-17.5 J kg^{-1}K^{-1}, 11.2 K, 3.7) and HoNiIn (-12.7 J kg^{-1}K^{-1}, 20 K, 3.0), exhibit comparable performance but have lower *SRI*. Therefore, it is

Published in Handbook on the Physics and Chemistry of Rare Earths, Volume 64 (2023) Pages 175-246
https://doi.org/10.1016/bs.hpcre.2023.10.004

possible to achieve good MCE performance by combining with less critical metals, such as Ni, Cu, Al, etc., and this implies that high-performing magnetocaloric materials at low temperatures are not restricted to high material criticalities.

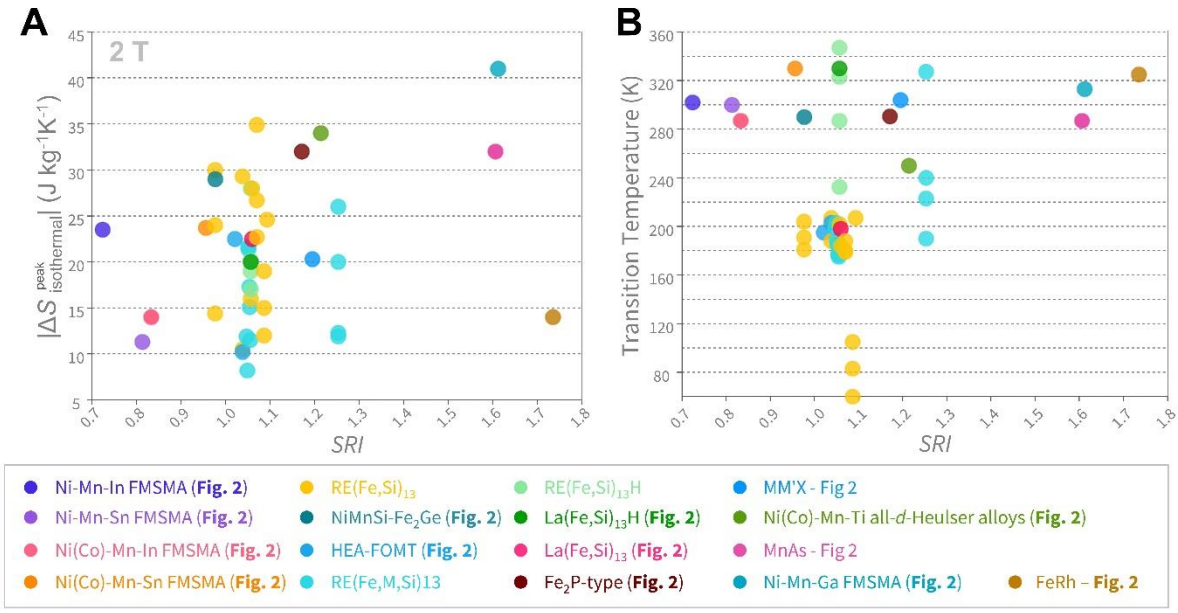

Figure 32. Performance comparison (2 T) of magnetocaloric materials standing on the "*giant* $Gd_5Si_2Ge_2$" with *SRI* lower than 2.0: **(A)** $\left|\Delta S^{peak}_{isothermal}\right|$ and **(B)** transition temperatures.

4 Epilogue and future outlook

Since the discovery of $Gd_5Si_2Ge_2$ and the subsequent use of the term "giant magnetocaloric effect (GMCE)" to describe it, research on magnetocaloric materials has evolved to focus on room-temperature applications as well as on the hunt for additional compounds that exhibit first-order thermomagnetic phase transition (FOMT). The "*giant* $Gd_5Si_2Ge_2$" led to the discovery of several new compounds showing FOMT and GMCE values, including MnAs, Fe_2P, $La(Fe,Si)_{13}$, MM'X, ferromagnetic shape memory alloys, RE_2In, and high-entropy alloys with FOMT (HEA-FOMT), etc. A wide array of variant compositions is also reported today for their families. As well as investigating their thermomagnetic and other properties to better understand their potential applications, magnetocaloric research led to the discovery of new quantitative criterion for evaluating the order of thermomagnetic phase transitions and the synergistic effect of multi-caloric effects aided by multi-stimuli.

Modern environmental concerns about energy and climate change today spurred interest in gas liquefaction applications, which has led to a resurgence of interest in cryogenic magnetocaloric materials. A large number of existing prototypes began testing with Gd, a

SOMT material but evolved to use FOMT compounds, such as Fe_2P-type and $NaZn_{13}$-type materials. Considering these are mainly for ambient temperature applications, the ultimate choice in material selection comes down to those with FOMT and RE-free compositions. Nevertheless, many of these compositions are not as effective at cryogenic temperatures, narrowing the options considerably for developing low-temperature prototypes. Therefore, cryogenic magnetocaloric materials ultimately rely on rare earth elements, which poses sustainability and material criticality concerns. Developing new materials with comparable or better magnetocaloric properties that are more sustainable and have a lower material criticality is therefore crucial. This can be achieved by compensating the critical elements for less critical ones during the search and development of materials that are optimized for cryogenic applications.

As a first step in this endeavor, this chapter identifies magnetocaloric compounds that stand on the "*giant* $Gd_5Si_2Ge_2$", i.e., compounds with large MCE values that meet the GMCE threshold. Their current criticality analysis was also performed, finding that their overall level of material criticality is medium to high. This will be useful for designing compositions with optimized performance and medium criticality by balancing critical and non-critical elements. Additionally, the upcoming material design concept, inspired by the HEA idea, has the potential to balance criticality in large proportions. It also offers combinatorial capabilities, such as large MCE values with optimized mechanical properties, and tunable transition temperatures and criticality. Through the recent discovery of a directed search strategy, the challenge of rationally searching the large HEA compositional space has been solved, so high-performance magnetocaloric compounds with material criticality can be realized soon for cryogenic applications.

5 Acknowledgements

Work funded by PID2019-105720RB-I00/AEI/10.13039/501100011033, Air Force Office of Scientific Research (FA8655-21-1-7044), the Clean Hydrogen Partnership and its members within the project HyLICAL (Grant no. 101101461), the European Innovation Council, funded by the European Union, via project CoCoMag (Grant no. 101099736), and the Research Council of Norway within project LIQUID-H is also acknowledged. J.Y.L. acknowledges EMERGIA 2021 fellowship from Junta de la Andalucía (ref. EMC21_00418).

6 References

[1] P. Weiss, A. Piccard, Le phénomène magnétocalorique, J. Phys. Theor. Appl. 7(1) (1917) 103-109.
[2] W.F. Giauque, D.P. MacDougall, Attainment of Temperatures Below 1° Absolute by Demagnetization of Gd_{2}(SO_{4})_{3}·8H_{2}O, Phys Rev 43(9) (1933) 768-768.
[3] V.K. Pecharsky, K.A. Gschneidner, Giant Magnetocaloric Effect in $Gd_5(Si_2Ge_2)$, Phys Rev Lett 78(23) (1997) 4494-4497.

[4] V.K. Pecharsky, K.A. Gschneidner, Magnetocaloric effect and magnetic refrigeration, J Magn Magn Mater 200(1-3) (1999) 44-56.
[5] S.A. Nikitin, G. Myalikgulyev, A.M. Tishin, M.P. Annaorazov, K.A. Asatryan, A.L. Tyurin, The magnetocaloric effect in Fe49Rh51 compound, Phys Lett A 148(6-7) (1990) 363-366.
[6] M.P. Annaorazov, K.A. Asatryan, G. Myalikgulyev, S.A. Nikitin, A.M. Tishin, A.L. Tyurin, Alloys of the Fe-Rh system as a new class of working material for magnetic refrigerators, Cryogenics 32(10) (1992) 867-872.
[7] Z.B. Guo, Y.W. Du, J.S. Zhu, H. Huang, W.P. Ding, D. Feng, Large magnetic entropy change in perovskite-type manganese oxides, Phys Rev Lett 78(6) (1997) 1142-1145.
[8] V.K. Pecharsky, K.A. Gschneidner, Tunable magnetic regenerator alloys with a giant magnetocaloric effect for magnetic refrigeration from similar to 20 to similar to 290 K, Appl Phys Lett 70(24) (1997) 3299-3301.
[9] K.A. Gschneidner, V.K. Pecharsky, Magnetocaloric materials, Annu Rev Mater Sci 30 (2000) 387-429.
[10] E. Bruck, Developments in magnetocaloric refrigeration, J Phys D Appl Phys 38(23) (2005) R381-R391.
[11] V. Franco, J.S. Blazquez, J.J. Ipus, J.Y. Law, L.M. Moreno-Ramirez, A. Conde, Magnetocaloric effect: From materials research to refrigeration devices, Prog Mater Sci 93 (2018) 112-232.
[12] L.M. Moreno-Ramírez, J.Y. Law, Á. Díaz-García, V. Franco, Advanced Magnetocaloric Materials, in Encyclopedia of Materials: Electronics, Elsevier, 1 (2023) 616-632, https://doi.org/10.1016/B978-0-12-819728-8.00068-1
[13] J.Y. Law, V. Franco, Review on magnetocaloric high-entropy alloys: Design and analysis methods, J Mater Res 38(1) (2023) 37-51.
[14] J.Y. Law, L.M. Moreno-Ramirez, Á. Díaz-García, V. Franco, Current perspective in magnetocaloric materials research, J Appl Phys 133 (2023) 040903.
[15] Á. Díaz-García, J.Y. Law, L.M. Moreno-Ramirez, R. Schäfer, V. Franco, Unpublished, (2023).
[16] A. Biswas, R.K. Chouhan, A. Thayer, Y. Mudryk, I.Z. Hlova, O. Dolotko, V.K. Pecharsky, Unusual first-order magnetic phase transition and large magnetocaloric effect in Nd_2In, Physical Review Materials 6(11) (2022) 114406.
[17] J.Y. Law, L.M. Moreno-Ramírez, Á. Díaz-García, A. Martín-Cid, S. Kobayashi, S. Kawaguchi, T. Nakamura, V. Franco, MnFeNiGeSi high-entropy alloy with large magnetocaloric effect, J Alloy Compd 855 (2021) 157424.
[18] J.Y. Law, Á. Díaz-García, L.M. Moreno-Ramírez, V. Franco, Increased magnetocaloric response of FeMnNiGeSi high-entropy alloys, Acta Mater 212 (2021) 116931.
[19] A. Biswas, N.A. Zarkevich, A.K. Pathak, O. Dolotko, I.Z. Hlova, A.V. Smirnov, Y. Mudryk, D.D. Johnson, V.K. Pecharsky, First-order magnetic phase transition in Pr_2In with negligible thermomagnetic hysteresis, Phys Rev B 101(22) (2020) 224402.
[20] F. Guillou, A.K. Pathak, D. Paudyal, Y. Mudryk, F. Wilhelm, A. Rogalev, V.K. Pecharsky, Non-hysteretic first-order phase transition with large latent heat and giant low-field magnetocaloric effect, Nat. Commun. 9(1) (2018) 2925.
[21] Z.Y. Wei, E.K. Liu, J.H. Chen, Y. Li, G.D. Liu, H.Z. Luo, X.K. Xi, H.W. Zhang, W.H. Wang, G.H. Wu, Realization of multifunctional shape-memory ferromagnets in all-d-metal Heusler phases, Appl Phys Lett 107(2) (2015) 022406.
[22] H. Wada, S. Tomekawa, M. Shiga, Magnetocaloric properties of a first-order magnetic transition system $ErCo_2$, Cryogenics 39(11) (1999) 915-919.
[23] H. Wada, Y. Tanabe, Giant magnetocaloric effect of $MnAs_{1-x}Sb_x$, Appl Phys Lett 79(20) (2001) 3302-3304.
[24] T. Samanta, D.L. Lepkowski, A.U. Saleheen, A. Shankar, J. Prestigiacomo, I. Dubenko, A. Quetz, I.W.H. Oswald, G.T. McCandless, J.Y. Chan, P.W. Adams, D.P. Young, N. Ali, S. Stadler, Hydrostatic pressure-induced modifications of structural transitions lead to large enhancements of magnetocaloric effects in MnNiSi-based systems, Phys Rev B 91(2) (2015) 5.
[25] J.C.B. Monteiro, R.D. dos Reis, F.G. Gandra, The physical properties of Gd3Ru: A real candidate for a practical cryogenic refrigerator, Appl Phys Lett 106(19) (2015) 194106.
[26] D.X. Li, T. Yamamura, S. Nimori, Y. Homma, F. Honda, D. Aoki, Giant and isotropic low temperature magnetocaloric effect in magnetic semiconductor EuSe, Appl Phys Lett 102(15) (2013) 152409.
[27] E. Talik, M. Klimczak, Giant magnetocaloric effect in Tb3Rh, J Alloy Compd 486(1-2) (2009) L30-L33.
[28] C.L. Zhang, D.H. Wang, Q.Q. Cao, Z.D. Han, H.C. Xuan, Y.W. Du, Magnetostructural phase transition and magnetocaloric effect in off-stoichiometric Mn1.9-xNixGe alloys, Appl Phys Lett 93(12) (2008) 122505.

[29] T. Krenke, E. Duman, M. Acet, E.F. Wassermann, X. Moya, L. Manosa, A. Planes, Inverse magnetocaloric effect in ferromagnetic Ni-Mn-Sn alloys, Nat Mater 4(6) (2005) 450-454.
[30] F. Albertini, F. Canepa, S. Cirafici, E.A. Franceschi, M. Napoletano, A. Paoluzi, L. Pareti, M. Solzi, Composition dependence of magnetic and magnetothermal properties of Ni-Mn-Ga shape memory alloys, J Magn Magn Mater 272 (2004) 2111-2112.
[31] M. Pasquale, C.P. Sasso, L.H. Lewis, Magnetic entropy in Ni2MnGa single crystals, J Appl Phys 95(11) (2004) 6918-6920.
[32] A. Fujita, S. Fujieda, Y. Hasegawa, K. Fukamichi, Itinerant-electron metamagnetic transition and large magnetocaloric effects in $La(Fe_xSi_{1-x})_{13}$ compounds and their hydrides, Phys Rev B 67(10) (2003) 104416.
[33] O. Tegus, E. Bruck, K.H.J. Buschow, F.R. de Boer, Transition-metal-based magnetic refrigerants for room-temperature applications, Nature 415(6868) (2002) 150-152.
[34] F.X. Hu, B.G. Shen, J.R. Sun, Z.H. Cheng, G.H. Rao, X.X. Zhang, Influence of negative lattice expansion and metamagnetic transition on magnetic entropy change in the compound LaFe11.4Si1.6, Appl Phys Lett 78(23) (2001) 3675-3677.
[35] E. Bruck, O. Tegus, X.W. Li, F.R. de Boer, K.H.J. Buschow, Magnetic refrigeration towards room-temperature applications, Physica B 327(2-4) (2003) 431-437.
[36] J. Lai, X. You, J. Law, V. Franco, B. Huang, D. Bessas, M. Maschek, D. Zeng, N. van Dijk, E. Brück, Ultra-low hysteresis in giant magnetocaloric Mn1-V Fe0.95(P,Si,B) compounds, J Alloy Compd 930 (2023) 167336.
[37] V. Franco, J.Y. Law, A. Conde, V. Brabander, D. Karpenkov, I. Radulov, K. Skokov, O. Gutfleisch, Predicting the tricritical point composition of a series of LaFeSi magnetocaloric alloys via universal scaling, Journal of Physics D: Applied Physics 50(41) (2017) 414004.
[38] J.Y. Law, V. Franco, L.M. Moreno-Ramirez, A. Conde, D.Y. Karpenkov, I. Radulov, K.P. Skokov, O. Gutfleisch, A quantitative criterion for determining the order of magnetic phase transitions using the magnetocaloric effect, Nat. Commun. 9(1) (2018) 2680.
[39] L.M. Moreno-Ramírez, J.Y. Law, J.M. Borrego, A. Barcza, J.-M. Greneche, V. Franco, First-order phase transition in high-performance La(Fe,Mn,Si)13H despite negligible hysteresis, J Alloy Compd 950 (2023) 169883.
[40] Á. Díaz-García, J. Revuelta, L.M. Moreno-Ramírez, J.Y. Law, C. Mayer, V. Franco, Additive manufacturing of magnetocaloric $(La,Ce)(Fe,Mn,Si)_{13}$–H particles via polymer-based composite filaments, Composites Communications 35 (2022) 101352.
[41] J.Y. Law, V. Franco, Magnetocaloric Composite Materials, in Encyclopedia of Materials: Composites, Elsevier, 2 (2021) 461-472, https://doi.org/10.1016/b978-0-12-819724-0.00038-0
[42] X. Lu, S. Zeng, Y. Zhang, P. Zhang, Q. Jiang, J. Liu, Effect of annealing on microstructure and magnetocaloric properties of plastically deformed La0.7Ce0.3Fe13.68Mn0.2Si1.4 alloys, Journal of Materials Research and Technology 18 (2022) 2282-2291.
[43] J. Lai, H. Sepehri-Amin, X. Tang, J. Li, Y. Matsushita, T. Ohkubo, A.T. Saito, K. Hono, Reduction of hysteresis in (La1-xCex) y(MnzFe11.4-z)Si1.6 magnetocaloric compounds for cryogenic magnetic refrigeration, Acta Mater 220 (2021) 117286.
[44] E.K. Liu, W.H. Wang, L. Feng, W. Zhu, G.J. Li, J.L. Chen, H.W. Zhang, G.H. Wu, C.B. Jiang, H.B. Xu, F. de Boer, Stable magnetostructural coupling with tunable magnetoresponsive effects in hexagonal ferromagnets, Nat. Commun. 3 (2012) 873.
[45] T. Samanta, I. Dubenko, A. Quetz, S. Stadler, N. Ali, Giant magnetocaloric effects near room temperature in Mn1-xCuxCoGe, Appl Phys Lett 101(24) (2012) 242405.
[46] J.Y. Law, V. Franco, Pushing the limits of magnetocaloric high-entropy alloys, APL Materials 9(8) (2021) 080702.
[47] M. Li, Y. Bai, C. Zhang, Y. Song, S. Jiang, D. Grouset, M. Zhang, Review on the research of hydrogen storage system fast refueling in fuel cell vehicle, Int J Hydrogen Energ 44(21) (2019) 10677-10693.
[48] M. Aziz, Liquid Hydrogen: A Review on Liquefaction, Storage, Transportation, and Safety, Energies 14(18) (2021).
[49] A. Kitanovski, Energy Applications of Magnetocaloric Materials, Advanced Energy Materials 10(10) (2020) 1903741.
[50] V. Franco, Magnetocaloric Characterization of Materials, in Magnetic Measurement Techniques for Materials Characterization, Springer International Publishing, (2021) 697-726, https://doi.org/10.1007/978-3-030-70443-8_23

[51] V. Franco, Á. Díaz-García, L.M. Moreno-Ramirez, J.Y. Law, Magnetocaloric Characterization for the Study of Phase Transitions, in Magnetic Cooling: From fundamentals to high efficiency refrigeration Wiley. In press, (2023)
[52] C. Romero-Muniz, J.Y. Law, J. Revuelta-Losada, L.M. Moreno-Ramirez, V. Franco, Magnetocaloric materials for hydrogen liquefaction, The Innovations: Materials (2023) Accepted.
[53] A.M. Tishin, Y.I. Spichkin, The Magnetocaloric Effect and its Applications, Institute of Physics Publishing, Bristol, 2003.
[54] T. Johansson, B. Lebech, M. Nielsen, H.B. Møller, A.R. Mackintosh, Crystal Fields and the Magnetic Properties of Praseodymium and Neodymium, Phys Rev Lett 25(8) (1970) 524-526.
[55] C.B. Zimm, P.M. Ratzmann, J.A. Barclay, G.F. Green, J.N. Chafe, The Magnetocaloric Effect in Neodymium, in Advances in Cryogenic Engineering Materials: Part A, Springer US, (1990) 763-768, https://doi.org/10.1007/978-1-4613-9880-6_99
[56] K.A. Gschneidner, V.K. Pecharsky, The influence of magnetic field on the thermal properties of solids, Mat Sci Eng a-Struct 287(2) (2000) 301-310.
[57] N. Terada, H. Mamiya, High-efficiency magnetic refrigeration using holmium, Nat. Commun. 12(1) (2021) 1212.
[58] K.A. Gschneidner, V.K. Pecharsky, A.O. Tsokol, Recent developments in magnetocaloric materials, Rep Prog Phys 68(6) (2005) 1479-1539.
[59] Y. Mudryk, V.K. Pecharsky, K.A. Gschneidner, Chapter 262 - R5T4 Compounds: An Extraordinary Versatile Model System for the Solid State Science, in Handbook on the Physics and Chemistry of Rare Earths, Elsevier, 44 (2014) 283-449, https://doi.org/10.1016/B978-0-444-62711-7.00262-0
[60] V.K. Pecharsky, K.A. Gschneidner, Phase relationships and crystallography in the pseudobinary system Gd5Si4 Gd5Ge4, J Alloy Compd 260(1) (1997) 98-106.
[61] K.A. Gschneidner, V.K. Pecharsky, A.O. Pecharsky, V.V. Ivtchenko, E.M. Levin, The nonpareil R-5(SixGe1-x)(4) phases, J Alloy Compd 303 (2000) 214-222.
[62] V.V. Ivtchenko, V.K. Pecharsky, K.A. Gschneidner, Magnetothermal Properties of Dy5(SixGe1−x)4 Alloys, in Advances in Cryogenic Engineering Materials: Volume 46, Part A, Springer US, (2000) 405-412, https://doi.org/10.1007/978-1-4615-4293-3_52
[63] Y.I. Spichkin, V.K. Pecharsky, K.A. Gschneidner, Preparation, crystal structure, magnetic and magnetothermal properties of (GdxR5-x)Si-4, where R=Pr and Tb, alloys, J Appl Phys 89(3) (2001) 1738-1745.
[64] H. Huang, A.O. Pecharsky, V.K. Pecharsky, K.A. Gschneidner, Preparation, crystal structure and magnetocaloric properties of Tb-5(SixGe4-x), in Advances in Cryogenic Engineering, Vols 48a and B, Amer Inst Physics, 614 (2002) 11-18,
[65] A.O. Pecharsky, K.A. Gschneidner, V.K. Pecharsky, The giant magnetocaloric effect of optimally prepared Gd5Si2Ge2, J Appl Phys 93(8) (2003) 4722-4728.
[66] D.H. Ryan, M. Elouneg-Jamroz, J. van Lierop, Z. Altounian, H.B. Wang, Field and temperature induced magnetic transition in Gd_5Sn_4: A giant magnetocaloric material, Phys Rev Lett 90(11) (2003) 117202.
[67] Y. Zhuo, R. Chahine, T.K. Bose, Magnetic entropy change in the Ge-rich alloys Gd-Si-Ge, Ieee T Magn 39(5) (2003) 3358-3360.
[68] A.O. Pecharsky, K.A. Gschneidner, V.K. Pecharsky, D.L. Schlagel, T.A. Lograsso, Phase relationships and structural, magnetic, and thermodynamic properties of alloys in the pseudobinary Er5Si4-Er5Ge4 system, Phys Rev B 70(14) (2004) 144419.
[69] L. Morellon, P.A. Algarabel, C. Magen, M.R. Ibarra, Giant magnetoresistance in the Ge-rich magnetocaloric compound, Gd-5(Si0.1Ge0.9)(4), J Magn Magn Mater 237(2) (2001) 119-123.
[70] R. Nirmala, D.C. Kundaliya, S.R. Shinde, A.G. Joshi, A.V. Morozkin, S.K. Malik, Magnetism and magnetocaloric effect in (DyxGd5-x)Si2Ge2 (0 <= x <= 5) compounds, J Appl Phys 101(12) (2007) 123901.
[71] R. Nirmala, A.K. Nigam, S.K. Malik, Magnetic and magnetocaloric properties of Tb5Si2Sb2, Solid State Commun 146(3-4) (2008) 121-123.
[72] H. Zhang, Y. Mudryk, Q. Cao, V.K. Pecharsky, K.A. Gschneidner, Y. Long, Phase relationships, and structural, magnetic, and magnetocaloric properties in the Ce_5Si_4-Ce_5Ge_4 system, J Appl Phys 107(1) (2010) 013909.
[73] A.M.G. Carvalho, J.C.G. Tedesco, M.J.M. Pires, M.E. Soffner, A.O. Guimaraes, A.M. Mansanares, A.A. Coelho, Large magnetocaloric effect and refrigerant capacity near room temperature in as-cast Gd5Ge2Si2-xSnx compounds, Appl Phys Lett 102(19) (2013) 192410.

[74] R. Nirmala, A.V. Morozkin, R. Rajivgandhi, A.K. Nigam, S. Quezado, S.K. Malik, Metamagnetism-enhanced magnetocaloric effect in the rare earth intermetallic compound Ho5Ge4, J Magn Magn Mater 418 (2016) 118-121.
[75] K. Matsumoto, T. Okano, T. Kouen, S. Abe, T. Numazawa, K. Kamiya, S. Nimori, Magnetic entropy change of magnetic refrigerants with first order phase transition suitable for hydrogen refrigeration, Ieee T Appl Supercon 14(2) (2004) 1738-1741.
[76] Y. Mudryk, D. Paudyal, V.K. Pecharsky, K.A. Gschneidner, Magnetostructural transition in Gd5Si0.5Ge3.5: Magnetic and x-ray powder diffraction measurements, and theoretical calculations, Phys Rev B 77(2) (2008) 024408.
[77] R. Rawat, I. Das, The similar dependence of the magnetocaloric effect and magnetoresistance in TmCu and TmAg compounds and its implications, J Phys-Condens Mat 13(19) (2001) L379-L387.
[78] V.S.R. de Sousa, P.J. von Ranke, F.C.G. Gandra, The influence of spontaneous and field-induced spin reorientation transitions on the magnetocaloric properties of HoZn and ErZn, J Appl Phys 109(6) (2011) 063904.
[79] L.W. Li, Y. Yuan, Y.K. Zhang, T. Namiki, K. Nishimura, R. Pottgen, S.Q. Zhou, Giant low field magnetocaloric effect and field-induced metamagnetic transition in TmZn, Appl Phys Lett 107(13) (2015) 132401.
[80] L.W. Li, Y. Yuan, Y.K. Zhang, R. Pottgen, S.Q. Zhou, Magnetic phase transitions and large magnetic entropy change with a wide temperature span in HoZn, J Alloy Compd 643 (2015) 147-151.
[81] L.W. Li, Y. Yuan, C. Xu, Y. Qi, S.Q. Zhou, Observation of large magnetocaloric effect in equiatomic binary compound ErZn, Aip Advances 7(5) (2017) 5.
[82] J.Y. Law, L.M. Moreno-Ramírez, J.S. Blázquez, V. Franco, A. Conde, Gd+GdZn biphasic magnetic composites synthesized in a single preparation step: Increasing refrigerant capacity without decreasing magnetic entropy change, J Alloy Compd 675 (2016) 244-247.
[83] X.J. Wang, L.J. Wang, Q.M. Ma, G. Sun, Y.K. Zhang, J.Z. Cui, Magnetic phase transitions and large magnetocaloric effects in equiatomic binary DyZn compound, J Alloy Compd 694 (2017) 613-616.
[84] L. Li, Y. Yuan, Y. Qi, Q. Wang, S. Zhou, Achievement of a table-like magnetocaloric effect in the dual-phase ErZn2/ErZn composite, Materials Research Letters 6(1) (2018) 67-71.
[85] C.L. Wang, J.D. Zou, J. Liu, Y. Mudryk, K.A. Gschneidner, Y. Long, V. Smetana, G.J. Miller, V.K. Pecharsky, Crystal structure, magnetic properties, and the magnetocaloric effect of Gd_5Rh_4 and GdRh, J Appl Phys 113(17) (2013).
[86] W. Hermes, T. Harmening, R. Pottgen, Ferromagnetism and Magnetocaloric Effect around 95 K in the Laves Phase EuRh1.2Zn0.8, Chem Mater 21(14) (2009) 3325-3331.
[87] Y.J. Wang, Y.S. Du, Y.Q. Zhang, L. Li, L. Ma, J. Wang, J.T. Zhao, G.H. Rao, Low-temperature magnetic properties and large magnetocaloric effects in the RE_3Rh_2 (RE = Nd, Ho and Er) intermetallics, Intermetallics 127 (2020) 106989.
[88] P. Kumar, N.K. Singh, A.K. Nayak, A. Haldar, K.G. Suresh, A.K. Nigam, Large reversible magnetocaloric effect in Er3Co compound, J Appl Phys 107(9) (2010) 09A932.
[89] L.H. Yang, H. Zhang, F.X. Hu, J.R. Sun, L.Q. Pan, B.G. Shen, Magnetic and magnetocaloric properties of equiatomic alloys RAl (R = Ho and Er), J Alloy Compd 596 (2014) 58-62.
[90] K.A. Gschneidner, H. Takeya, J.O. Moorman, V.K. Pecharsky, (Dy0.5Er0.5)Al2: A large magnetocaloric effect material for low temperature magnetic refrigeration, Appl Phys Lett 64(2) (1994) 253-255.
[91] V.K. Pecharsky, K.A. Gschneidner, S.Y. Dan'kov, A.M. Tishin, Magnetocaloric properties of Gd3Al2, Kluwer Academic/Plenum Publ, New York, 1999.
[92] J.Q. Deng, J.L. Yan, J.L. Huang, J.M. Zhu, X. Chen, Y.H. Zhuang, The influence of Co substitution on the magnetocaloric effect of Gd(Al,Fe)(2), Phys Scripta 75(5) (2007) 604-607.
[93] H. Zhang, Z.Y. Xu, X.Q. Zheng, J. Shen, F.X. Hua, J.R. Sun, B.G. Shen, Giant magnetic refrigerant capacity in Ho3Al2 compound, Solid State Commun 152(13) (2012) 1127-1130.
[94] M.M. Prusty, J.A. Chelvane, A.V. Morozkin, K. Gururaj, K.G. Pradeep, P.L. Paulose, R. Nirmala, Magnetocaloric effect in melt-spun rare earth intermetallic compound ErAl2, AIP Advances 12(3) (2022).
[95] W. Liu, T. Gottschall, F. Scheibel, E. Bykov, N. Fortunato, A. Aubert, H. Zhang, K. Skokov, O. Gutfleisch, Designing magnetocaloric materials for hydrogen liquefaction with light rare-earth Laves phases, Journal of Physics: Energy 5(3) (2023) 034001.
[96] H. Zhang, L.H. Yang, J.Y. Li, Z. Wang, E. Niu, R.M. Liu, Z.B. Li, F.X. Hu, J.R. Sun, B.G. Shen, Magnetic properties and magnetocaloric effect in Tb3Al2 compound, J Alloy Compd 615 (2014) 406-409.

[97] Y. Li, H. Zhang, T. Yan, K. Long, C. Cheng, Y. Xue, H. Zhou, Ieee, Successive Magnetic Transitions and Magnetocaloric Effect in Dy3Al2 Compound, 2015 Ieee Magnetics Conference (Intermag) (2015) 1.
[98] N.K. Singh, P. Kumar, Z. Mao, D. Paudyal, V. Neu, K.G. Suresh, V.K. Pecharsky, K.A. Gschneidner, Magnetic, magnetocaloric and magnetoresistance properties of Nd7Pd3, J Phys-Condens Mat 21(45) (2009) 456004.
[99] L. Li, O. Niehaus, M. Johnscher, R. Pottgen, Magnetic properties and tuneable magnetocaloric effect with large temperature span in GdCd1-xRux solid solutions, Intermetallics 60 (2015) 9-12.
[100] J.C.B. Monteiro, F.G. Gandra, Magnetocaloric properties of (Gd1-xErx)(3)Ru alloys and their composites, J Alloy Compd 803 (2019) 1178-1183.
[101] Y. Shang, Y. Yuan, Y. Cao, R.L. Hadimani, Y. Mozharivskyj, H. Fu, Structure, magnetic properties, and magnetocaloric effect of polycrystalline Ho3M (M = Rh, Ru) alloys, J Magn Magn Mater 497 (2020) 166055.
[102] Y.S. Du, C.R. Li, G. Cheng, X.F. Wu, J.J. Huo, J.Q. Wei, J. Wang, Investigation on the Magnetocaloric Effect of the Pr7Pd3 Compound, J Supercond Nov Magn 31(8) (2018) 2573-2577.
[103] X.Q. Zheng, Z.Y. Xu, B. Zhang, F.X. Hu, B.G. Shen, The normal and inverse magnetocaloric effect in RCu2 (R=Tb, Dy, Ho, Er) compounds, J Magn Magn Mater 421 (2017) 448-452.
[104] R. Rajivgandhi, J.A. Chelvane, R. Nirmala, Magnetic and magnetocaloric properties of the intermetallic compound ErCu2, AIP Conference Proceedings 1832(1) (2017).
[105] R. Rajivgandhi, J.A. Chelvane, A.K. Nigam, S.K. Malik, R. Nirmala, Preservation of large low temperature magnetocaloric effect in metamagnetic intermetallic compounds RCu2 (R = Gd, Tb, Dy, Ho and Er) upon rapid solidification, J Alloy Compd 815 (2020) 152659.
[106] J. Chen, B.G. Shen, Q.Y. Dong, F.X. Hu, J.R. Sun, Large reversible magnetocaloric effect caused by two successive magnetic transitions in ErGa compound, Appl Phys Lett 95(13) (2009) 132504.
[107] R.D. dos Reis, L.M. da Silva, A.O. dos Santos, A.M.N. Medina, L.P. Cardoso, F.G. Gandra, Study of the magnetocaloric properties of the antiferromagnetic compounds RGa2 (R = Ce, Pr, Nd, Dy, Ho and Er), J Phys-Condens Mat 22(48) (2010) 486002.
[108] J. Chen, B.G. Shen, Q.Y. Dong, J.R. Sun, Giant magnetocaloric effect in HoGa compound over a large temperature span, Solid State Commun 150(3-4) (2010) 157-159.
[109] X.Q. Zheng, J. Chen, J. Shen, H. Zhang, Z.Y. Xu, W.W. Gao, J.F. Wu, F.X. Hu, J.R. Sun, B.G. Shen, Large refrigerant capacity of RGa (R = Tb and Dy) compounds, J Appl Phys 111(7) (2012) 07A917.
[110] Z.J. Mo, J. Shen, L.Q. Yan, C.C. Tang, J. Lin, J.F. Wu, J.R. Sun, L.C. Wang, X.Q. Zheng, B.G. Shen, Low field induced giant magnetocaloric effect in TmGa compound, Appl Phys Lett 103(5) (2013).
[111] S.X. Yang, X.Q. Zheng, W.Y. Yang, J.W. Xu, J. Liu, L. Xi, H. Zhang, L.C. Wang, Z.Y. Xu, J.Y. Zhang, Y.F. Wu, X.B. Ma, D.F. Chen, J.B. Yang, S.G. Wang, B.G. Shen, Tunable magnetic properties and magnetocaloric effect of TmGa by Ho substitution, Phys Rev B 102(17) (2020) 174441.
[112] X.Q. Zheng, J. Chen, L.C. Wang, R.R. Wu, F.X. Hu, J.R. Sun, B.G. Shen, Magnetic properties and magnetocaloric effects of GdxEr1-xGa (0 <= x <= 1) compounds, J Appl Phys 115(17) (2014) 17A905.
[113] X.Q. Zheng, J. Chen, Z.Y. Xu, Z.J. Mo, F.X. Hu, J.R. Sun, B.G. Shen, Nearly constant magnetic entropy change and adiabatic temperature change in PrGa compound, J Appl Phys 115(17) (2014) 17A938.
[114] X.Q. Zheng, J.W. Xu, S.H. Shao, H. Zhang, J.Y. Zhang, S.G. Wang, Z.Y. Xu, L.C. Wang, J. Chen, B.G. Shen, Large magnetocaloric effect of NdGa compound due to successive magnetic transitions, AIP Advances 8(5) (2018).
[115] Q. Zhang, J.H. Cho, B. Li, W.J. Hu, Z.D. Zhang, Magnetocaloric effect in Ho2In over a wide temperature range, Appl Phys Lett 94(18) (2009) 182501.
[116] Q. Zhang, X.G. Liu, F. Yang, W.J. Feng, X.G. Zhao, D.J. Kang, Z.D. Zhang, Large reversible magnetocaloric effect in Dy2In, J Phys D Appl Phys 42(5) (2009) 055011.
[117] Q. Zhang, J.H. Cho, J. Du, F. Yang, X.G. Liu, W.J. Feng, Y.J. Zhang, J. Li, Z.D. Zhang, Large reversible magnetocaloric effect in Tb2In, Solid State Commun 149(9-10) (2009) 396-399.
[118] W. Liu, F. Scheibel, T. Gottschall, E. Bykov, I. Dirba, K. Skokov, O. Gutfleisch, Large magnetic entropy change in Nd_2In near the boiling temperature of natural gas, Appl Phys Lett 119(2) (2021).
[119] W. Liu, E. Bykov, S. Taskaev, M. Bogush, V. Khovaylo, N. Fortunato, A. Aubert, H. Zhang, T. Gottschall, J. Wosnitza, F. Scheibel, K. Skokov, O. Gutfleisch, A study on rare-earth Laves phases for magnetocaloric liquefaction of hydrogen, Applied Materials Today 29 (2022) 101624.
[120] H. Zhang, B.G. Shen, Z.Y. Xu, J. Chen, J. Shen, F.X. Hu, J.R. Sun, Large reversible magnetocaloric effect in Er_2In compound, J Alloy Compd 509(5) (2011) 2602-2605.

[121] F. Guillou, H. Yibole, R. Hamane, V. Hardy, Y.B. Sun, J.J. Zhao, Y. Mudryk, V.K. Pecharsky, Crystal structure and physical properties of Yb2In and Eu2-xYbxIn alloys, Physical Review Materials 4(10) (2020) 104402.
[122] A. Biswas, R.K. Chouhan, O. Dolotko, A. Thayer, S. Lapidus, Y. Mudryk, V.K. Pecharsky, Correlating Crystallography, Magnetism, and Electronic Structure Across Anhysteretic First-Order Phase Transition in Pr_2In, ECS Journal of Solid State Science and Technology 11(4) (2022) 043005.
[123] J.C.B. Monteiro, G.A. Lombardi, R.D. dos Reis, H.E. Freitas, L.P. Cardoso, A.M. Mansanares, F.G. Gandra, Heat flux measurements of Tb3M series (M = Co, Rh and Ru): Specific heat and magnetocaloric properties, Physica B 503 (2016) 64-69.
[124] X.Q. Zheng, B.G. Shen, The magnetic properties and magnetocaloric effects in binary R-T (R = Pr, Gd, Tb, Dy, Ho, Er, Tm; T = Ga, Ni, Co, Cu) intermetallic compounds, Chinese Phys B 26(2) (2017) 41.
[125] J. Le Roy, J.-M. Moreau, D. Paccard, E. Parthé, R3T2 compounds (R = rare earth or Y; T = Rh, Pd, Pt) with the rhombohedral Er3Ni2 structure type, Acta Crystallographica Section B 33(8) (1977) 2414-2417.
[126] J.-M. Moreau, D. Paccard, E. Parthé, The tetragonal crystal structure of R3Rh2 compounds with R = Gd, Tb, Dy, Ho, Er, Y, Acta Crystallographica Section B 32(6) (1976) 1767-1771.
[127] A.O. Pecharsky, Y. Mozharivskyj, K.W. Dennis, K.A. Gschneidner, R.W. McCallum, G.J. Miller, V.K. Pecharsky, Preparation, crystal structure, heat capacity, magnetism, and the magnetocaloric effect of Pr5Ni1.9Si3 and PrNi, Phys Rev B 68(13) (2003) 134452.
[128] S.K. Tripathy, K.G. Suresh, R. Nirmala, A.K. Nigam, S.K. Malik, Magnetocaloric effect in the intermetallic compound DyNi, Solid State Commun 134(5) (2005) 323-327.
[129] P. Kumar, K.G. Suresh, A.K. Nigam, O. Gutfleisch, Large reversible magnetocaloric effect in RNi compounds, J Phys D Appl Phys 41(24) (2008) 245006.
[130] H. Drulis, A. Hackemer, A. Zaleski, Y.L. Yaropolov, S.A. Nikitin, V.N. Verbetsky, The magnetocaloric effect and low temperature specific heat of SmNi, Solid State Commun 151(18) (2011) 1240-1243.
[131] W.L. Zuo, F.X. Hu, J.R. Sun, B.G. Shen, Large reversible magnetocaloric effect in RMn2 (R = Tb, Dy, Ho, Er) compounds, J Alloy Compd 575 (2013) 162-167.
[132] X.Q. Zheng, B. Zhang, H. Wu, F.X. Hu, Q.Z. Huang, B.G. Shen, Large magnetocaloric effect of HoxEr1-xNi (0 <= x <= 1) compounds, J Appl Phys 120(16) (2016) 7.
[133] R. Rajivgandhi, J.A. Chelvane, A.K. Nigam, J.G. Park, S.K. Malik, R. Nirmala, Effect of microstructure and texture on the magnetic and magnetocaloric properties of the melt-spun rare earth intermetallic compound DyNi, J Magn Magn Mater 418 (2016) 9-13.
[134] R. Rajivgandhi, J. Arout Chelvane, S. Quezado, S.K. Malik, R. Nirmala, Effect of rapid quenching on the magnetism and magnetocaloric effect of equiatomic rare earth intermetallic compounds RNi (R=Gd, Tb and Ho), J Magn Magn Mater 433 (2017) 169-177.
[135] J. Kurian, M.R. Rahul, J. Arout Chelvane, A.V. Morozkin, A.K. Nigam, G. Phanikumar, R. Nirmala, Enhanced magnetocaloric effect in undercooled rare earth intermetallic compounds RNi (R = Gd, Ho and Er), J Magn Magn Mater 499 (2020) 166302.
[136] J. Cwik, Y. Koshkid'ko, N.A. de Oliveira, K. Nenkov, A. Hackemer, E. Dilmieva, N. Kolchugina, S. Nikitin, K. Rogacki, Magnetocaloric effect in Laves-phase rare-earth compounds with the second-order magnetic phase transition: Estimation of the high-field properties, Acta Mater 133 (2017) 230-239.
[137] J. Ćwik, Y. Koshkid'ko, K. Nenkov, E.A. Tereshina, K. Rogacki, Structural, magnetic and magnetocaloric properties of HoNi2 and ErNi2 compounds ordered at low temperatures, J Alloy Compd 735 (2018) 1088-1095.
[138] J. Lai, X. Tang, H. Sepehri-Amin, K. Hono, Tuning magnetocaloric effect of $Ho_{1-x}Gd_xNi_2$ and $HoNi_{2-y}Co_y$ alloys around hydrogen liquefaction temperature, Scripta Mater 188 (2020) 302-306.
[139] S. Taskaev, V. Khovaylo, K. Skokov, W. Liu, E. Bykov, M. Ulyanov, D. Bataev, A. Basharova, M. Kononova, D. Plakhotskiy, M. Bogush, T. Gottschall, O. Gutfleisch, Magnetocaloric effect in GdNi2 for cryogenic gas liquefaction studied in magnetic fields up to 50 T, J Appl Phys 127(23) (2020).
[140] A. Haldar, I. Dhiman, A. Das, K.G. Suresh, A.K. Nigam, Magnetic, magnetocaloric and neutron diffraction studies on TbNi5-xMx (M = Co and Fe) compounds, J Alloy Compd 509(9) (2011) 3760-3765.
[141] Q.Y. Dong, J. Chen, J. Shen, J.R. Sun, B.G. Shen, Magnetic properties and magnetocaloric effects in R3Ni2 (R = Ho and Er) compounds, Appl Phys Lett 99(13) (2011).

[142] A. Provino, V. Smetana, D. Paudyal, K.A. Gschneidner, A.V. Mudring, V.K. Pecharsky, P. Manfrinetti, M. Putti, Gd3Ni2 and Gd3CoxNi2-x: magnetism and unexpected Co/Ni crystallographic ordering, Journal of Materials Chemistry C 4(25) (2016) 6078-6089.
[143] H. Wada, Y. Tanabe, M. Shiga, H. Sugawara, H. Sato, Magnetocaloric effects of Laves phase $Er(Co_{1-x}Ni_x)_2$ compounds, J Alloy Compd 316(1-2) (2001) 245-249.
[144] N.H. Duc, D.T.K. Anh, P.E. Brommer, Metamagnetism, giant magnetoresistance and magnetocaloric effects in RCO2-based compounds in the vicinity of the Curie temperature, Physica B 319(1-4) (2002) 1-8.
[145] T. Tohei, H. Wada, Change in the character of magnetocaloric effect with Ni substitution in Ho(Co1-xNix)(2), J Magn Magn Mater 280(1) (2004) 101-107.
[146] K.W. Zhou, Y.H. Zhuang, J.Q. Li, J.Q. Deng, Q.M. Zhu, Magnetocaloric effects in (Gd1-xTbx)Co-2, Solid State Commun 137(5) (2006) 275-277.
[147] Z. Gu, B. Zhou, J. Li, W. Ao, G. Cheng, J. Zhao, Magnetocaloric effect of GdCo2−xAlx compounds, Solid State Commun 141(10) (2007) 548-550.
[148] Y.Y. Zhu, K. Asamoto, Y. Nishimura, T. Kouen, S. Abe, K. Matsumoto, T. Numazawa, Magnetocaloric effect of (Er(x)R(1-x))Co(2) (R = Ho, Dy) for magnetic refrigeration between 20 and 80 K, Cryogenics 51(9) (2011) 494-498.
[149] M. Balli, D. Fruchart, D. Gignoux, Magnetic behaviour and experimental study of the magnetocaloric effect in the pseudobinary Laves phase $Er_{1-x}Dy_xCo_2$, J Alloy Compd 509(9) (2011) 3907-3912.
[150] L.A. Burrola-Gandara, M.C. Grijalva-Castillo, C.R. Santillan-Rodriguez, J.A. Matutes-Aquino, Magnetocaloric effect in Sm-$Co_{2-x}Fe_x$ alloys, J Appl Phys 111(7) (2012) 07A942.
[151] B. Li, J. Du, W.J. Ren, W.J. Hu, Q. Zhang, D. Li, Z.D. Zhang, Large reversible magnetocaloric effect in Tb3Co compound, Appl Phys Lett 92(24) (2008) 242504.
[152] J. Shen, J.L. Zhao, F.X. Hu, G.H. Rao, G.Y. Liu, J.F. Wu, Y.X. Li, J.R. Sun, B.G. Shen, Magnetocaloric effect in antiferromagnetic Dy3Co compound, Appl Phys a-Mater 99(4) (2010) 853-858.
[153] J. Shen, J.L. Zhao, F.X. Hu, J.F. Wu, J.R. Sun, B.G. Shen, Order of magnetic transition and large magnetocaloric effect in Er3Co, Chinese Phys B 19(4) (2010) 047502.
[154] J. Shen, J.F. Wu, Magnetocaloric effect and magnetic phase transition in Ho3Co, J Appl Phys 109(7) (2011) 07A931.
[155] Z.J. Mo, J. Shen, L.Q. Yan, J.F. Wu, C.C. Tang, B.G. Shen, Low-field induced large reversible magnetocaloric effect in Tm3Co compound, J Alloy Compd 572 (2013) 1-4.
[156] J.Q. Deng, Y.H. Zhuang, J.Q. Li, J.L. Huang, Magnetic properties of Tb12Co7, Physica B 391(2) (2007) 331-334.
[157] X. Chen, Y.H. Zhuang, Magnetocaloric effect of Gd12Co7, Solid State Commun 148(7-8) (2008) 322-325.
[158] X.Q. Zheng, X.P. Shao, J. Chen, Z.Y. Xu, F.X. Hu, J.R. Sun, B.G. Shen, Giant magnetocaloric effect in Ho12Co7 compound, Appl Phys Lett 102(2) (2013) 022421.
[159] X. Zheng, B. Zhang, Y. Li, H. Wu, H. Zhang, J. Zhang, S. Wang, Q. Huang, B. Shen, Large magnetocaloric effect in Er12Co7 compound and the enhancement of δTFWHM by Ho-substitution, J Alloy Compd 680 (2016) 617-622.
[160] L.M. Moreno-Ramírez, C. Romero-Muñiz, J.Y. Law, V. Franco, A. Conde, I.A. Radulov, F. Maccari, K.P. Skokov, O. Gutfleisch, The role of Ni in modifying the order of the phase transition of $La(Fe,Ni,Si)_{13}$, Acta Mater 160 (2018) 137-146.
[161] L.M. Moreno-Ramírez, C. Romero-Muñiz, J.Y. Law, V. Franco, A. Conde, I.A. Radulov, F. Maccari, K.P. Skokov, O. Gutfleisch, Tunable first order transition in $La(Fe,Cr,Si)_{13}$ compounds: Retaining magnetocaloric response despite a magnetic moment reduction, Acta Mater 175 (2019) 406-414.
[162] K. Lowe, J. Liu, K. Skokov, J.D. Moore, H. Sepehri-Amin, K. Hono, M. Katter, O. Gutfleisch, The effect of the thermal decomposition reaction on the mechanical and magnetocaloric properties of La(Fe,Si,Co)(13), Acta Mater 60(10) (2012) 4268-4276.
[163] J. Liu, C. He, M.X. Zhang, A.R. Yan, A systematic study of the microstructure, phase formation and magnetocaloric properties in off-stoichiometric La-Fe-Si alloys, Acta Mater 118 (2016) 44-53.
[164] S.A. Nikitin, A.M. Tishin, Magnetocaloric effect in HoCo2 compound, Cryogenics 31(3) (1991) 166-167.
[165] B.K. Banerjee, On a generalised approach to first and second order magnetic transitions, Phys Lett 12(1) (1964) 16-17.

[166] C.M. Bonilla, J. Herrero-Albillos, F. Bartolome, L.M. Garcia, M. Parra-Borderias, V. Franco, Universal behavior for magnetic entropy change in magnetocaloric materials: An analysis on the nature of phase transitions, Phys Rev B 81(22) (2010) 224424.
[167] S.K. Tripathy, K.G. Suresh, A.K. Nigam, A comparative study of the magnetocaloric effect in Gd3Co and Gd3Ni, J Magn Magn Mater 306(1) (2006) 24-29.
[168] W. Adams, J.-M. Moreau, E. Parthé, J. Schweizer, $R_{12}Co_7$ compounds with R = Gd, Tb, Dy, Ho, Er, Acta Cryst. B32 (1976) 2697-2699.
[169] Y. Makihara, Y. Andoh, Y. Hashimoto, H. Fujii, M. Hasuo, T. Okamoto, Magnetic Characteristics of Laves Phase RMn2 Compounds (R=Gd, Tb, Dy, Ho and Er), J Phys Soc Jpn 52(2) (1983) 629-636.
[170] S.K. Malik, W.E. Wallace, Magnetic behavior of cubic laves phase RMn2 (R = Gd, Dy and Ho) compounds, J Magn Magn Mater 24(1) (1981) 23-28.
[171] Y. Liu, X. Fu, Q. Yu, M. Zhang, J. Liu, Significant reduction of phase-transition hysteresis for magnetocaloric $(La_{1-x}Ce)_2Fe11Si_2H$ alloys by microstructural manipulation, Acta Mater 207 (2021).
[172] C. Bean, D. Rodbell, Magnetic Disorder as a First-Order Phase Transformation, Phys Rev 126(1) (1962) 104-115.
[173] L.M. Moreno-Ramírez, J.Y. Law, S.S. Pramana, A.K. Giri, V. Franco, Analysis of the magnetic field dependence of the isothermal entropy change of inverse magnetocaloric materials, Results in Physics 22 (2021) 103933.
[174] D. Guo, L.M. Moreno-Ramírez, C. Romero-Muñiz, Y. Zhang, J.Y. Law, V. Franco, J. Wang, Z. Ren, First- and second-order phase transitions in RE_6Co_2Ga (RE = Ho, Dy or Gd) cryogenic magnetocaloric materials, Science China Materials 64(11) (2021) 2846-2857.
[175] A.N. Khan, L.M. Moreno-Ramírez, Á. Díaz-García, J.Y. Law, V. Franco, All-d-metal Ni(Co)-Mn(X)-Ti (X = Fe or Cr) Heusler alloys: Enhanced magnetocaloric effect for moderate magnetic fields, J Alloy Compd 931 (2023) 167559.
[176] J.Y. Law, Á. Díaz-García, L.M. Moreno-Ramírez, V. Franco, A. Conde, A.K. Giri, How concurrent thermomagnetic transitions can affect magnetocaloric effect: the $Ni_{49-x}Mn_{36+x}In_{15}$ Heusler alloy case, Acta Mater 166 (2019) 459-465.
[177] S. Fujieda, A. Fujita, N. Kawamoto, K. Fukamichi, Strong magnetocaloric effects in La1-zCez(Fex-yMnySi1-x)(13) at low temperatures, Appl Phys Lett 89(6) (2006) 062504.
[178] S. Fujieda, A. Fujita, K. Fukamichi, Control of large magnetocaloric effects and hysteresis of La1-zCez(Fe0.86Si0.14)(13) compounds, Ieee T Magn 41(10) (2005) 2787-2789.
[179] H. Zhang, J. Shen, Z.Y. Xu, X.Q. Zheng, F.X. Hu, J.R. Sun, B.G. Shen, Simultaneous enhancements of Curie temperature and magnetocaloric effects in the $La_{1-x}Ce_xFe_{11.5}Si_{1.5}C_y$ compounds, J Magn Magn Mater 324(4) (2012) 484-487.
[180] S. Fujieda, A. Fujita, K. Fukamichi, Enhancement of magnetocaloric effects in La1-zPrz(Fe0.88Si0.12)(13) and their hydrides, J Appl Phys 102(2) (2007) 023907.
[181] S. Mican, R. Tetean, Magnetic properties and magnetocaloric effect in La0.7Nd0.3Fe13-xSix compounds, J Solid State Chem 187 (2012) 238-243.
[182] J. Shen, Y.X. Li, J. Zhang, B. Gao, F.X. Hu, H.W. Zhang, Y.Z. Chen, C.B. Rong, J.R. Sun, Large magnetic entropy change and low hysteresis loss in the Nd- and Co-doped La(Fe,Si)(13) compounds, J Appl Phys 103(7) (2008) 07B317.
[183] X. Chen, Y. Chen, Y. Tang, The effect of different temperature annealing on phase relation of LaFe11.5Si1.5 and the magnetocaloric effects of La0.8Ce0.2Fe11.5−xCoxSi1.5 alloys, J Magn Magn Mater 323(24) (2011) 3177-3183.
[184] J. Shen, Y.X. Li, J.R. Sun, B.G. Shen, Effect of R substitution on magnetic properties and magnetocaloric effects of La1-xRxFe11.5Si1.5 compounds with R=Ce, Pr and Nd, Chinese Phys B 18(5) (2009) 2058-2062.
[185] J. Chen, Magnetic properties and magnetocaloric effects in Ni2In-type RCuSi and CrB-type RGa compounds, Ph.D. Thesis (in Chinese), Graduate University of Chinese Academy of Sciences China, 2010.
[186] J. Chen, B.G. Shen, Q.Y. Dong, F.X. Hu, J.R. Sun, Giant reversible magnetocaloric effect in metamagnetic HoCuSi compound, Appl Phys Lett 96(15) (2010) 152501.
[187] J. Chen, B.G. Shen, Q.Y. Dong, J.R. Sun, Giant magnetic entropy change in antiferromagnetic DyCuSi compound, Solid State Commun 150(31-32) (2010) 1429-1431.

[188] R. Rawat, I. Das, Magnetocaloric and magnetoresistance studies of GdPd2Si, J Phys-Condens Mat 13(3) (2001) L57-L63.
[189] R. Rawat, I. Das, Heat capacity and magnetocaloric studies of RPd2Si (R = Gd,Th and Dy), J Phys-Condens Mat 18(3) (2006) 1051-1059.
[190] L.W. Li, W.D. Hutchison, D.X. Huo, T. Namiki, Z.H. Qian, K. Nishimura, Low-field giant reversible magnetocaloric effect in intermetallic compound ErCr2Si2, Scripta Mater 67(3) (2012) 237-240.
[191] L. Li, G. Hu, I. Umehara, D. Huo, W.D. Hutchison, T. Namiki, K. Nishimura, Magnetic properties and magnetocaloric effect of GdCr2Si2 compound under hydrostatic pressure, J Alloy Compd 575 (2013) 1-4.
[192] S.B. Gupta, K.G. Suresh, Giant low field magnetocaloric effect in soft ferromagnetic ErRuSi, Appl Phys Lett 102(2) (2013) 022408.
[193] T. Samanta, I. Das, S. Banerjee, Giant magnetocaloric effect in antiferromagnetic ErRu2Si2 compound, Appl Phys Lett 91(15) (2007) 152506.
[194] T. Paramanik, K. Das, T. Samanta, I. Das, Observation of large magnetocaloric effect in HoRu2Si2, J Appl Phys 115(8) (2014).
[195] L.W. Li, K. Nishimura, G. Usui, D.X. Huo, Z.H. Qian, Study of the magnetic properties and magnetocaloric effect in RCo2B2 (R = Tb, Dy and Ho) compounds, Intermetallics 23 (2012) 101-105.
[196] J.L. Wang, S.J. Campbell, R. Zeng, C.K. Poh, S.X. Dou, S.J. Kennedy, Re-entrant ferromagnet $PrMn_2Ge_{0.8}Si_{1.2}$: Magnetocaloric effect, J Appl Phys 105(7) (2009) 07A909.
[197] J.L. Wang, S.J. Campbell, J.M. Cadogan, A.J. Studer, R. Zeng, S.X. Dou, Magnetocaloric effect in layered $NdMn_2Ge_{0.4}Si_{1.6}$, Appl Phys Lett 98(23) (2011) 232509.
[198] L.W. Li, K. Nishimura, W.D. Hutchison, Z.H. Qian, D.X. Huo, T. NamiKi, Giant reversible magnetocaloric effect in ErMn2Si2 compound with a second order magnetic phase transition, Appl Phys Lett 100(15) (2012) 152403.
[199] H. Zhang, Y.J. Sun, E. Niu, L.H. Yang, J. Shen, F.X. Hu, J.R. Sun, B.G. Shen, Large magnetocaloric effects of RFeSi (R = Tb and Dy) compounds for magnetic refrigeration in nitrogen and natural gas liquefaction, Appl Phys Lett 103(20) (2013) 202412.
[200] H. Zhang, B.G. Shen, Z.Y. Xu, J. Shen, F.X. Hu, J.R. Sun, Y. Long, Large reversible magnetocaloric effects in ErFeSi compound under low magnetic field change around liquid hydrogen temperature, Appl Phys Lett 102(9) (2013) 092401.
[201] M.F. Md Din, J.L. Wang, S.J. Campbell, A.J. Studer, M. Avdeev, S.J. Kennedy, Q.F. Gu, R. Zeng, S.X. Dou, Magnetic phase transitions and entropy change in layered NdMn1.7Cr0.3Si2, Appl Phys Lett 104(4) (2014) 042401.
[202] H. Zhang, B.G. Shen, Magnetocaloric effects in RTX intermetallic compounds (R = Gd-Tm, T = Fe-Cu and Pd, X = Al and Si), Chinese Phys B 24(12) (2015) 127504.
[203] Y. Ma, X. Dong, Y. Qi, L. Li, Investigation of the magnetic and magnetocaloric properties in metamagnetic REFe2Si2 (RE = Pr and Nd) compounds, J Magn Magn Mater 471 (2019) 25-29.
[204] Y. Zhang, J. Zhu, S. Li, Z. Zhang, J. Wang, Z. Ren, Magnetic properties and promising magnetocaloric performances in the antiferromagnetic GdFe2Si2 compound, Science China Materials 65(5) (2022) 1345-1352.
[205] S. Gupta, K.G. Suresh, Observation of giant magnetocaloric effect in HoCoSi, Mater Lett 113 (2013) 195-197.
[206] H. Zhang, Y.Y. Wu, Y. Long, H.S. Wang, K.X. Zhong, F.X. Hu, J.R. Sun, B.G. Shen, Large reversible magnetocaloric effect in antiferromagnetic HoNiSi compound, J Appl Phys 116(21) (2014) 5.
[207] H. Zhang, Y.W. Li, E.K. Liu, Y.J. Ke, J.L. Jin, Y. Long, B.G. Shen, Giant rotating magnetocaloric effect induced by highly texturing in polycrystalline DyNiSi compound, Sci Rep 5 (2015) 10.
[208] T. Tolinski, M. Falkowski, K. Synoradzki, A. Hoser, N. Stusser, Magnetocaloric effect in the ferromagnetic GdNi4M (M = Al, Si) and antiferromagnetic NdNiAl4 compounds, J Alloy Compd 523 (2012) 43-48.
[209] S. Pakhira, C. Mazumdar, R. Ranganathan, S. Giri, M. Avdeev, Large magnetic cooling power involving frustrated antiferromagnetic spin-glass state in R2NiSi3 (R = Gd,Er), Phys Rev B 94(10) (2016) 15.
[210] Y. Zhang, Q.Y. Dong, L.C. Wang, M. Zhang, H.T. Yan, J.R. Sun, F.X. Hu, B.G. Shen, Giant low-field reversible magnetocaloric effect in HoCoGe compound, RSC Adv. 6(108) (2016) 106171-106176.
[211] Y. Zhang, Q. Dong, X. Zheng, Y. Liu, S. Zuo, J. Xiong, B. Zhang, X. Zhao, R. Li, D. Liu, F.-x. Hu, J. Sun, T. Zhao, B. Shen, Complex magnetic properties and large magnetocaloric effects in RCoGe (R=Tb, Dy) compounds, AIP Advances 8(5) (2018).
[212] L.M. da Silva, A.O. dos Santos, A.A. Coelho, L.P. Cardoso, Magnetic properties and magnetocaloric effect of the HoAgGa compound, Appl Phys Lett 103(16) (2013) 162413.

[213] D. Guo, L.M. Moreno-Ramírez, J.-Y. Law, Y. Zhang, V. Franco, Excellent cryogenic magnetocaloric properties in heavy rare-earth based HRENiGa2 (HRE = Dy, Ho, or Er) compounds, Science China Materials 66(1) (2023) 249-256.
[214] L.C. Wang, L. Cui, Q.Y. Dong, Z.J. Mo, Z.Y. Xu, F.X. Hu, J.R. Sun, B.G. Shen, Large magnetocaloric effect with a wide working temperature span in the R_2CoGa_3 (R = Gd, Dy, and Ho) compounds, J Appl Phys 115(23) (2014) 233913.
[215] Y. Zhang, D. Guo, S. Geng, X. Lu, G. Wilde, Structure, magnetic and cryogenic magneto-caloric properties in intermetallic gallium compounds RE2Co2Ga (RE = Dy, Ho, Er, and Tm), J Appl Phys 124(4) (2018).
[216] Y. Zhang, Y. Yang, C. Hou, D. Guo, X. Li, Z. Ren, G. Wilde, Metamagnetic transition and magnetocaloric properties in antiferromagnetic Ho2Ni2Ga and Tm2Ni2Ga compounds, Intermetallics 94 (2018) 17-21.
[217] D. Guo, H. Li, Y. Zhang, Magnetic Phase Transition and Magnetocaloric Effect in Ternary Er2Ni2Ga Compound, Ieee T Magn 55(1) (2019) 2500204.
[218] Q.Y. Dong, B.G. Shen, J. Chen, J. Shen, J.R. Sun, Large reversible magnetocaloric effect in DyCuAl compound, J Appl Phys 105(11) (2009) 113902.
[219] Q.Y. Dong, J. Chen, J. Shen, J.R. Sun, B.G. Shen, Large magnetic entropy change and refrigerant capacity in rare-earth intermetallic RCuAl (R=Ho and Er) compounds, J Magn Magn Mater 324(17) (2012) 2676-2678.
[220] L.C. Wang, Q.Y. Dong, Z.J. Mo, Z.Y. Xu, F.X. Hu, J.R. Sun, B.G. Shen, Low-temperature reversible giant magnetocaloric effect in the HoCuAl compound, J Appl Phys 114(16) (2013) 163915.
[221] Z.J. Mo, J. Shen, L.Q. Yan, J.F. Wu, L.C. Wang, J. Lin, C.C. Tang, B.G. Shen, Low-field induced giant magnetocaloric effect in TmCuAl compound, Appl Phys Lett 102(19) (2013).
[222] X.X. Zhang, F.W. Wang, G.H. Wen, Magnetic entropy change in RCoAl (R = Gd, Tb, Dy, and Ho) compounds: candidate materials for providing magnetic refrigeration in the temperature range 10 K to 100 K, J Phys-Condens Mat 13(31) (2001) L747-L752.
[223] M. Klimczak, E. Talik, Magnetocaloric effect of GdTX (T = Mn, Fe, Ni, Pd, X=Al, In) and GdFe6Al6 ternary compounds, in International Conference on Magnetism, Iop Publishing Ltd, 200 (2010) 092009, 10.1088/1742-6596/200/9/092009
[224] J.W. Xu, X.Q. Zheng, S.X. Yang, S.H. Shao, J.Q. Liu, J.Y. Zhang, S.G. Wang, Z.Y. Xu, L.C. Wang, S. Zhang, Z.Q. Zhang, B.G. Shen, Low working temperature near liquid helium boiling point of $RNiAl_2$ (R = Tm, Tb and Gd) compounds with large magnetocaloric effect, J Appl Phys 125(22) (2019).
[225] L.J. Meng, Y.S. Jia, Y. Qi, Q. Wang, L.W. Li, Investigation of the magnetism and magnetocaloric effect in the R2CoAl3 (R = Gd, Tb, Dy, and Ho) compounds, J Alloy Compd 715 (2017) 242-246.
[226] D.X. Li, S. Nimori, D. Aoki, Magnetic entropy change and relative cooling power of Gd3Ni6Al2 and Tb3Ni6Al2 compounds, Solid State Commun 156 (2013) 54-58.
[227] J.W. Xu, X.Q. Zheng, S.X. Yang, L. Xi, D.S. Wang, C.F. Liu, J.Y. Zhang, Y.F. Wu, J.X. Shen, S.G. Wang, B.G. Shen, Large reversible magnetic entropy change of $R_3Ni_6Al_2$ (R = Dy, Ho and Er) compounds, J Alloy Compd 879 (2021) 160468.
[228] A.V. Morozkin, V.K. Genchel, A.V. Garshev, V.O. Yapaskurt, O. Isnard, J.L. Yao, R. Nirmala, S. Quezado, S.K. Malik, Magnetic ordering of Mo2NiB2-type {Gd, Tb, Dy)2Co2Al compounds by magnetization and neutron diffraction study, J Magn Magn Mater 442 (2017) 36-44.
[229] X. Dong, J. Feng, Y. Yi, L. Li, Investigation of the crystal structure and cryogenic magnetic properties of RE2T2Al (RE = Dy, Ho, Er, and Tm; T = Co and Ni) compounds, J Appl Phys 124(9) (2018).
[230] L. Li, O. Niehaus, B. Gerke, R. Pottgen, Magnetism and Magnetocaloric Effect in EuAuZn, Ieee T Magn 50(11) (2014) 4.
[231] Z. Zhang, S. Stein, L. Li, R. Pöttgen, Magnetocaloric effect and critical behavior in ternary equiatomic magnesium compounds REPtMg (RE = Tb, Dy and Ho), Intermetallics 109 (2019) 24-29.
[232] Y. Zhang, Y. Yang, X. Xu, S. Geng, L. Hou, X. Li, Z. Ren, G. Wilde, Excellent magnetocaloric properties in RE_2Cu_2Cd (RE = Dy and Tm) compounds and its composite materials, Sci Rep 6 (2016) 34192.
[233] Y. Yang, Y.K. Zhang, X. Xu, S.H. Geng, L. Hou, X. Li, Z.M. Ren, G. Wilde, Magnetic and magnetocaloric properties of the ternary cadmium based intermetallic compounds of Gd_2Cu_2Cd and Er_2Cu_2Cd, J Alloy Compd 692 (2017) 665-669.
[234] Y. Yi, L. Li, K. Su, Y. Qi, D. Huo, Large magnetocaloric effect in a wide temperature range induced by two successive magnetic phase transitions in Ho_2Cu_2Cd compound, Intermetallics 80 (2017) 22-25.

[235] L. Li, O. Niehaus, M. Kersting, R. Pöttgen, Reversible table-like magnetocaloric effect in Eu4PdMg over a very large temperature span, Appl Phys Lett 104(9) (2014) 092416.
[236] L.W. Li, O. Niehaus, M. Kersting, R. Pottgen, Large Reversible Magnetocaloric Effect Around Liquid Hydrogen Temperature in Er4PdMg Compound, Ieee T Magn 51(11) (2015) 4.
[237] L.W. Li, O. Niehaus, M. Kersting, R. Pottgen, Magnetic properties and magnetocaloric effect in the rare earth-rich phases RE4PtMg (RE = Ho and Er), Intermetallics 62 (2015) 17-21.
[238] L. Li, D. Huo, K. Su, R. Pöttgen, Magnetic properties and large magnetic entropy change in rare earth-rich cadmium compounds of RE4CoCd (RE = Tm and Ho), Intermetallics 93 (2018) 343-346.
[239] D. Guo, Y. Wang, H. Li, R. Guan, H. Xu, Y. Zhang, Observation of large magnetocaloric effect in ternary Er-based Er4CoCd compound, J Magn Magn Mater 489 (2019) 165462.
[240] W. Hermes, U.C. Rodewald, R. Pottgen, Large reversible magnetocaloric effect due to a rather unstable antiferromagnetic ground state in Er4NiCd, J Appl Phys 108(11) (2010) 113919.
[241] Z.-J. Mo, J. Shen, L.-Q. Yan, X.-Q. Gao, L.-C. Wang, C.-C. Tang, J.-F. Wu, J.-r. Sun, B.-G. Shen, Magnetic properties and magnetocaloric effect in the RCu2Si2 and RCu2Ge2 (R = Ho, Er) compounds, J Appl Phys 115(7) (2014) 073905.
[242] A. Herrero, A. Oleaga, A. Provino, I.R. Aseguinolaza, A. Salazar, D. Peddis, P. Manfrinetti, Crystallographic, magnetic and magnetocaloric properties in novel intermetallic materials R3CoNi (R = Tb, Dy, Ho, Er, Tm, Lu), J Alloy Compd 865 (2021) 158948.
[243] R. Mondal, R. Nirmala, J.A. Chelvane, A.K. Nigam, Magnetocaloric effect in the rare earth intermetallic compounds RCoNi (R=Gd, Tb, Dy, and Ho), J Appl Phys 113(17) (2013).
[244] M.F.M. Din, J.L. Wang, R. Zeng, S.J. Kennedy, S.J. Campbell, S.X. Dou, Magnetic Properties and Magnetocaloric Effect in Layered NdMn1.9V0.1Si2, EPJ Web of Conferences 75 (2014) 04001.
[245] I. Ijjaali, R. Welter, G. Venturini, B. Malaman, Refinements of the TiNiSi-type RMnSi (R=Tb, Lu, Sc) and DyCoSi structures from single crystal X-ray diffraction, J Alloy Compd 292(1) (1999) 4-10.
[246] J. Leciejewicz, N. Stüsser, M. Kolenda, A. Szytuła, A. Zygmunt, Magnetic ordering in HoCoSi and TbCoGe, J Alloy Compd 240(1) (1996) 164-169.
[247] A.E. Dwight, P.P. Vaishnava, C.W. Kimball, J.L. Matykiewicv, Crystal structure and Mössbauer effect study of evuiatomic (Sc,Y,Ln)-Co-(Si,Ge,Sn) ternary compounds (Ln Gd — Tm, Lu), Journal of the Less Common Metals 119(2) (1986) 319-326.
[248] R. Welter, G. Venturini, E. Ressouche, B. Malaman, Magnetic properties of RCoSi (R La—Sm, Gd, Tb) compounds from susceptibility measurements and neutron diffraction studies, J Alloy Compd 210(1) (1994) 279-286.
[249] Z.Y. Xu, Magnetism and magnetocaloric effects in rare earth transition metal compounds with low temperature transition, Graduate University of Chinese Academy of Sciences, China, 2012.
[250] H. Zhang, C. Xing, H. Zhou, X. Zheng, X. Miao, L. He, J. Chen, H. Lu, E. Liu, W. Han, H. Zhang, Y. Wang, Y. Long, L. van Eijk, E. Brück, Giant anisotropic magnetocaloric effect by coherent orientation of crystallographic texture and rare-earth ion moments in HoNiSi ploycrystal, Acta Mater 193 (2020) 210-220.
[251] P. Javorský, P.C.M. Gubbens, A.M. Mulders, K. Prokeš, N. Stüsser, T.J. Gortenmulder, R.W.A. Hendrikx, Incommensurate magnetic structure in TmCuAl at low temperatures, J Magn Magn Mater 251(2) (2002) 123-128.
[252] N.K. Singh, K.G. Suresh, R. Nirmala, A.K. Nigam, S.K. Malik, Correlation between magnetism and magnetocaloric effect in the intermetallic compound DyNiAl, J Appl Phys 99(8) (2006) 08K904.
[253] N.K. Singh, K.G. Suresh, R. Nirmala, A.K. Nigam, S.K. Malik, Effect of magnetic polarons on the magnetic, magnetocaloric, and magnetoresistance properties of the intermetallic compound HoNiAl, J Appl Phys 101(9) (2007) 093904.
[254] Z.-J. Mo, J. Shen, G.-F. Chen, L.-Q. Yan, X. Zheng, J.-F. Wu, C.-C. Tang, J.-R. sun, B.-G. Shen, Evolution of magnetic properties and magnetocaloric effect in TmNi1−xCuxAl (x = 0, 0.1, 0.3, 0.5, 0.7, 0.9, 1) compounds, J Appl Phys 115(17) (2014).
[255] L.C. Wang, Q.Y. Dong, J. Lu, X.P. Shao, Z.J. Mo, Z.Y. Xu, J.R. Sun, F.X. Hu, B.G. Shen, Low-temperature large reversible magnetocaloric effects of $ErNi_{1-x}Cu_xAl$ (x = 0.2, 0.5, 0.8) intermetallic compounds, J Appl Phys 114(21) (2013) 213907.

[256] L. Cui, L.C. Wang, Q.Y. Dong, F.H. Liu, Z.J. Mo, Y. Zhang, E. Niu, Z.Y. Xu, F.X. Hu, J.R. Sun, B.G. Shen, Effect of Cu doping on the magnetic and magnetocaloric properties in the HoNiAl intermetallic compound, J Alloy Compd 622 (2015) 24-28.
[257] A.G. Kuchin, S.P. Platonov, R.D. Mukhachev, A.V. Lukoyanov, A.S. Volegov, V.S. Gaviko, M.Y. Yakovleva, Large Magnetic Entropy Change in GdRuSi Optimal for Magnetocaloric Liquefaction of Nitrogen, Metals 13(2) (2023) 290.
[258] H. Zhang, Y.J. Sun, L.H. Yang, E. Niu, H.S. Wang, F.X. Hu, J.R. Sun, B.G. Shen, Successive inverse and normal magnetocaloric effects in HoFeSi compound, J Appl Phys 115(6) (2014) 063901.
[259] F. Hulliger, On the rare-earth palladium aluminides LnPdAl, J Alloy Compd 218(1) (1995) 44-46.
[260] Z. Xu, B. Shen, Large magnetocaloric effect in metamagnetic HoPdAl, Science China Technological Sciences 55(2) (2012) 445-450.
[261] Y.B. Tyvanchuk, Y.M. Kalyczak, Ł. Gondek, M. Rams, A. Szytuła, Z. Tomkowicz, Magnetic properties of RNi1−xIn1+x (R=Gd–Er) compounds, J Magn Magn Mater 277(3) (2004) 368-378.
[262] L. Gondek, A. Szytula, S. Baran, J. Hernandez-Velasco, Neutron diffraction studies of the hexagonal RTIn (R=rare earth, T=Au or Ni) compounds, J Magn Magn Mater 272-276 (2004) E443-E444.
[263] Ł. Gondek, A. Szytuła, S. Baran, M. Rams, J. Hernandez-Velasco, Y. Tyvanchuk, Magnetic structures of non-stoichiometric hexagonal RNi1−xIn1+x (R=Dy, Ho, Er) compounds, J Magn Magn Mater 278(3) (2004) 392-396.
[264] H. Zhang, Z.Y. Xu, X.Q. Zheng, J. Shen, F.X. Hu, J.R. Sun, B.G. Shen, Magnetocaloric effects in RNiIn (R = Gd-Er) intermetallic compounds, J Appl Phys 109(12) (2011) 123926.
[265] Z.J. Mo, J. Shen, L.Q. Yan, C.C. Tang, L.C. Wang, J.F. Wu, J.R. Sun, B.G. Shen, Magnetic property and magnetocaloric effect in TmCoAl compound, Intermetallics 56 (2015) 75-78.
[266] R.C. O'Handley, Modern magnetic materials : principles and applications, Wiley, New York, 2000.
[267] J.A. Chelvane, T. Das, R.N. Mahato, A.V. Morozkin, J. Lamsal, W.B. Yelon, R. Nirmala, S.K. Malik, Magnetic structure and magnetic entropy change in the intermetallic compound DyCoAl, J Appl Phys 107(9) (2010) 09A906.
[268] D.X. Li, Y. Homma, F. Honda, T. Yamamura, D. Aoki, Large Magnetocaloric Effect and Magnetic Properties in ErCoAl, in 20th International Conference on Magnetism, Icm 2015, Elsevier Science Bv, 75 (2015) 1300-1305, 10.1016/j.phpro.2015.12.145
[269] P.B.d. Castro, K. Terashima, T.D. Yamamoto, Z. Hou, S. Iwasaki, R. Matsumoto, S. Adachi, Y. Saito, P. Song, H. Takeya, Y. Takano, Machine-learning-guided discovery of the gigantic magnetocaloric effect in HoB2 near the hydrogen liquefaction temperature, NPG Asia Materials 12(1) (2020) 35.
[270] P.B.d. Castro, K. Terashima, T.D. Yamamoto, S. Iwasaki, R. Matsumoto, S. Adachi, Y. Saito, H. Takeya, Y. Takano, Effect of Dy substitution in the giant magnetocaloric properties of HoB2, Sci Technol Adv Mat 21(1) (2020) 849-855.
[271] P. Baptista de Castro, K. Terashima, T.D. Yamamoto, S. Iwasaki, A.T. Saito, R. Matsumoto, S. Adachi, Y. Saito, M. ElMassalami, H. Takeya, Y. Takano, Enhancement of giant refrigerant capacity in $Ho_{1-x}Gd_xB_2$ alloys ($0.1 \leqslant x \leqslant 0.4$), J Alloy Compd 865 (2021) 158881.
[272] D.X. Li, T. Yamamura, S. Nimori, Y. Homma, F. Honda, Y. Haga, D. Aoki, Large reversible magnetocaloric effect in ferromagnetic semiconductor EuS, Solid State Commun 193 (2014) 6-10.
[273] L. Li, S. Hirai, E. Nakamura, H.B. Yuan, Influences of Eu2O3 characters and sulfurization conditions on the preparation of EuS and its large magnetocaloric effect, J Alloy Compd 687 (2016) 413-420.
[274] C. Delacotte, T.A. Pomelova, T. Stephant, T. Guizouarn, S. Cordier, N.G. Naumov, P. Lemoine, NaGdS2: A Promising Sulfide for Cryogenic Magnetic Cooling, Chem Mater 34(4) (2022) 1829-1837.
[275] T.A. Yamamoto, T. Nakagawa, K. Sako, T. Arakawa, H. Nitani, Magnetocaloric effect of rare earth mono-nitrides, TbN and HoN, J Alloy Compd 376(1-2) (2004) 17-22.
[276] T. Nakagawa, K. Sako, T. Arakawa, T.A. Yamamoto, Magnetocaloric effect of mononitride containing gadolinium and dysprosium GdxDy1-xN, J Alloy Compd 364(1-2) (2004) 53-58.
[277] T. Nakagawa, K. Sako, T. Arakawa, N. Tomioka, T.A. Yamamoto, K. Kamiya, T. Numazawa, Magnetocaloric effects of binary rare earth mononitrides, GdxTb1-xN and TbxHo1-xN, J Alloy Compd 408 (2006) 187-190.
[278] T. Nakagawa, T. Arakawa, K. Sako, N. Tomioka, T.A. Yamamoto, T. Kusunose, K. Niihara, K. Kamiya, T. Numazawa, Magnetocaloric effects of ferromagnetic erbium mononitride, J Alloy Compd 408 (2006) 191-195.
[279] Y. Hirayama, T. Nakagawa, T. Kusunose, T.A. Yamamoto, Magnetocaloric Effect of Rare Earth Nitrides, Ieee T Magn 44(11) (2008) 2997-3000.

[280] K.P. Shinde, S.H. Jang, J.W. Kim, D.S. Kim, M. Ranot, K.C. Chung, Magnetocaloric properties of TbN, DyN and HoN nanopowders prepared by the plasma arc discharge method, Dalton T 44(47) (2015) 20386-20391.
[281] N. Terada, K. Terashima, P.B. de Castro, C.V. Colin, H. Mamiya, T.D. Yamamoto, H. Takeya, O. Sakai, Y. Takano, H. Kitazawa, Relationship between magnetic ordering and gigantic magnetocaloric effect in ${\mathrm{HoB}}_{2}$ studied by neutron diffraction experiment, Phys Rev B 102(9) (2020) 094435.
[282] T. Utaki, K. Kamiya, T. Nakagawa, A. Yamamoto, T. Numazawa, Research on a Magnetic Refrigeration Cycle for Hydrogen Liquefaction, in: S.D. Miller, R.G. Ross Jr (Eds.) Cryocoolers, International Cryocooler Conference, Inc., Boulder, CO, , 2007, pp. 645 - 653.
[283] T. Numazawa, K. Kamiya, T. Utaki, K. Matsumoto, Magnetic refrigerator for hydrogen liquefaction, Cryogenics 62 (2014) 185-192.
[284] H. Meng, B. Li, Z. Han, Y.Q. Zhang, X.W. Wang, Z.D. Zhang, Reversible magnetocaloric effect and refrigeration capacity enhanced by two successive magnetic transitions in DyB2, Sci. China-Technol. Sci. 55(2) (2012) 501-504.
[285] J. Li, Y. Liu, X. Lu, Y. Zhang, J. Guo, M. Zhang, J. Liu, Enhanced refrigeration capacity in Ho1-xDyxB2 compounds around liquid hydrogen temperature, J Alloy Compd 864 (2021) 158757.
[286] S. Iwasaki, T.D. Yamamoto, P. Baptista de Castro, K. Terashima, H. Takeya, Y. Takano, Al substitution effect on magnetic properties of magnetocaloric material HoB2, Solid State Commun 342 (2022) 114616.
[287] Z. Han, D. Li, H. Meng, X.H. Liu, Z.D. Zhang, Magnetocaloric effect in terbium diboride, J Alloy Compd 498(2) (2010) 118-120.
[288] L.J. Meng, C. Xu, Y. Yuan, Y. Qi, S.Q. Zhou, L.W. Li, Magnetic properties and giant reversible magnetocaloric effect in GdCoC2, RSC Adv. 6(78) (2016) 74765-74768.
[289] L.J. Meng, Y.S. Jia, L.W. Li, Large reversible magnetocaloric effect in the RECoC2 (RE = Ho and Er) compounds, Intermetallics 85 (2017) 69-73.
[290] Y. Zhang, S. Li, L. Hu, X. Wang, L. Li, M. Yan, Excellent magnetocaloric performance in the carbide compounds RE2Cr2C3 (RE = Er, Ho, and Dy) and their composites, Materials Today Physics 27 (2022) 100786.
[291] L. Li, M. Kadonaga, D. Huo, Z. Qian, T. Namiki, K. Nishimura, Low field giant magnetocaloric effect in RNiBC (R = Er and Gd) and enhanced refrigerant capacity in its composite materials, Appl Phys Lett 101(12) (2012).
[292] Y. Zhang, D. Guo, B. Wu, H. Wang, R. Guan, X. Li, Z. Ren, Magnetic properties and magneto-caloric performances in RECo2B2C (RE = Gd, Tb and Dy) compounds, J Alloy Compd 817 (2020) 152780.
[293] P. Bredy, P. Seyfert, Measurement of magnetic field induced changes in the entropy of europium sulphide, Cryogenics 28(9) (1988) 605-606.
[294] S. Nishio, T. Nakagawa, T. Arakawa, N. Tomioka, T.A. Yamamoto, T. Kusunose, K. Niihara, T. Numazawa, K. Kamiya, Specific heat and thermal conductivity of HoN and ErN at cryogenic temperatures, J Appl Phys 99(8) (2006) 08K901.
[295] D. Kim, J. Ahn, B. Sinha, J. Kim, C. Choi, Novel route to prepare HoN nanoparticles for magnetic refrigerant in cryogenic temperature, Int J Hydrogen Energ 40(35) (2015) 11465-11469.
[296] K.P. Shinde, S.H. Jang, M. Ranot, B.B. Sinha, J.W. Kim, K.C. Chung, Large magnetic entropy change at cryogenic temperature in rare earth HoN nanoparticles, RSC Adv. 6(79) (2016) 75562-75569.
[297] K. Ahn, A.O. Pecharsky, K.A. Gschneidner, V.K. Pecharsky, Preparation, heat capacity, magnetic properties, and the magnetocaloric effect of EuO, J Appl Phys 97(6) (2005) 063901.
[298] Y.T. Su, Y. Sui, X.J. Wang, J.G. Cheng, Y. Wang, W.F. Liu, X.Y. Liu, Large magnetocaloric properties in single-crystal dysprosium titanate, Mater Lett 72 (2012) 15-17.
[299] Y. Su, Y. Sui, J.G. Cheng, J.S. Zhou, X. Wang, Y. Wang, J.B. Goodenough, Critical behavior of the ferromagnetic perovskites RTiO3 (R= Dy, Ho, Er, Tm, Yb) by magnetocaloric measurements, Phys Rev B 87(19) (2013) 195102.
[300] Z.J. Mo, J. Shen, L. Li, Y. Liu, C.C. Tang, F.X. Hu, J.R. Sun, B.G. Shen, Observation of giant magnetocaloric effect in EuTiO3, Mater Lett 158 (2015) 282-284.
[301] A. Midya, P. Mandal, K. Rubi, R.F. Chen, J.S. Wang, R. Mahendiran, G. Lorusso, M. Evangelisti, Large adiabatic temperature and magnetic entropy changes in EuTiO3, Phys Rev B 93(9) (2016) 094422.
[302] S. Roy, N. Khan, P. Mandal, Giant low-field magnetocaloric effect in single-crystalline EuTi0.85Nb0.15O3, Apl Materials 4(2) (2016) 026102.
[303] A. McDannald, L. Kuna, M. Jain, Magnetic and magnetocaloric properties of bulk dysprosium chromite, J Appl Phys 114(11) (2013) 113904.

[304] L.H. Yin, J. Yang, P. Tong, X. Luo, C.B. Park, K.W. Shin, W.H. Song, J.M. Dai, K.H. Kim, X.B. Zhu, Y.P. Sun, Role of rare earth ions in the magnetic, magnetocaloric and magnetoelectric properties of $RCrO_3$ (R = Dy, Nd, Tb, Er) crystals, Journal of Materials Chemistry C 4(47) (2016) 11198-11204.
[305] E. Palacios, C. Tomasi, R. Saez-Puche, A.J. Dos Santos-Garcia, F. Fernandez-Martinez, R. Burriel, Effect of Gd polarization on the large magnetocaloric effect of GdCrO4 in a broad temperature range, Phys Rev B 93(6) (2016) 064420.
[306] A. Midya, N. Khan, D. Bhoi, P. Mandal, 3d-4f spin interaction induced giant magnetocaloric effect in zircon-type DyCrO4 and HoCrO4 compounds, Appl Phys Lett 103(9) (2013) 092402.
[307] A. Midya, N. Khan, D. Bhoi, P. Mandal, 3d-4f spin interaction and field-induced metamagnetism in RCrO4 (R=Ho, Gd, Lu) compounds, J Appl Phys 115(17) (2014) 17E114.
[308] Q.Y. Dong, Y. Ma, Y.J. Ke, X.Q. Zhang, L.C. Wang, B.G. Shen, J.R. Sun, Z.H. Cheng, Ericsson-like giant magnetocaloric effect in $GdCrO_4$-$ErCrO_4$ composite oxides near liquid hydrogen temperature, Mater Lett 161 (2015) 669-673.
[309] A. Midya, N. Khan, D. Bhoi, P. Mandal, Giant magnetocaloric effect in antiferromagnetic DyVO4 compound, Physica B 448 (2014) 43-45.
[310] K. Rubi, P. Kumar, D.V. Maheswar Repaka, R. Chen, J.-S. Wang, R. Mahendiran, Giant magnetocaloric effect in magnetoelectric $Eu_{1-x}Ba_xTiO_3$, Appl Phys Lett 104(3) (2014) 032407.
[311] E. Palacios, M. Evangelisti, R. Sáez-Puche, A.J. Dos Santos-García, F. Fernández-Martínez, C. Cascales, M. Castro, R. Burriel, O. Fabelo, J.A. Rodríguez-Velamazán, Magnetic structures and magnetocaloric effect in RVO4 R=Gd, Nd, Phys Rev B 97(21) (2018) 214401.
[312] K. Dey, A. Indra, S. Majumdar, S. Giri, Cryogenic magnetocaloric effect in zircon-type RVO4 (R = Gd, Ho, Er, and Yb), Journal of Materials Chemistry C 5(7) (2017) 1646-1650.
[313] M. Balli, S. Mansouri, D.Z. Dimitrov, P. Fournier, S. Jandl, J.-Y. Juang, Strong conventional and rotating magnetocaloric effects in $TbVO_4$ crystals over a wide cryogenic temperature range, Physical Review Materials 4(11) (2020) 114411.
[314] G.N.P. Oliveira, A.L. Pires, P. Machado, A.M. Pereira, J.P. Araújo, A.M.L. Lopes, Effect of chemical pressure on the magnetocaloric effect of perovskite-like RCrO3 (R-Yb, Er, Sm and Y), J Alloy Compd 797 (2019) 269-276.
[315] R.X. Huang, S.X. Cao, W. Ren, S. Zhan, B.J. Kang, J.C. Zhang, Large rotating field entropy change in ErFeO3 single crystal with angular distribution contribution, Appl Phys Lett 103(16) (2013) 162412.
[316] Y.-J. Ke, X.-Q. Zhang, H. Ge, Y. Ma, Z.-H. Cheng, Low field induced giant anisotropic magnetocaloric effect in DyFeO3 single crystal, Chinese Phys B 24(3) (2015) 037501.
[317] Y.J. Ke, X.Q. Zhang, Y. Ma, Z.H. Cheng, Anisotropic magnetic entropy change in RFeO3 single crystals(R = Tb, Tm, or Y), Sci Rep 6 (2016) 19775.
[318] Y.-J. Ke, X.-Q. Zhang, J.-F. Wang, Z.-H. Cheng, Giant magnetic entropy change in gadolinium orthoferrite near liquid hydrogen temperature, J Alloy Compd 739 (2018) 897-900.
[319] M. Das, S. Roy, P. Mandal, Giant reversible magnetocaloric effect in a multiferroic GdFeO3 single crystal, Phys Rev B 96(17) (2017) 8.
[320] X. Bohigas, J. Tejada, E. del Barco, X.X. Zhang, M. Sales, Tunable magnetocaloric effect in ceramic perovskites, Appl Phys Lett 73(3) (1998) 390-392.
[321] L.W. Li, J. Wang, K.P. Su, D.X. Huo, Y. Qi, Magnetic properties and magnetocaloric effect in metamagnetic RE2Cu2O5 (RE = Dy and Ho) cuprates, J Alloy Compd 658 (2016) 500-504.
[322] M. Das, S. Roy, N. Khan, P. Mandal, Giant magnetocaloric effect in an exchange-frustrated GdCrTiO5 antiferromagnet, Phys Rev B 98(10) (2018) 104420.
[323] L. Li, K. Su, D. Huo, Large reversible normal and inverse magneto-caloric effects in the RE2BaCuO5 (RE = Dy and Er) compounds, J Alloy Compd 735 (2018) 773-776.
[324] P. Xu, L. Hu, Z. Zhang, H. Wang, L. Li, Electronic structure, magnetic properties and magnetocaloric performance in rare earths (RE) based RE_2BaZnO_5 (RE = Gd, Dy, Ho, and Er) compounds, Acta Mater 236 (2022) 118114.
[325] S. Ghara, F. Fauth, E. Suard, J. Rodriquez-Carvajal, A. Sundaresan, Synthesis, Structure, and Physical Properties of the Polar Magnet DyCrWO6, Inorg Chem 57(20) (2018) 12827-12835.
[326] C. Dhital, D. Pham, T. Lawal, C. Bucholz, A. Poyraz, Q. Zhang, R. Nepal, R. Jin, R. Rai, Crystal and magnetic structure of polar oxide HoCrWO6, J Magn Magn Mater 514 (2020) 167219.

[327] Y. Tian, J. Ouyang, H. Xiao, Y. Zhang, Structural and magnetocaloric properties in the aeschynite type GdCrWO6 and ErCrWO6 oxides, Ceram. Int. 47(20) (2021) 29197-29204.
[328] R.C. Sahoo, S. Das, T.K. Nath, Role of Gd spin ordering on magnetocaloric effect and ferromagnetism in Sr substituted Gd2CoMnO6 double perovskite, J Appl Phys 124(10) (2018) 103901
[329] Z. Dong, Z. Wang, S. Yin, Structural, magnetic and cryogenic magneto-caloric properties in RE2FeCrO6 (RE = Er and Tm) compounds, Ceram. Int. 46(17) (2020) 26632-26636.
[330] Y.S. Jia, Q. Wang, P. Wang, L.W. Li, Structural, magnetic and magnetocaloric properties in R2CoMnO6 (R = Dy, Ho, and Er), Ceram. Int. 43(17) (2017) 15856-15861.
[331] Y.Q. Cai, Y.Y. Jiao, Q. Cui, J.W. Cai, Y. Li, B.S. Wang, M.T. Fernández-Díaz, M.A. McGuire, J.Q. Yan, J.A. Alonso, J.G. Cheng, Giant reversible magnetocaloric effect in the pyrochlore $Er_2Mn_2O_7$ due to a cooperative two-sublattice ferromagnetic order, Physical Review Materials 1(6) (2017) 064408.
[332] Y. Zhang, H. Li, D. Guo, Z. Ren, G. Wilde, Cryogenic magnetic properties in the pyrochlore RE2TiMnO7 (RE = Dy and Ho) compounds, Ceram. Int. 44(13) (2018) 15681-15685.
[333] R. Li, G. Li, C. Greaves, Gaudefroyite: a mineral with excellent magnetocaloric effect suitable for liquefying hydrogen, Journal of Materials Chemistry A 6(13) (2018) 5260-5264.
[334] R.D. McMichael, J.J. Ritter, R.D. Shull, Enhanced magnetocaloric effect in Gd3Ga5xFexO12, J Appl Phys 73(10) (1993) 6946-6948.
[335] P. Mukherjee, S.E. Dutton, Enhanced Magnetocaloric Effect from Cr Substitution in Ising Lanthanide Gallium Garnets Ln(3)CrGa(4)O(12) (Ln = Tb, Dy, Ho), Adv Funct Mater 27(32) (2017) 1701950.
[336] D. Neupane, L. Hulsebosch, K.S.S. Ali, R. Bhattarai, X. Shen, A.K. Pathak, S.R. Mishra, Enhanced magnetocaloric effect in aluminum doped Gd3Fe5-xAlxO12 garnet: Structural, magnetic, and Mössbauer study, Materialia 21 (2022) 101301.
[337] J. Sultana, J. Mohapatra, J.P. Liu, S.R. Mishra, Structural, magnetic, and magnetocaloric properties of chromium doped Gd3Fe5-xCrxO12 garnet compound, AIP Advances 13(2) (2023).
[338] R. Li, Enhancing the Magnetocaloric Effect of a Paramagnet to above Liquid Hydrogen Temperature, Energy Technology 7(5) (2019) 1801070.
[339] R.K. Li, C.C. Wu, M.J. Xia, LiCaTb5(BO3)6: A new magneto-optical crystal promising as Faraday rotator, Optical Materials 62 (2016) 452-457.
[340] V. Tkáč, A. Orendáčová, E. Čižmár, M. Orendáč, A. Feher, A.G. Anders, Giant reversible rotating cryomagnetocaloric effect inKEr(MoO4)2induced by a crystal-field anisotropy, Phys Rev B 92(2) (2015) 024406.
[341] D.B. Miracle, O.N. Senkov, A critical review of high entropy alloys and related concepts, Acta Mater 122 (2017) 448-511.
[342] D.B. Miracle, High entropy alloys as a bold step forward in alloy development, Nat. Commun. 10(1) (2019) 1805.
[343] TMS, Defining Pathways for Realizing the Revolutionary Potential of High Entropy Alloys, TMS, Pittsburgh, PA, 2021.
[344] V. Franco, J.S. Blazquez, C.F. Conde, A. Conde, A Finemet-type alloy as a low-cost candidate for high-temperature magnetic refrigeration, Appl Phys Lett 88(4) (2006) 042505.
[345] V. Franco, J.S. Blazquez, A. Conde, Field dependence of the magnetocaloric effect in materials with a second order phase transition: A master curve for the magnetic entropy change, Appl Phys Lett 89(22) (2006) 222512.
[346] V. Franco, A. Conde, Scaling laws for the magnetocaloric effect in second order phase transitions: From physics to applications for the characterization of materials, Int J Refrig 33(3) (2010) 465-473.
[347] S. Guo, C.T. Liu, Phase stability in high entropy alloys: Formation of solid-solution phase or amorphous phase, Progress in Natural Science: Materials International 21(6) (2011) 433-446.
[348] Z. Dong, Z. Wang, S. Yin, Magnetic properties and large cryogenic magneto-caloric effect of $Er_{0.2}Tm_{0.2}Ho_{0.2}Cu_{0.2}Co_{0.2}$ amorphous ribbon, Intermetallics 124 (2020) 106879.
[349] J.T. Huo, D.Q. Zhao, H.Y. Bai, E. Axinte, W.H. Wang, Giant magnetocaloric effect in Tm-based bulk metallic glasses, J Non-Cryst Solids 359 (2013) 1-4.
[350] J. Huo, L. Huo, H. Men, X. Wang, A. Inoue, J. Wang, C. Chang, R.-W. Li, The magnetocaloric effect of Gd-Tb-Dy-Al-M (M = Fe, Co and Ni) high-entropy bulk metallic glasses, Intermetallics 58 (2015) 31-35.
[351] K. Yao, Y. Xu, Magnetic properties, magnetic transition and large magneto-caloric effect in the $Ho_{0.2}Er_{0.2}Tm_{0.2}Ni_{0.2}Cu_{0.2}$ amorphous ribbon, Solid State Commun 345 (2022) 114702.

[352] Y. Wang, D. Guo, B. Wu, S. Geng, Y. Zhang, Magnetocaloric effect and refrigeration performance in $RE_{60}Co_{20}Ni_{20}$ (RE = Ho and Er) amorphous ribbons, J Magn Magn Mater 498 (2020) 166179.
[353] Y. Zhang, J. Zhu, S. Li, J. Wang, Z. Ren, Achievement of giant cryogenic refrigerant capacity in quinary rare-earths based high-entropy amorphous alloy, J Mater Sci Technol 102 (2022) 66-71.
[354] I. Tereshina, J. Cwik, E. Tereshina, G. Politova, G. Burkhanov, V. Chzhan, A. Ilyushin, M. Miller, A. Zaleski, K. Nenkov, L. Schultz, Multifunctional Phenomena in Rare-Earth Intermetallic Compounds With a Laves Phase Structure: Giant Magnetostriction and Magnetocaloric Effect, Ieee T Magn 50(11) (2014) 4.
[355] I.S. Tereshina, G.A. Politova, E.A. Tereshina, G.S. Burkhanov, O.D. Chistyakov, S.A. Nikitin, Magnetocaloric effect in (Tb,Dy,R)(Co,Fe)(2) (R = Ho, Er) multicomponent compounds, in 2nd International Symposium on Advanced Magnetic Materials and Applications, Iop Publishing Ltd, 266 (2011) 012077, 10.1088/1742-6596/266/1/012077
[356] I.S. Tereshina, V.B. Chzhan, E.A. Tereshina, S. Khmelevskyi, G.S. Burkhanov, A.S. Ilyushin, M.A. Paukov, L. Havela, A.Y. Karpenkov, J. Cwik, Y.S. Koshkid'ko, M. Miller, K. Nenkov, L. Schultz, Magnetostructural phase transitions and magnetocaloric effect in Tb-Dy-Ho-Co-Al alloys with a Laves phase structure, J Appl Phys 120(1) (2016) 10.
[357] J. Cwik, Magnetism and magnetocaloric effect in multicomponent Laves-phase compounds: Study and comparative analysis, J Solid State Chem 209 (2014) 13-22.
[358] G.A. Politova, I.S. Tereshina, J. Cwik, Multifunctional phenomena in Tb-Dy-Gd(Ho)-Co(Al) compounds with a Laves phase structure: Magnetostriction and magnetocaloric effect, J Alloy Compd 843 (2020).
[359] P.K. Jesla, J.A. Chelvane, A.K. Nigam, R. Nirmala, Magnetocaloric effect in a multicomponent Laves phase intermetallic compound $Gd_{0.2}Tb_{0.2}Dy_{0.2}Ho_{0.2}Er_{0.2}Al_2$, AIP Conference Proceedings, 2020, p. 030565.
[360] W.-L. Zuo, A. Murtaza, L. Wang, A. Ghani, Y. Ding, L. Liu, T. Jin, M. Fang, X. Ke, S. Yang, Exploring the heat capacity and magnetocaloric behaviors of rare-earth based multicomponent (Ce0.71Pr0.07Nd0.22)2Fe17-xSix alloys, J Alloy Compd 960 (2023) 171042.
[361] EuropeanCommission, Study on the Critical Raw Materials for the EU 2023 – Final Report (2023).doi: 10.2873/725585.
[362] Methodology for establishing the EU list of critical raw materials – Guidelines (2017).doi: https://doi.org/10.2873/769526.
[363] EuropeanCommission, Study on the EU's list of Critical Raw Materials – Final Report (2020).doi: https://doi.org/10.2873/725585.
[364] E. Commission, European Commision, Study on the review of the list of Critical Raw Materials – Criticality Assessments (2017).doi: https://doi.org/10.2873/876644.